Role of the Microvasculature in the Development of Muscle Insulin Resistance

By

Philippe St-Pierre, RT, B.Sc., M.Sc.

Submitted in fulfilment of the requirements for the degree of
Doctor of Philosophy (Medical Research)

Menzies Research Institute
University of Tasmania

May 2010

TABLE OF CONTENT

TABLE OF FIGURES

TABLE OF TABLES

ACKNOWLEDGEMENTS

First of all, I would like to thank both my supervisors: Prof Stephen Rattigan and Prof Michael Clark. Not only have they given me the opportunity to study in their lab, but they have also given me all the help and support necessary to complete this incredible adventure. For it all, I will always be thankful.

I was also very lucky to be part an awesome group of people. I would like to extend my gratitude to Renée Dwyer, Carol Bussey, Dino Premilovac, Eloise Bradley, Kathleen Downey, Michelle Keske, Stephen Richards, John Newman, Barbara Arnts and Geoffrey Appleby. You have been my surrogate family during these last 4 years. It has been a real pleasure to share that time with you.

I would like to acknowledge the work discussed in Chapter 6 on the angiogenic process done by Georgia Siltman. Also big thanks to Renée, Eloise, Dino, Carol and Jennifer Lavers for correcting my dodgy English.

Last, but definitely not least, I want to thank my friends (Marie-Eve, Julie, Sam, J-F and Alexis) and my family (Mom, Dad and Vincent) that I left back home. It has not always been easy, but even through the distance you have always been with me. I do not think I could have done it without your support. I also want to mention my godfather and my grandfather, to which this thesis is dedicated. I miss you both greatly.

STATEMENT

The work in this thesis has been taken exclusively for the use of a Ph.D. in the area of Biochemistry, and has not been used for any other higher degree or graduate diploma in any university. All written and experimental work is my own, except which has been referenced accordingly.

PHILIPPE ST-PIERRE

AUTHORITY OF ACCESS

This thesis may be available for loan and limited copying in accordance with the Copyright Act 1968.

PHILIPPE ST-PIERRE

ABSTRACT

Type 2 diabetes is a disease characterised by a decrease in the sensitivity to insulin. Recently evidence has suggested an involvement of the microvasculature in the development of type 2 diabetes. Microvascular perfusion is increased by insulin and impairment of this response may contribute to muscle insulin resistance by limiting insulin and glucose delivery to skeletal muscle myocytes. This thesis focuses on the involvement of the microvascular perfusion in the development of insulin resistance.

Two different models were used to assess the impact of the microvascular perfusion on the insulin-mediated glucose disposal. Firstly, 4 weeks of high-fat diet (HFD model) feeding to rats was used as a pre-diabetic model of insulin resistance. Secondly, partial blockage of skeletal muscle microvascular beds with 15 μm diameter latex microspheres (MS model) was used to assess the effect of decreased muscle microvascular perfusion on insulin sensitivity.

In each model, insulin sensitivity was determined during hyperinsulinaemic isoglycaemic clamps in anaesthetized rats. Femoral arterial blood flow (FBF) and microvascular perfusion (assessed by the hindleg metabolism of infused 1-methylxanthine) were measured. Hindleg glucose uptake was determined from arteriovenous difference and FBF and muscle glucose uptake from [^{14}C]-2-deoxyglucose uptake.

Insulin-mediated increases in femoral blood flow and glucose uptake were blunted in the HFD rats compared to those on the normal diet, while insulin-induced microvascular perfusion was completely abolished. To see whether contraction responses were intact on the HFD, the functional response to electrical stimulation in the HFD rats was explored. The contraction-mediated increase in microvascular perfusion and glucose uptake was unaffected by the HFD.

In the MS model, microsphere occlusion of hindleg muscle microvasculature diminished microvascular perfusion as well as insulin-mediated glucose uptake, thus causing a vascular-derived acute state of insulin resistance. Next, the long-term effect of microsphere occlusion was assessed. Surprisingly, insulin responses following chronic microsphere occlusion were restored by 2 weeks of

recovery post-injection. This may be explained by a rapid angiogenic response in occluded muscle vasculature.

Collectively, this thesis demonstrates two key findings that highlight the potential role of the microvasculature in the development of skeletal muscle insulin resistance: (i) that insulin- but not contraction-mediated microvascular responses are impaired in a pre-diabetic model of insulin resistance, and (ii) that acute physical reduction of microvascular flow impairs muscle insulin sensitivity. This furthers our understanding of the aetiology of type 2 diabetes and emphasizes the microvasculature as an interesting therapeutic target for the management of type 2 diabetes.

ABBREVIATIONS

ALP	Allopurinol
AI	Acoustic Intensity
AMPK	5' AMP-activated protein kinase
AS160	Akt Substrate 160
BG	Blood Glucose
BPM	Beats per Minutes
2-DG	2-Deoxyglucose
Cr	Creatine
CEU	Contrast Enhanced Ultrasound
EC	Energy Charge
EDL	Extensor Digitorum Longus
eNOS	Endothelial Nitric Oxide Synthase
ER	Endoplasmic Reticulum
ET-1	Endothelin-1
FA	Fatty Acids
FBF	Femoral Blood Flow
FFA	Free Fatty Acids
GIR	Glucose Infusion Rate
GLUT-4	Glucose Transporter 4
HFD	High Fat Diet
HGU	Hindlimb Glucose Uptake
HLPC	High Liquid Performance Chromatography
HR	Heart Rate

Hz	Hertz
IKK	IκB-α Kinase
IMCL	Intramyocellular Lipid
IRS	Insulin Receptor Substrate
JNK	c-jun NH2-terminal kinase
LDF	Laser Doppler Flowmetry
LPL	Lipoprotein lipase
MAP	Mean Arterial Pressure
MBF	Microvascular Blood Flow
MBV	Microvascular Blood Volume
MFR	Microvascular Flow Rate
MGS	Media Growth Supplement
mmHg	Millimetre of mercury
MS	Microspheres
1-MU	1-Methyluric
1-MX	1-Methylxanthine
ND	Normal Diet
NO	Nitric Oxide
NOS	Nitric Oxide Synthase
OXY	Oxypurinol
PCA	Perchloric acid
PCr	Phospho-creatine
PCr/Cr	Phospho-creatine to creatine ratio
PI3-K	Phosphatidyl Inositol-3 Kinase
PG	Plasma Glucose
PL	Plasma Lactate

R'g	Rate of Glucose Uptake
Ra	Rate of appearance
Rd	Rate of disappearance
RG	Red Gastrocnemius
ROS	Reactive Oxygen Species
RT	Room Temperature
SEM	Standard Error of the Mean
SHR	Spontaneously Hypertensive Rats
TG	Triglycerides
TNF-α	Tumor Necrosis Factor-α
UPR	Unfolded Protein Response
VEGF	Vascular Endothelial Growth Factor
WG	White Gastrocnemius
XO	Xanthine Oxidase
ZDF	Zucker Diabetic Fatty

PREFACE

Some of the data presented in this thesis has been published or presented at scientific meetings and has been listed below

Publications directly arising from this thesis

St-Pierre P, Genders AJ, Keske MA, Richards SR, Rattigan S. Loss of insulin-mediated microvascular perfusion in skeletal muscle is associated with the development of insulin resistance. Diabetes, Obesity and Metabolism. Accepted for publication on May 3, 2010.

Presentation at scientific meetings

St-Pierre P, Genders AJ, Keske MA, Richards SM, Rattigan S. Insulin-, but not Contraction-, Mediated Microvascular Perfusion in Skeletal Muscle is Markedly Blunted by High Fat Feeding. Annual Scientific Meeting of the Australian Diabetes Society, August 2009 (oral presentation)

Newman JM, Dwyer RM, **St-Pierre P**, Richards SM, Clark MG, Rattigan S. Microvascular vasomotion is enhanced by insulin and inhibited by acute insulin resistance in rat muscle. Annual Scientific Meeting of the Australian Diabetes Society, August 2009. (oral presentation)

St-Pierre P, Keske MA, Clark MG, Richards SM, Rattigan S. In vivo assessment of microvascular perfusion and glucose uptake: Effect of acute microsphere embolism. European Society for Microcirculation, *Journal of Vascular Research* 45 (Suppl. 2):87, 2008 (poster presentation)

Rattigan S, **St-Pierre P**, Genders AJ, Keith L, Keske MA, Richards SR. High fat feeding induced loss of insulin-mediated vascular sensitivity in muscle. European Association for the Study of Diabetes, *Diabetologia* 51 [Suppl. 1]: S253, 2008 (poster presentation)

Other publications

Newman JM, Dwyer RM, **St-Pierre P**, Richards SM, Clark MG, Rattigan S. Decreased microvascular vasomotion and myogenic response in rat skeletal muscle in association with acute insulin resistance. *Journal of Physiology* 587(Pt 11):2579-2588, 2009

CHAPTER 1:

INTRODUCTION

1.1 INTRODUCTION

In 2004-05, more than half (53 %) of the Australian population, or 7.4 million people were either overweight or obese (ABS 2008). Obesity poses a major risk to long-term health by increasing the risk of chronic illnesses such as diabetes. An estimated 5 % of the Australian population in 2008 has diagnosed type 2 diabetes with an annual health cost estimated of one billion (ABS 2008). Globally, the World Health Organization estimated the prevalence of type 2 diabetes at 160 million in 2000, and the prevalence is expected to double before 2030 (WHO 2009).

Type 2 diabetes is a chronic disease that occurs when the body cannot effectively use the insulin it produces, leading to a rise in blood glucose. Over time, type 2 diabetes lead to many complication including: heart disease and stroke, hypertension, atherosclerosis, nephropathy, neuropathy, and retinopathy (WHO 2009). Even though type 2 diabetes has been a subject of intensive research, the underlying mechanisms remain relatively poorly understood. Unravelling how insulin resistance progresses to diabetes would be invaluable as it may lead to the therapeutic strategies to prevent the development of this disease. In addition, determining the role of obesity, and how it influences the rate of this progression, is an important factor to consider.

1.2 PHYSIOLOGICAL EFFECTS OF INSULIN

The metabolic actions of insulin have been known since the 1920s, but in the last 2 decades, the novel vascular actions of insulin have been uncovered. These include an increase in total blood flow and enhanced microvascular recruitment. This increase in blood flow and recruitment is responsible for approximately 50 % of insulin-mediated glucose uptake in skeletal muscle (Youd 2000). Interestingly, in late stage type 2 diabetes, the vascular actions of insulin have been shown to be impaired (Wallis 2002, Clerk 2007). A decreased in the vascular actions of insulin will lead to decreased delivery of insulin and glucose

to the skeletal muscle and a decrease in insulin-mediated glucose uptake. This thesis explores the possibility that impaired microvascular recruitment may be a major initial defect leading to insulin resistance.

Insulin mediates its main metabolic action via the PI3K/Akt intracellular pathway (Figure 1). Upon reaching a target cells, insulin binds to its tyrosine kinase receptor, leading to activation of insulin receptor substrate (IRS) by phosphorylation on the tyrosine residue (White 1994). This creates a Src homology 2 (SH2)-binding domain on IRS, which the regulatory p85 subunit of PI3K will bind, in turn activating its catalytic p110 subunit (Folli 1992, Vincent 2003). This results in phosphorylation of the 3'-OH position of the inositol ring of plasma membrane inositol phospholipids, generating increased levels of phophatidylinositol-3,4,5 triphosphate (PIP_3). This molecule is specifically recognised by protein containing pleck-strin homology (PH) domains. The 3'-phosphoinositide-dependent kinase 1 (PDK-1) possess such a domain (Mora 2004), and upon its activation, will phosphorylate the Thr^{308} residue of Akt (Alessi 1996). Akt is a very important intracellular signalling intermediate known for its regulation of many downstream proteins (Gual 2005).

In skeletal muscle, Akt activation leads to an increase in glucose uptake by recruiting the transmembrane glucose transporter GLUT-4 to the plasmatic membrane and the T-tubule (Kim 2006). This mechanism involves the activation of Akt substrate 160 (AS160) (Bruss 2005). In the endothelial cell of the skeletal muscle vasculature, insulin leads to the Akt-mediated phosphorylation of eNOS on Ser^{1177} (Zeng 2000) and the production of nitric oxide (NO). This molecule is an important mediator of the endothelial dependent vasodilation (Moncada 1987). Therefore, insulin can increase the vasodilation of vessels through an increased release of NO by the stimulation of endothelial cell (Scherrer 1994). It is interesting that both metabolic and vascular actions of insulin share similar intracellular signalling pathways.

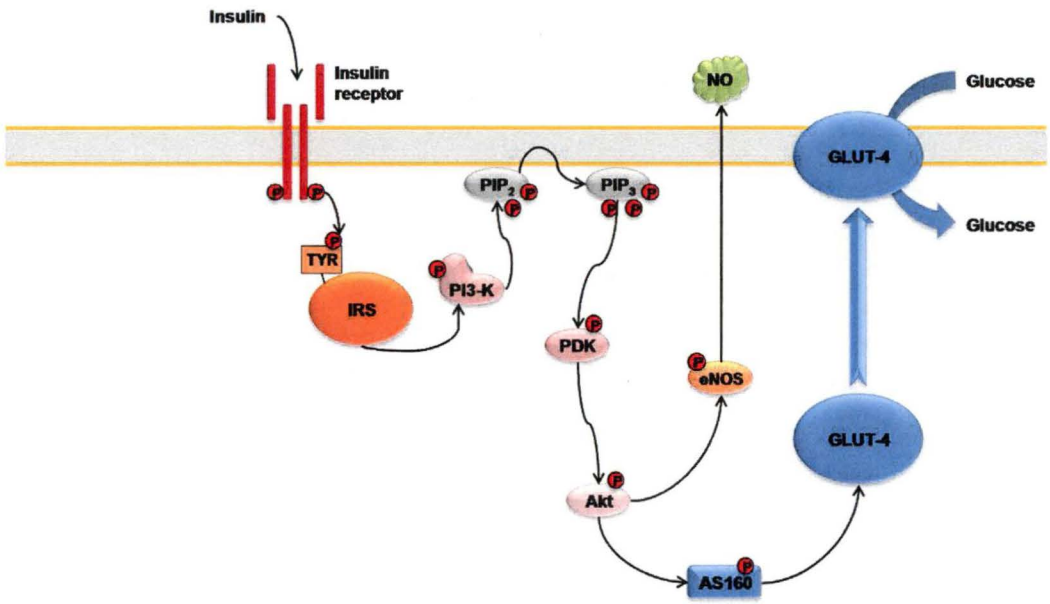

Figure 1: Insulin signalling.
Intracellular insulin signalling of the PI3K/Akt pathway. Activation of this pathway in the myocyte leads to the recruitment to the membrane of glucose transporter GLUT-4. In the endothelial cell this pathway results in NO production, a know vasodilatator. Adapted from (Muniyappa 2007)

It should be mentioned that the binding of insulin to its receptor also activates a second intracellular pathway, the Ras/MAPK pathway. This pathway is responsible for effects of insulin on gene expression, cell growth and differentiation (Muniyappa 2007). Furthermore, the Ras/MAPK pathway has been shown to be intact in states of insulin resistance, while the PI3K/Akt is defective (Jiang 1999, Cusi 2000). As insulin resistance is accompanied by compensatory hyperinsulinemia, this increases will led to the over activation of the Ras/MAPK pathway. As the MAPK pathway have been shown to be able to phosphorylate IRS-1 on serine residues (De Fea 1997), this can further impair the activation of the PI3K pathway (Dunaif 1995).

1.3 AETIOLOGY OF THE DEVELOPMENT OF TYPE 2 DIABETES

Insulin, a peptide hormone synthetised in the pancreas by the β-cells of the islet of Langerhans, is secreted in response to increased blood glucose. Insulin is the main hypoglycaemic hormone and its action is diminished in type 2 diabetes. The type 2 diabetic state is defined as a loss of control of the blood glucose by the body. The aetiology of diabetes can split into three phase (Figure 2). First, the insulin resistant phase occurs when there is a failure of insulin to exert its normal effects. Physiological concentrations of insulin fail to suppress hepatic glucose output and to increase glucose disposal into muscle. Therefore, in order to achieve normal level of blood glucose, the pancreas needs to secrete abnormally high amounts of insulin. The second phase occurs when this high insulin secretion is no longer able to maintain the glycaemia within normal range (fasting value <130 mg/dl) (ADA 2009). It is at this point that insulin resistance/diabetes is usually diagnosed. The third phase occurs after chronic exposure (many years) to the diabetic phenotype. Over a long period, the pancreas is unable to sustain these high levels of secretion and β-cell failure occurs. Therefore, the production of insulin by the pancreas becomes insufficient to maintain normal blood glucose levels and uncontrolled hyperglycemia results. These three phases are illustrated in Figure 2. As the insulin resistant phase occurs very early in the pathogenesis of diabetes, understanding its evolution is crucial in the prevention of type 2 diabetes.

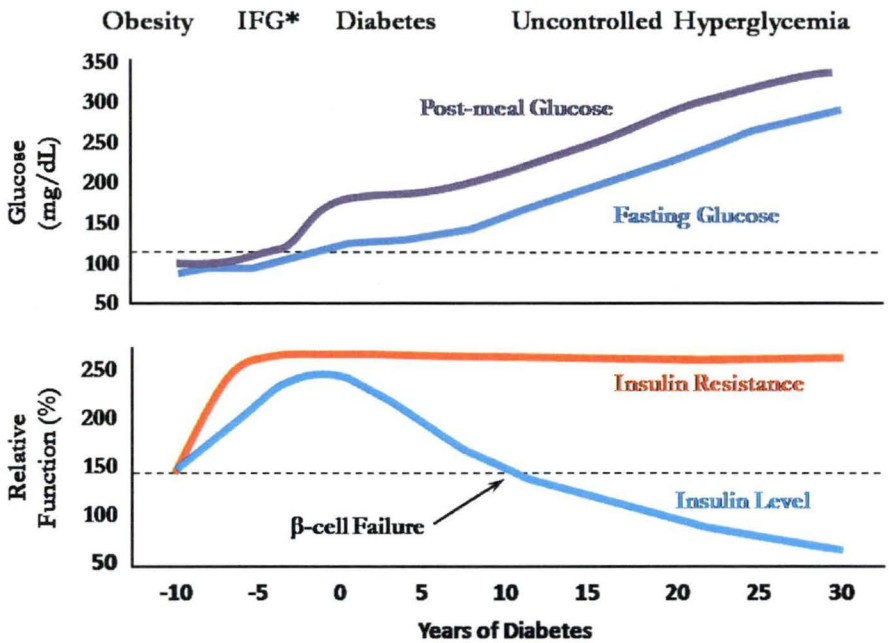

Figure 2: Aetiology of type 2 diabetes.
Graphic representation of blood glucose and pancreatic function during the development of Type 2 diabetes over the years. The development of type 2 diabetes can be separated into 3 phases. (1) The insulin resistant stage, often associated with obesity, is characterised by an increase in blood insulin. This is required as the body is less responsive to the actions of insulin. Early on, the increase in blood insulin is sufficient to maintain blood glucose in a normal range. (2) This is followed by the diabetic state, where the fasting blood glucose is higher than 130 mg/dl. This occurs when the overproduction of insulin become insufficient to maintain blood glucose within physiological range. (3) The later phase happens when the pancreatic production of insulin falls and β-cell failure occurs. This is a very late stage in the progression of the disease, and afflicted subject would require daily injection of exogenous insulin to maintain their blood glucose.
IFG = impaired fasting glucose.
(Adapted from International Diabetes Center (IDC), Minneapolis, Minnesota)

Type 2 diabetes is a difficult disease to investigate as it appears to results from a combination of factors. The occurrence and severity of this disease in each patient depends on environmental factors such as their level of fitness, weight, and diet but also on genetic predisposition. Despite this, skeletal muscle insulin resistance, define by decrease insulin-mediated glucose uptake in the skeletal muscle, is a common feature of the disease and a major contributor to its development (Reaven 1988, Defronzo 1991). Insulin-mediated glucose uptake is

regulated at three points in skeletal muscle: Firstly, by the delivery of blood rich in insulin and glucose to the muscle, secondly by the trans-endothelium transport of insulin from the circulation to the interstitium, and thirdly by the intracellular signalling pathway leading to glucose uptake once insulin is bound to its receptor on the cell surface of the myocyte. This thesis focuses on the first point of control and discusses how impairment of the delivery of insulin and glucose to the skeletal muscle could be implicated in the early development of insulin resistance. Furthermore, it is important to discern between bulk delivery of blood and the effective delivery of glucose. Increase in total blood flow does not necessary correlate with increase delivery of insulin and glucose to the skeletal muscle (Rattigan 1997). The redistribution of blood flow within discrete region of the muscle is crucial to the proper disposal of glucose. This point will be explored in further details in section 1.5.2.1.1 and 1.5.2.2.

1.4 SKELETAL MUSCLE INSULIN RESISTANCE

The skeletal muscle is an extremely important organ for insulin-mediated glucose disposal, as it accounts for about 80 % of the insulin-mediated glucose uptake after a meal (Defronzo 1988). In addition, muscle insulin resistance is a precursor to the hyperglycemia observed in patients with glucose intolerance or type 2 diabetes (Reaven 1988, Defronzo 1991) underscoring the contribution of the skeletal muscle to the insulin resistant phenotype. Therefore, skeletal muscle is a prime target for the early defects in the development of insulin resistance, although the exact mechanism remained largely unknown. Different cellular mechanisms have been proposed to explain the skeletal muscle insulin resistance, with the major theories outlined below.

1.4.1 Fatty Acid Excess

Increases in circulating free fatty acid (FFA) are observed in type 2 diabetes patients (Reaven 1988) and have therefore been hypothesised to be responsible for the insulin resistance (Reaven 1988). The elevated FFA could be a result of

an increased dietary intake, but could also result from a resistance to insulin at the adipocyte leading to an increased activity of the hormone-sensitive lipase resulting in breakdown of triglycerides and release of FFA into the circulation (Roden 1996).

Two mechanisms have been proposed by which FFA may induce skeletal muscle insulin resistance. The first is that the decrease in glucose uptake could result from an interaction between lipid and glucose metabolism known as the fatty acid cycle or Randle cycle (Randle 1965). High circulating FFA levels leads to an increased oxidation of fatty acid and increased intra-mitochondrial content of acetyl-CoA. As a result, there is an increase in reduced/oxidized nicotinamide adenine dinucleotide ($NADH/NAD^+$) ratio, which in turn inhibits the pyruvate dehydrogenase (PDH) activity. The increase fatty acid oxidation will also lead to an accumulation of cytosolic citrate that will in turn inhibits PFK-1 (Garland 1963). Inhibition of PDH and PFK-1 leads to an increase glucose-6-phosphate levels that will inhibit hexokinase and then lead to decrease glucose uptake. However, the importance of this mechanism was called into question when it was revealed that reduction in carbohydrate oxidation was responsible for only one-third of the fatty acid-dependent decrease in glucose uptake (Boden 1994).

The second mechanism by which FFA could decrease insulin-mediated glucose uptake is by a direct action on the insulin signalling (Shulman 2000). Increased circulating FFA will increase intracellular concentration of fatty acid metabolites, fatty acyl Co-A, ceramides and diacylglycerol (DAG) (Shulman 2000, Machann 2004, Summers 2006). Accumulation of these intracellular fatty acid metabolites have been shown to impair the PI3K/Akt insulin signalling cascade by activating PKC (θ, βII, and δ) and subsequent serine phosphorylation of IRS-1 (Griffin 1999, Itani 2002, Yu 2002, Guo 2007). IRS-1 is central in the insulin PI3K/Akt pathway (see Figure 1) and serine phosphorylation prevents the downstream transmission of the insulin activation (Gual 2005).

Infusion of intralipids and heparin has been used to study the effect of increased circulating FFA on insulin sensitivity. This procedure has been shown to cause insulin resistance in both rodents (Kraegen 2008) and human (Ferrannini 1983, Bonadonna 1989, Boden 1994, Dresner 1999). Intralipid infusion prevented up to 50 % of the normal insulin-stimulated glucose uptake during a hyperinsulinaemic clamp and after glucose ingestion and was associated with impairment of IRS-1 activation (Dresner 1999).

The potential importance of FFA in the early development of insulin resistance is further supported by temporal studies of the obese Zucker rat (Liu 2002). Six-week-old obese Zucker rats, presenting only mild insulin resistance, have a 2-fold increase in the peripheral and portal levels of FFA when compared to their lean counterparts. This demonstrates that the increase in FFA precedes the appearance of hyperglycaemia and insulin resistance that is not apparent until ~15 weeks of age in this model. These studies indicate that an increase in FFA may well be implicated in the early development of insulin resistance.

1.4.2 Tumor Necrosis Factor-α

Obesity is now known to be a chronic low inflammatory state (Hotamisligil 2006, Lee 2009), and this inflammatory state may be involved in the development of insulin resistance. Tumor necrosis factor-α (TNF-α), a proinflammatory cytokine, is produced and secreted from the adipose tissue and plays a major role in mediating immune responses (Wellen 2005). Furthermore, TNF-α has been implicated as a critical mediator of insulin resistance, particularly in relation to obesity (Hotamisligil 1993, Hofmann 1994, Hotamisligil 1996). Expression of TNF-α is strongly correlated with reduced insulin-stimulated glucose disposal (Saghizadeh 1996, Kern 2001) and genetic ablation of TNF-α restores skeletal muscle insulin sensitivity in obese rodents (Uysal 1997). TNF-α has been shown to impair insulin signalling by phosphorylation of IRS-1 on Ser^{312}, Ser ^{636}, and Ser^{1101} (Gual 2005, Schenk 2008). A number of different protein kinases have been implicated in the

inhibition of IRS signalling by TNF-α and include PKC (Yu 2002), IκB-α kinase (Gao 2002) and c-jun NH2-terminal kinase (Aguirre 2000). All these kinases were initially indentified as critical mediators of inflammatory signalling (Gual 2005). Given its association with obesity, TNF-α may, with FFA, also be an important mediator in the early development of insulin resistance.

Infusion of TNF-α *in vivo* has been shown to inhibit insulin-mediated glucose uptake in rats. Acute infusion of TNF-α in the anaesthetised rat induced mild systemic insulin resistance, as seen by the 21 % decrease in glucose infusion rate during euglycaemic hyperinsulinaemic clamp (Youd 2000), and a ~50 % decrease in insulin-mediated skeletal muscle glucose uptake. Similar effects were observed in humans, where TNF-α infusion decrease the glucose infusion rate during hyperinsulinaemic clamp and prevented activation of the IRS and AS160 by insulin in the skeletal muscle (Plomgaard 2005). While *in vivo* experiments with systemic infusion of TNF-α leads to muscle insulin resistance, incubated skeletal muscle have failed to show any effect of TNF-α on insulin signalling and glucose uptake (Furnsinn 1997, Nolte 1998). Explanation for this may reside in the experimental procedure used. Indeed, incubated muscle does not involve the vasculature for nutrient delivery. However, in vivo, vascular delivery has been shown to be important and compromised by TNF-α (Youd 2000, Zhang 2003). In these studies, TNF-α was shown to prevent the insulin-mediated microvascular recruitment, leading to impaired glucose uptake. Therefore, the effect of TNF-α on impaired insulin sensitivity may be due to its vascular actions rather than actions within the myocyte. The physiological importance of the vascular actions will be further discussed in section 1.5.

1.4.3 Endothelial Dysfunction

As stated previously in section 1.2, NO is a potent vasodilator produced by endothelial cells. Endothelial dysfunction is defined as impairment of the NO synthesis and/or increase degradation of NO in response to stimuli, such as acetylcholine, and insulin. (Li 2000). Macro- and micro-vascular actions of

insulin have been shown to rely on the production of NO (Baron 1994, Scherrer 1994, Steinberg 1994, Vincent 2003, Potenza 2009), and impairment in this NO production has been shown to be present in insulin resistant muscle (Williams 1996, Young 1998, Vincent 2003, Muniyappa 2007, Kearney 2008).

Oxidative stress is thought to be partially responsible for endothelial dysfunction in type 2 diabetes, and can be explained by an overproduction of superoxide induced by chronic hyperglycaemia (Brownlee 1981). Increased presence of superoxide molecule has been shown to affect caveolae formation, endothelial NOS expression, and endothelial NOS-caveolin interactions (Peterson 1999), all leading to decrease NO bioavailability. Moreover, elevated glucose has also been shown to impair endothelial cell function via IKK downregulation of the IRS/PI3K pathway (Kim 2005). However, available data tends to favour the view that endothelial dysfunction precedes the development of type 2 diabetes (Anastasiou 1998, Lesniewski 2008) and even the skeletal muscle insulin resistance (Jansson 2007, Serne 2007). Therefore, it is unlikely that oxidative stress due to chronic hyperglycemia is responsible for endothelial dysfunction in the initial stage of insulin resistance.

Interestingly, both TNF-α and FFA have been shown to impair the insulin-mediated production of NO. In healthy humans, infusion of either TNF-α or FFA lead to impairment of the insulin-mediated increase in total blood flow (Steinberg 2000, Rask-Madsen 2003). In both cases, a decrease in insulin-mediated NO production was identified as the cause. Furthermore, similarly to hyperglycaemia, increased exposure to FFA can activate IKK, which in turn will inactivate elements of the insulin-signalling pathway, resulting in a further decrease in endothelial NO production (Kim 2005). This association with endothelial dysfunction supports the notion that TNF-α and FFA are early factors in the development of insulin resistance.

1.4.4 Endoplasmic Reticulum Stress

In the last 5 years, endoplasmic reticulum (ER) stress has been proposed as a molecular mechanism responsible for insulin resistance (Ozcan 2004, Eizirik 2008). ER stress occurs when the influx of misfolded or unfolded peptides exceeds the ER processing capacity (Boden 2009). ER stress triggers the unfolded protein response (UPR) that will either slow the protein synthesis, increase production of chaperone to properly fold the protein, or increases degradation of the unfolded proteins (Schroder 2005). Activation of the UPR has been shown to activate several serine/threonine kinases, including IKK and JNK, which can induce insulin resistance via serine phosphorylation of IRS-1 (Zhang 2008). Thus, the ER may be a proximal site that senses nutritional excess and translates it into metabolic responses.

1.4.5 Leptin and Adiponectin Resistance

Leptin and adiponectin are two adipokines that have recently stimulated much interest and may well be involved in the development insulin resistance. Leptin influences body weight homeostasis through effects on food intake and energy expenditure (Sierra-Honigmann 1998) while adiponectin is a known to be a insulin-sensitizing hormone (Lihn 2005) and to promote eNOS activity and the bioavailability of NO (Chen 2003, Tan 2004, Li 2007). Both adipokines have been shown to activate 5' AMP-activated protein kinase (AMPK) in the skeletal muscle and, as such, increase the rate of fatty acid oxidation and decrease muscle lipid content, which may in part be the underlying mechanism to their insulin sensitizing effect (Minokoshi 2002, Hardie 2003, Hattori 2008).

Resistance to leptin and adiponectin results in the accumulation of intramuscular lipids, such as DAG and ceramides, which, as discussed above, may contribute to the development of insulin resistance (Dyck 2006). Resistance to adiponectin has been shown to precede the accumulation of skeletal muscle lipids and insulin resistance in high-fat-fed rats (Mullen 2009). Furthermore, it is interesting to note that TNF-α decreases the expression of adiponectin (Bruun 2003).

The difficulty to indentify only one culprit for the development of insulin resistance illustrates the complexity of this disease. Insulin resistance has such a complex pathophysiology that one single causative molecular culprit is unlikely to exist. While myocyte insulin resistance in fully establish type 2 diabetes is without question, the mechanism(s) leading to this is far from resolved. A novel new possibility is that the loss of myocyte insulin signalling may be a secondary response after a primary loss of vascular function. The evidence related to the different vascular actions of insulin, which supports such a proposition is discussed below.

1.5 VASCULAR ACTIONS OF INSULIN

1.5.1 Macrovascular Effect of Insulin

The first observation of a vascular effect of insulin was made in 1939 by Abramson and colleagues (Abramson 1939). In this study, it was found that a bolus dose of 40-280U of insulin led to increased blood flow to the leg, forearm and hand of patients with schizophrenia. They found that insulin increased blood flow up to eight times, but since the experimental procedure did not include a compensatory glucose infusion, the vasodilatation attributed to insulin may also have been due to an increase in adrenaline levels resulting from the fall in blood glucose. However, in the early 1990s, Baron and colleagues demonstrated that increases in total blood flow was a novel action of insulin (Laakso 1990). The hyperinsulinaemic euglycaemic clamp (the gold standard to evaluate the insulin sensitivity) was used to eliminate the possible effects of counterregulatory hormones. Their studies were designed to assess the dose-dependent effects of insulin on glucose uptake and leg blood flow. They observed that leg blood flow increased in an insulin dose-dependent fashion along with whole body and muscle glucose uptake. The insulin-mediated flow response in lean men, (first increase in total blood flow at 300 pmol/l of serum insulin) was positively correlated with muscle glucose clearance. These findings were also confirmed

by others using various techniques to assess total blood flow in both human (Anderson 1991, Baron 1993, Utriainen 1995, Tack 1996, Ueda 1998) and animals (Liang 1982, Rattigan 1997, Vincent 2002, Zhang 2004).

However, there was considerable variation between reported studies in the magnitude of the blood flow response to insulin, and some groups failed to observe any changes in flow with insulin (Jackson 1986, Yki-Jarvinen 1987, Ebeling 1993, Sakai 1993). This led to considerable controversy as to whether insulin action on total blood flow was physiologically relevant (Yki-Jarvinen 1998, Steinberg 1999). While different measuring techniques have shown an insulin-mediated action on the total blood flow, the debate is centred on the experimental design. Many of the studies describing insulin-mediated increase in total blood flow used supra-physiologic or pharmacological dose of insulin (Baron 1993, Raitakari 1996, Bonadonna 1998), while studies showing small effects use more physiologically relevant doses of insulin that required several hours of insulin infusion before a change in blood flow was seen. (Laakso 1990, Anderson 1991, Vollenweider 1993). Moreover, an increase in FBF is not always associated with an increase in myocyte glucose uptake (Scherrer 1994, Nuutila 1996, Rattigan 1999).

This led Baron and colleagues (Baron 1994) to postulate that, although not measured in their studies, the distribution of blood flow within the muscle microvasculature may be a more crucial factor in insulin sensitivity. This important microvascular action of insulin was confirmed by direct measures in subsequent studies by others. (Rattigan 1997, Coggins 2001, Serne 2001, Vincent 2002, de Jongh 2004, Vincent 2004, Zhang 2004).

1.5.2 Microvascular Effect of Insulin

1.5.2.1 Structure of the Skeletal Muscle Microcirculation

Figure 3 depicts the general circulation found within the skeletal muscle. The muscle vascular tree is comprised of three different types of vessels: arteries, capillaries and veins. The blood circulatory system within muscle starts with the feeding arteries, which are generally classified as first-order arteriole (Sweeney 1989). In the subsequent branches, assigned higher order numbers, a reduction in arteriole diameters is observed until the capillaries are reached (Murrant 2000). As the diameter decreases, the smooth muscle cell content of the arterial vessel also decreases. Arterioles of 1st to 3rd order (> 50 μm diameter) are thought to control the resistance and, as such, the total blood flow though the skeletal muscle (Segal 1986, Murrant 2000). The smaller arterioles of the 3rd through 5th order (10-40 μm diameter) are thought to control the capillary blood flow distribution and capillary recruitment (Honig 1982, Clerk 2004). Capillaries, which arise from a 5th order arterioles, are grouped together to form a capillary module made of ~15 capillaries. This module runs along the muscle fibre, with three to four capillaries generally surrounding each fibre. Each capillary is composed of a single layer of endothelial cells, which allows efficient exchange of gas and other molecules between the blood and the myocytes. Resistance in the microvasculature can also be regulated by capillary recruitment itself and is of particularly importance during hyperaemia (Jayaweera 1999). The capillaries module terminates at post-capillaries venules. As the venules combine, an increase in diameter size and amount of smooth muscle cells surrounding the endothelial lined lumen occurs.

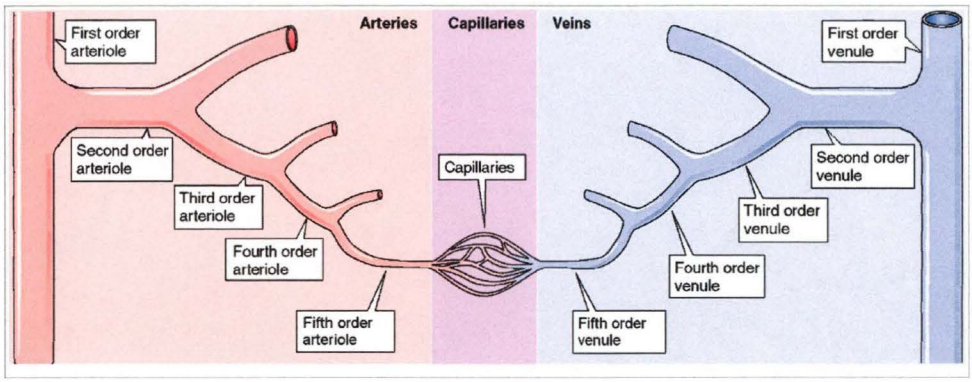

Figure 3: Microvascular tree.
The microvasculature is comprised of three different types of vessels: arteries, capillaries and veins. The skeletal muscle vascular system starts with the arteries, which are responsible for delivering the blood rich in nutrients and oxygen within the muscle. As arteries go deeper into the organ, the diameter and the smooth muscle cell content diminish. At the capillary level, only a single layer of endothelial cell exists. Capillaries allow efficient exchange of gas and other molecules between the blood and the myocytes. Venous vessels connected to the capillary beds groups together as they make their way out of the muscle. As such, their diameter and smooth muscle cell content increases.
(Adapted from (Boron 2003))

The term microvasculature generally refers to vessels < 150 μm in diameter (Levy 2001). It therefore includes the capillaries and the smaller arterioles and venules. The primary function of the microcirculation is to optimise the delivery of nutrients and removals of waste products (Murrant 2000). As such, the perfusion of a tissue can be modulated by contraction of the smooth muscle cells of the terminal arterioles (5^{th} order arterioles), therefore affecting the access of blood to this portion of the capillary module.

The circulatory system in muscle however has a further level of complexity that involves two circuits in parallel. Early evidence for two circulatory systems in the muscle comes from a study of Pappenheimer in 1940s (Pappenheimer 1941). Clark and colleagues have since shown that distributions of blood toward one or the other of these two separate flow routes (nutritive and non-nutritive) result in very different metabolic effects (Clark 1995)

1.5.2.1.1 Non-Nutritive and Nutritive Routes

The muscle microcirculation (Figure 4) is comprised of two distinct pathways: the non-nutritive and the nutritive route. Blood flow distribution between those two routes is under the control of vasoactive substances and the sympathetic nervous system (Clark 1995). Even though these two routes are contiguous and parallel inside the muscle, their functions are very different.

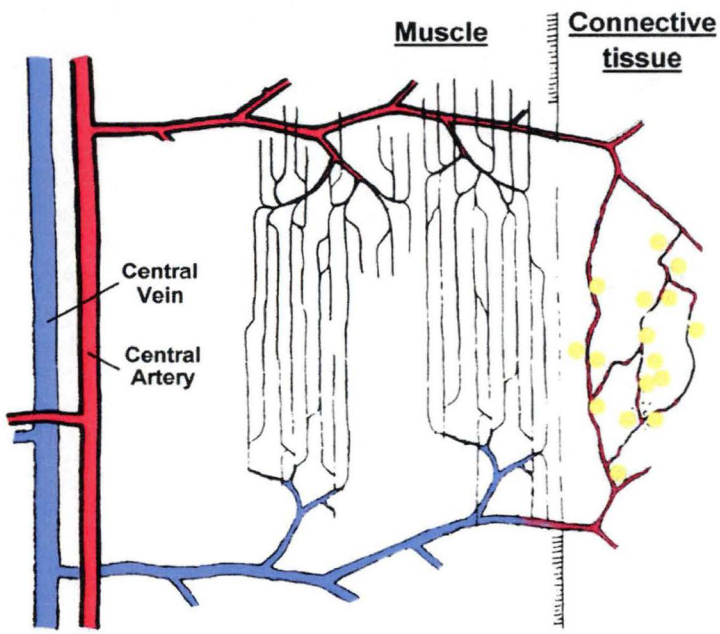

Figure 4: Schematic representation of the muscle vascular system.
Transverse arteriole supplies both capillaries of the nutritive route (irrigating the myocytes) and the non-nutritive route (in close association with the connective tissue of the skeletal muscle).
(Adapted from (Borgstrom 1988))

The nutritive route contains vessels that are considered to have extensive contact with the myocyte (Clark 1995). This network is composed of extremely tortuous capillaries that are evenly distributed inside the muscle, wrapping around the muscle fibre to allow efficient exchange. By providing a large surface area for optimal exchange within the muscle cells, the nutritive route allows exchange

between the blood and the muscle fibre. On the other hand, the non-nutritive route is more closely associated with the connective tissue of the perimysium and epimycium of the skeletal muscle, such as tendons (Newman 1997) and adipose tissue (Clerk 2000). Vessels composing this route are shorter, and possibly of slightly greater diameter (Vincent 2001) therefore giving this route a high capacitance with a low resistance. As this route irrigates cells with low metabolic activity, it is scarcely implicated in nutrient exchange. Several studies using different techniques have suggested that at rest non-nutritive flow is predominant (Clark 2000). Under insulin stimulation or exercise, there is a greater percentage of the nutritive capillaries perfused with the potential for increased delivery of nutrients, oxygen and hormone to the myocytes (Clark 2000, Clark 2006). This increased is called microvascular recruitment.

1.5.2.2 Microvascular Recruitment

The term microvascular recruitment is used to describe an increase in capillary surface area within the skeletal muscle, which leads to increased delivery of glucose and insulin to the myocytes. Insulin-mediated microvascular recruitment is a result of the vasodilatory action of insulin, largely NO-dependent (Scherrer 1994, Steinberg 1994, Vincent 2003), on the terminal arterioles controlling the access of blood and nutrients to the nutritive flow route. Changes in microvascular recruitment are independent of total blood flow and measurements of microvascular recruitment have been successfully assessed by many different techniques (Clark 2008), including 1-methylxanthine (1-MX) metabolism and contrast-enhanced ultrasound (CEU). These techniques have been pivotal in assessing the effect of insulin action on microvascular recruitment.

1.5.2.2.1 1-Methylxanthine Metabolism

The Hobart Muscle Research Group has demonstrated that insulin can increase microvascular recruitment (Rattigan 1997). The 1-MX technique is a biochemical assay for the measurement of capillary surface area due to increase

microvascular recruitment. Xanthine oxidase (XO) is an enzyme present at the luminal surface of capillaries and is practically absent from the bigger vessels (Jarasch 1986, Parks 1986). Perfused capillary surface area can be assessed by infusing 1-MX, a specific substrate of XO, into the blood stream. Increases in the capillary surface area will results in increase conversion of 1-MX to 1-methyluric (1-MU), which is independent of the total blood flow to the muscle (Rattigan 1997). Using the Fick principal (Zierler 1961), the amount of microvascular recruitment is determined by multiplying the arterio-venous difference by the arterial blood flow rate. 1-MX is an ideal substrate for measurement of microvascular recruitment as it is not vasoactive (Rattigan 1997) and does not affect metabolism (Rattigan 1997). Moreover, XO activity in the skeletal muscle does not change during acute treatment (Rattigan 1997, Rattigan 1997). Therefore, the 1-MX technique can be used to measure microvascular recruitment without adverse effects due to the 1-MX infusion.

The first direct evidence of insulin-mediated capillary recruitment was made by Rattigan and colleagues (Rattigan 1997), where they demonstrated that a 10 mU/min/kg insulin infusion was able to increase the 1-MX metabolism, and as such the microvascular recruitment. The dose of insulin used (10 mU/min/kg) in this study increased the total FBF. To ensure that the increase in 1-MX metabolism was not due to a macrovascular effect of insulin (i.e. total flow), the effects of epinephrine treatment was also determined. Epinephrine infusion was adjusted to produce an increase in total blood flow similar to insulin and it was found that the epinephrine-mediated increase in FBF was not associated with a rise in capillary perfusion (no change in 1-MX metabolism). Thus, it was concluded that insulin possesses a specific action on the microvascular recruitment that lead to increased delivery of blood to muscle. The physiology of the microvascular recruitment process was further assessed by Zhang and colleagues (Zhang 2004) where they found a dose-dependent effect of insulin infusion on capillary recruitment, total blood flow and muscle glucose uptake in the anaesthetised rat. It was noted that a low, physiological increase in insulin (~600 pmol/l) elicits an increase in capillary recruitment and glucose uptake, but not in total blood flow. This supported previous results indicating that glucose

uptake correlates well with microvascular recruitment but not with total blood flow (Rattigan 1999) demonstrating the physiological importance of the microvascular recruitment in the glucose disposal.

There are several limitations with the 1-MX technique. This technique requires an infusion protocol that leads to a constant concentration of 1-MX in the artery and requires a accurate measure of total blood flow to determine overall metabolism. Due to the volume of blood required for analysis it can only be used as an endpoint measurement in experimental animals. Furthermore, microvascular recruitment cannot be assessed in humans using the 1-MX technique, as the levels xanthine oxidase expression in human is far less than in rat (Rattigan 2005). Therefore, to circumvent these issues, a new technique to measured microvascular recruitment using contrast-enhanced ultrasound was developed.

1.5.2.2.2 Contrast-Enhanced Ultrasound Studies

Visualisation of the microvascular volume by contrast-enhanced ultrasound (CEU) is based on a technique initially develop for imaging the heart (Wei 1998). This technique involved a systemic infusion of phospholipids or albumin gas-filled microbubbles to provide contrast for the ultrasound detection. Microbubbles are imaged and destroyed using pulses of high mechanical index ultrasound from a transducer probe positioned over the tissue of interest (i.e. muscle of the hindleg). The intensity of the signal received from bursting the microbubbles is proportional to their concentration and is recorded as acoustic intensity (AI). By triggering the ultrasound pulses at different time intervals, the microbubbles can replenish the perfused vascular system between each pulse of ultrasound. At short ultrasound pulsing intervals (0-1 s) only the large rapidly filling vessels will be refilled while longer pulsing intervals (20-25 s) all vessels (arteries, arterioles, capillaries, venules and veins) that are carrying the blood flow will be replenished with microbubbles. Subtraction of the shorter time interval enables the measurement of the microvascular blood volume (Coggins

2001). The rate at which the capillary vessels fill may also be assessed and a measure of microvascular blood flow may be determined by multiplying the microvascular blood volume and microvascular fill rate.

Insulin-mediated increases in microvascular recruitment have been observed with the CEU technique (Coggins 2001, Vincent 2002, Vincent 2003, Zhang 2004). Direct comparison between 1-MX and CEU measurement during an hyperinsulinaemic clamp was made by Zhang and colleagues (Zhang 2004) as well as Dawson and colleagues (Dawson 2002). They were able to show that during the euglycaemic hyperinsulinaemic clamp using physiological doses of insulin (1.5, 3, and 10 mU/min/kg), similar proportional increases in microvascular recruitment were measured using both techniques. Furthermore, the microvascular recruitment required less insulin than enhancement of total blood flow. The data supports the notion that microvascular recruitment and total blood flow are controlled separately.

Another advantage of this technique is that CEU allows continuous measures of microvascular recruitment as opposed to the 1-MX method that can only be used to obtain endpoint measurement. CEU enables the time course of the microvascular recruitment and recruitment to be assessed in response to various stimuli. Increased microvascular recruitment was shown to be closely related to the rise in plasma insulin (Vincent 2006), and the insulin-mediated increase in capillary recruitment preceded insulin activation of the intracellular signalling pathway in the myocyte (Vincent 2004). Indeed, increases in muscle microvascular recruitment was noted after only 7 min of insulin infusion, while the increases in Akt phosphorylation and glucose uptake occur only after 30 min of infusion. This suggests that muscle metabolism is not fully responsible for the increase in perfusion during insulin stimulation. Furthermore, low, physiological 3 mU/min/kg insulin infusion was shown to elicit an increase in capillary recruitment and this effect precedes the increases in total blood flow by as much as 60-90 min (Vincent 2002). This was confirmed in human studies with a 1 mU/min/kg insulin infusion increasing microvascular recruitment by 20 min

prior to increases in forearm blood flow which occurred at 100 min (Eggleston 2007). These experiments imply that blood flow has been redistributed from perfused vessels into previously unperfused capillaries.

1.5.2.3 Microvascular Recruitment in Insulin Resistant State

Microvascular recruitment has been assessed in different rat models of type 2 diabetes. The obese Zucker rat, a genetic model of type 2 diabetes, has no insulin-mediated increase in microvascular recruitment and a blunting of the five-fold increase in insulin-mediated glucose uptake usually seen in their lean littermate (Wallis 2002). These observations are also true in the more severe model of type 2 diabetes, the Zucker Diabetic Fatty (ZDF) rat (Clerk 2007). During a euglycemic hyperinsulinaemic clamp, ZDF rats have a complete impairment of the insulin-mediated microvascular recruitment accompanied by a 60-70 % decrease in glucose utilisation. Interestingly, treatment with angiogensin-converting enzyme (ACE) inhibitor Quinapril reversed the impairment microvascular recruitment and partially restored the glucose utilisation. Considering this data, impairment of the microvascular recruitment is present in type 2 diabetes and may, along with myocyte insulin-resistance, be responsible for the decrease in insulin-mediated muscle glucose uptake

Impairment of the microvascular recruitment has also been observed in obese humans. In a study by Clerk and colleagues, microvascular recruitment of the forearm during a physiological insulin (1 mU/min/kg) clamp was assessed in both lean and obese patients (Clerk 2006). In lean subjects a 34 % increase in microvascular volume was observed, while there was no insulin-mediated change in the obese subjects. This microvascular dysfunction may affect the insulin-mediated glucose disposal by limiting the delivery of insulin and glucose to the skeletal muscle, thereby contributing to insulin resistance (Serne 1999, Serne 2001). These results are consistent with the data obtained in the skin capillaries of obese subject where impaired skin capillary recruitment, as well as

a decrease sensitivity of resistance vessels to insulin-induced endothelium dependent vasodilation, was observed during hyperinsulinemia (de Jongh 2004).

Evidence that the loss of insulin-mediated microvascular recruitment may precede and therefore be responsible for the skeletal muscle insulin resistance is also supported by results that show the effects of acute blockade of insulin-mediated microvascular recruitment. Infusion of intralipids (Clerk 2002), Tumor Necrosis Factor-α (TNF-α) (Youd 2000), α-methylserotonin (Rattigan 1999) and L-NAME (Vincent 2003) have all been shown to acutely block insulin-mediated microvascular recruitment. All of these infusions resulted in an approximate 50 % decrease of insulin-mediated skeletal muscle glucose uptake. Therefore, these data suggest that an impairment of insulin-mediated microvascular recruitment could very well be an initial stage of insulin resistance. It is noteworthy that both TNF-α and α-methylserotonin fail to affect the insulin-mediated glucose uptake in *in vitro* incubated muscle preparations (Nolte 1998, Rattigan 1999), suggesting that their effects are exclusively vascular.

1.5.2.4 Vasomotion

Vasomotion is defined as an oscillation of the vascular tone that is generated from the vascular wall itself (Nilsson 2003), which ensure distribution of blood within the different regions of the muscle. It is known that during rest, at any given time, about only a third of the muscle is actually perfused (Honig 1982). Therefore, vasomotion ensured that muscle is perfused sufficiently to sustain the prevailing metabolic demand and prevent hypoxia by periodically redistributing blood from one region of the muscle to another (Rucker 2000). Using mathematical analysis it was shown that vascular oscillation is comprised of five frequency components: heartbeat, respiratory, myogenic, neuronal and endothelial (Stefanovska 1999). Heartbeat, respiration and neuronal input oscillations are a result of separate and distal effects, and as such are not implicated in the "regional" vasomotion (or flowmotion). Flowmotion is a

consequence of the myogenic and endothelial inputs and may be affected locally by insulin.

Recently, it was reported that insulin influences vasomotion in the skeletal muscle (Newman 2009). Using Laser Doppler Flowmetry (LDF) to assess muscle vasomotion, insulin was shown to increase the total LDF signal, as well as the myogenic frequency component. When the same measurements were made in an acute model of insulin resistance (infused α-methylserotonin), effects of insulin on both total and myogenic frequency signals were blunted. This data gives support to the theory that insulin is able to act on the smooth muscle cell (responsible for the myogenic frequency) of the terminal arterial regulating the microvascular recruitment. Vascular dysfunction in insulin resistance may involve a specific loss of insulin to stimulate the vascular smooth muscle contribution to vasomotion/flowmotion in skeletal muscle.

1.5.2.5 Other Possible Impairments of the Microvasculature in Type 2 Diabetes

Others defects of the skeletal microvasculature could also be implicated in type 2 diabetes. These included a diminution in the number of capillaries and changes in the permeability of capillaries present inside the skeletal muscle. These two defects further emphasise the importance of the microvasculature in the type 2 diabetes.

1.5.2.5.1 Microvascular Rarefaction

A decrease in the actual number of vessels of the microcirculation is termed microvascular rarefaction. As is the case with impaired microvascular recruitment, microvascular rarefaction results in increase diffusion distance, therefore leading to decreased delivery of the nutrients and hormones to myocytes. While microvascular rarefaction has been observed in hypertension (Levy 2001, Serne 2001), it may also be present in the later stage of type 2

diabetes. Indeed, microvascular rarefaction was observed in the obese Zucker rat (Frisbee 2005) where there was a decrease in the microvessel density in gastrocnemius muscle of 15-17 weeks old Zucker rats. This rarefaction was only present when type 2 diabetes was apparent. In 6-7 weeks old Zucker rats where only insulin resistance was present, the microvascular density was unchanged. This is consistent with other studies where the capillary density is unchanged in the early stage of insulin resistance (Zou 2003, Fueger 2007). The relevance of the rarefaction hypothesis is also undermined by the fact that a minority of capillaries are functionally open at baseline (Honig 1982, Klitzman 1982), therefore mild rarefaction would not have much of an effect. Furthermore, Clerk and colleagues (Clerk 2007) did not detect significant rarefaction in a rat model of insulin resistance. Therefore, microvascular rarefaction may be a long-term consequence of the insulin resistance rather than a cause.

1.5.2.5.2 Capillaries Permeability

Trans-endothelial transport of insulin may also be implicated in the delivery of insulin to the muscle interstitium (Barrett 2009). Whether the movement of insulin through the endothelium is a passive or an active process is still a source of some controversy (King 1985, Steil 1996, Hamilton-Wessler 2002, Wang 2006). However, increase in vasopermeability to macromolecules of the skeletal muscle would result in an increase diffusion of the insulin to the interstitium, and therefore augment its effectiveness on the myocytes glucose uptake. Assessment of extravasation of albumin-bound Evans Blue in different models of insulin resistance was done to verify if impairment is present during insulin resistance. Extravasation of Evans Blue was shown to be decrease by 56 % after a 4 weeks high fructose feeding, compared to the ND (Chakir 1998). Interestingly, treatment with the insulin sensitiser Rosiglitazone has beneficial effect on the capillary permeability, with a ~40 % increase in extravasation of Evans Blue (St-Pierre 2004). However, it is not clear if change in permeability is a cause or a consequence of insulin resistance. Experiments in the obese Zucker rat showed a 30-50 % increased in capillary permeability when compared to their lean counterpart (St-Pierre 2006). This may therefore be an adaptive

mechanism compensating the loss of NO-dependent vasodilation and capillary recruitment noted in this model (Wallis 2002). Therefore, it is unlikely that capillary permeability is a key player in the initial stage of insulin resistance.

1.6 EXERCISE-MEDIATED METABOLIC AND HEMODYNAMIC EFFECTS

During exercise, turnover of ATP in skeletal muscle increases greatly, supported by metabolism of the glycogen and fatty acid stores, as well as enhanced utilisation of blood glucose. While relatively minor during the initial stage of contraction, contribution of blood glucose becomes more substantial as exercise continues and muscle glycogen stores are depleted. As with insulin, exercise-mediated glucose uptake involves the translocation of the GLUT-4 transporter to the plasma membrane and the T-Tubule (Roy 1996, Jessen 2005, Rose 2005). Interestingly, insulin- and exercise-mediated increases in glucose uptake are additive, meaning that they recruited distinct pools of GLUT4 transporter in the cells (Douen 1990).

To sustain the contraction, an increase in the delivery on nutrient and O_2 is required. Increase in microvascular recruitment occurs almost immediately after the initiation of contraction, preceding even the increase in total blood flow (Vincent 2006), and occurs at low intensities of muscle activity (Vincent 2006). The exact mechanisms responsible for the initial rise in blood flow are poorly understood, but appear to involve a local response from the capillaries themselves (Segal 2000) and/or from the mechanical stimulation of the contracting muscle, known as the muscle pump (Sheriff 1993). Thereafter, substance released from the contracting muscle, which included adenosine, potassium ions, acetylcholine, nitric oxide, and prostacyclin (reviewed in (Clifford 2004)), will induced a vasodilation of the feeding arteries, thus insuring a proper delivery of nutrient to sustain the contraction. The amplitude of the blood flow increase is proportional to the metabolic activity (Joyner 2007).

Exercise can be successfully used as a prevention treatment for development of obesity and TIID (Henriksen 2002, Anthony 2009) and to improve insulin sensitivity by ameliorating the vasodilatory dysfunction (De Filippis 2006). In insulin-resistant humans, insulin-stimulated skeletal muscle glucose transport has been shown to be improved in response to acute exercise (Minuk 1981, Hubinger 1987, Henriksen 2002) while both whole body and muscle glucose disposal are improved with aerobic exercise training (Hughes 1993, Dela 1995, Perseghin 1996, Henriksen 2002).

1.7 SUMMARY AND THESIS AIMS

The vascular actions of insulin, and more specifically its effects on microvascular recruitment, are an essential component of insulin's metabolic actions. In particular, the effect of insulin on skeletal muscle recruitment, which is responsible for ~50 % of insulin-mediated glucose disposal, is pertinent in assessing the progression of insulin resistance.

The work presented herein was therefore designed to investigate whether impairment in insulin's ability to increase microvascular recruitment is an early event in the pathogenesis of insulin resistance. Establishing this is important to understand the pathophysiology of insulin resistance. This thesis has used two different models of impaired recruitment and insulin resistance to investigate the progression of insulin resistance. Firstly, insulin-mediated microvascular recruitment was assessed for the first time, in a pre-diabetic model of insulin resistance, the 4 weeks high-fat diet fed rat. This model was used to determine changes in microvascular recruitment during the early stage of insulin resistance and its functional response to insulin and contraction. Secondly, partial blockage of skeletal muscle microvasculature with 15 μm diameter latex microspheres was used to occlude terminal arterials and enable determination of the effects of a decreased muscle microvascular recruitment on insulin sensitivity.

The aims of this thesis are:

1) To determine if an impairment in insulin-mediated microvascular recruitment is present in a pre-diabetic model of insulin resistance.
2) To assess the effect of contraction on muscle glucose uptake and microvascular recruitment in a pre-diabetic model of insulin-resistance
3) To develop a model of decreased microvascular recruitment using microsphere occlusion of the vasculature in order to evaluate the involvement of the microvasculature in insulin-mediated skeletal muscle glucose uptake *in vivo*.
4) To determine if a chronic reduction in insulin-mediated microvascular recruitment could be responsible for the insulin resistance in the myocyte observed in late stage of type 2 diabetes.

CHAPTER 2:

MATERIALS AND METHODS

2.1 ANIMAL CARE

All experiments were conducted on male Hooded Wistar rats reared in the University of Tasmania animal house. Animals were housed in a 12h light/dark cycle at a constant temperature of 21 ± 1 °C and allowed free access to water. For experiment requiring the determination of whole body glucose kinetics, rats were fasted. Food was removed around 5:00 PM on the evening before the study. All procedures were approved by the University of Tasmania Ethics Committee.

2.1.1 High-Fat Diet

A diet in high-fat content was purchase from Specialty Feeds (SF03-002, Glen Forrest, WA, Australia). Table 1 shows the comparison of the characteristics between the high-fat diet (HFD) with the chow routinely used in our facility (ND; Gibsons, Hobart). In the HFD, 60% of the energy comes from fat, consisting of mainly saturated and monounsaturated fat. The increase in the fat content was made at the expense of the carbohydrate content. The protein proportion was constant in both diets.

Table 1: Characteristics of the normal diet and the high-fat diet.

	Normal Diet		High-Fat Diet	
	% Total Energy	% Weight	% Total Energy	% Weight
Carbohydrate	71%	72%	26%	35%
Protein	19%	19%	14%	19%
Lipid	10%	5%	60%	36%
%SAT		21% Total lipid		60% Total lipid
%MONO		42% Total lipid		33% Total lipid
%POLY		37% Total lipid		7% Total lipid
Total	100%	96%	100%	90%

Sat: Saturated lipid, MONO: Monosaturated lipid, POLY: Polysaturated lipid.

The HFD was kept at 4 °C to prevent oxidation of the fatty acids and to ensure proper conservation. The diet contained all essential vitamins and nutrients.

For dietary intervention experiments, five week old male Hooded Wistar rats weighting approximately 110 grams were split into two groups. Each group was placed on a 4 week feeding of either the HFD or ND. All animal prior to the nutritional intervention received the ND.

2.2 *IN VIVO* EXPERIMENTS

2.2.1 Surgery

In vivo experiments were carried out in anaesthetized rats (50mg/100g body weight of pentobarbitone sodium) as shown in Figure 5. A 2 cm incision was made in the skin of the ventral side of the neck to allow access to the trachea and the neck vessels. A tracheotomy tube was inserted to facilitate spontaneous breathing during experiment. Polyethylene cannulas (PE60, Microtube Extrusions, North Rocks, NSW, Australia) were inserted in both jugular veins and secured using silk ligature (size 3/0 braided silk wax, Pearsalls Limited, England). The right jugular vein was used for the continuous infusion of pentobarbital and the left jugular was use to intravenously administer the various solutions required in the different experimental protocols. The right carotid artery was cannulated to monitor the arterial blood pressure using a pressure transducer (Transpac IV, Abbott Critical Systems, Morgan Hill, CA, USA), and was also used for arterial blood sampling.

The femoral vessels in both limbs were exposed via a small incision (~1.5 cm) in the overlaying skin. The epigastric vessels were then either ligated or used for the local injection of MS (see section 5.2.2 for more details). An ultrasonic probe (Transonic Systems, VB series 0.5 mm Ithaca, NY, USA) was positioned around the femoral artery just distal to the rectus abdominis muscle. The cavity

in the leg surrounding the probe was filled with lubrication jelly (H-R, Mohawk Medical Supply, Utica, NY, USA) to provide acoustic coupling to the probe. The probe was connected to the flow meter (Model T106 ultrasonic volume flow meter, Transonic systems, Ithaca, NY, USA). This was in turn interfaced with an IBM compatible PC computer that acquired the data (at sampling frequency of 100 Hz) for femoral blood flow, heart rate and blood pressure using WINDAQ data acquisition software (DATAQ Instruments, Akron, OH, USA). The surgical procedure generally lasted approximately 40 min. The animals were maintained under anaesthesia for the duration of the experiment using a continuous infusion of pentobarbital sodium (0.6 mg/min/kg). The femoral vein of the left leg was used for venous sampling, using an insulin syringe with an attached 29G needle (Becton Dickinson, USA). The body temperature of the animal was maintained at 35 °C using a water-jacketed platform and a heating lamp positioned above the rat.

For experiments exploring local effects, a second flow probe was positioned on the contralateral leg. Otherwise, only the right leg was assessed for total blood flow.

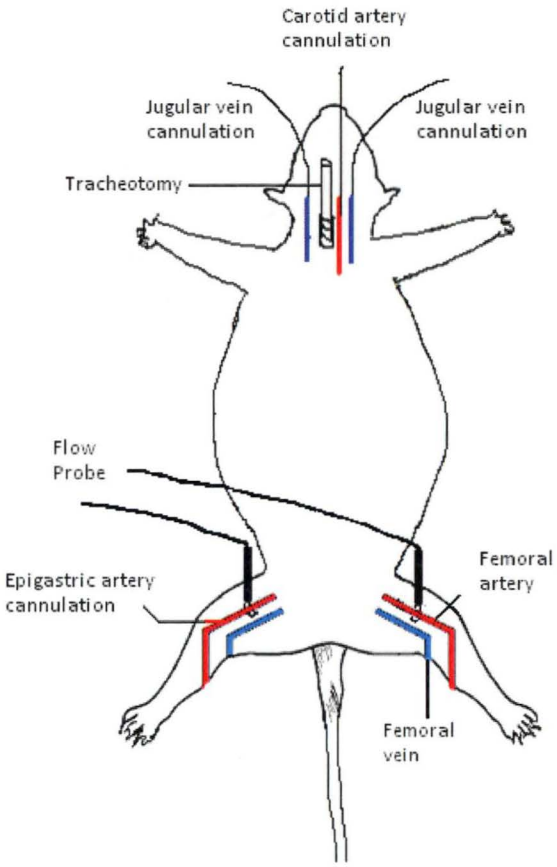

Figure 5: Schematic drawing of the *in vivo* surgery.
Surgery details are given in section 2.2.1. Briefly, the neck surgery involved the insertion of a tracheotomy tube to facilitate the spontaneous breathing and the cannulation of one carotid artery and both jugular veins to enable the blood sampling and the various intravenous infusions. The lower leg surgery involved the positioning of a Transonic flow probe around one or both of the femoral arteries to measure the femoral arterial blood pressure and, in the experiments requiring a local injection, the epigastric artery was cannulated. Diagram adapted from Mahajan *et al.* (Mahajan 2004).

2.2.2 Isoglycaemic Hyperinsulinaemic Clamp

Once the surgery was completed, a 60 min equilibration period was allowed so that leg blood flow and blood pressure could stabilise (Figure 6). Two arterial samples were taken at the end of equilibration and at regular intervals throughout the experimental procedure. Insulin (Humilin®, Lilly, USA) was

infused at a rate of 10 mU/min/kg of body weight during which blood glucose was maintained at isoglycaemia by infusion of a 30 % w/v solution of glucose. The insulin dose of 10 mU/min/kg of body weight was chosen to increase the insulinaemia to a high but physiological level. In control groups, saline infusion was matched to the volumes of insulin and glucose infused during the clamp.

At the end of the experiment, arterial and venous samples were collected (800 µl each). Blood glucose was measured on the arterial sample and plasma glucose was measured on both samples. Two 100 µl aliquot of each plasma sample were mixed with 20 µl of 2 M perchloric acid to precipitate proteins. Treated samples were later used to assess 1-methylxanthine (1-MX) concentration. Muscles from the right calf (soleus, plantaris, gastrocnemius red, gastrocnemius white, extensor digitorum longus and tibialis) were individually removed and immediately frozen in liquid nitrogen. Muscles were kept at -80 °C until assayed for 2-deoxyglucose (2-DG) uptake.

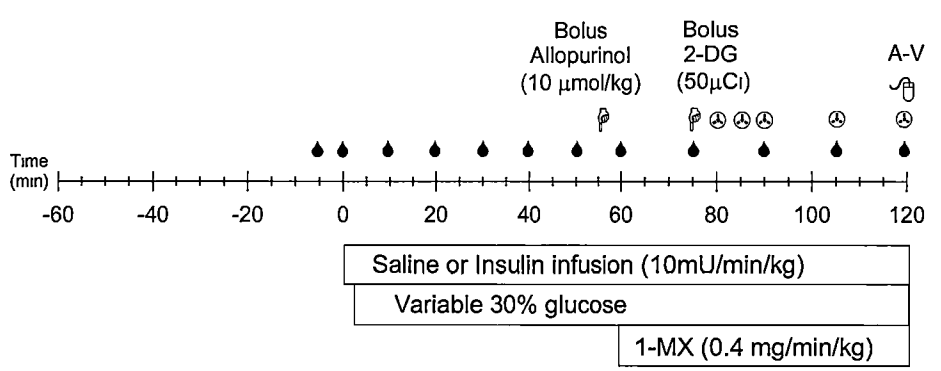

Figure 6: Isoglycaemic hyperinsulinaemic clamp.
Venous infusions are indicated by the bars. Bolus injections are shown by ℙ. Blood glucose was measured in arterial samples at the times indicated by ♦. Arterial samples for the determination of radioactivity are shown by ☮ and arterial and venous samples were collected for HPLC analysis at the time indicated by ☜.

2.2.3 Experimental Procedures

2.2.3.1 Analytical Methods

Blood and plasma glucose were determined using a glucose analyser by the glucose oxidase method (Model 2300 Stat plus, Yellow Springs Instruments, OH, USA). A sample of 25 µl was required for each determination. Enzyme immunoassay ELISA was used to assess the plasma level of insulin (Mercodia AB, Sweden) and TNF-α (Thermo Scientific, USA).

2.2.3.2 Hindlimb Glucose Uptake

To measure the glucose uptake across the lower hindlimb, glucose levels were determined in both arterial sample and venous sample from the femoral vessels, which drains blood from the lower leg. Hindlimb glucose uptake (HGU) was measure by the blood glucose arterio-venous difference multiplied by the femoral blood flow, and expressed as µmol/min.

2.2.3.3 2-Deoxyglucose Uptake

Muscle glucose uptake was measured using a modified version of the 2-deoxyglucose (2-DG) uptake technique (Kraegen 1985). Forty-five minutes before the completion of the experiment, a 200 µl bolus of 2-deoxy-d-[1-^{14}C]glucose (0.1mCi/ml, Sigma) was injected via of the jugular vein. Arterial samples were collected at 5, 10, 15, 30 and 45 min to determine plasma clearance of the radioactivity. The plasma samples (25 µl) were then added to 4 ml of Biodegradable Counting Scintillant-BCA (Amersham Pharmaca Biotech, IL, USA) and glucose radioactivity was determined using a scintillation counter (Perkin Elmer Inc, Tri-Carb 2800TR, IL, USA).

At the end of the experiments, calf muscles (soleus, plantaris, gastrocnemius red, gastrocnemius white, extensor digitorum longus and tibialis anterior) were collected and were immediately freeze-clamped using liquid nitrogen-cooled tongs. Muscles were kept at -80°C until assayed for 2-DG uptake.

The frozen muscles were ground under liquid nitrogen and 100 mg of muscle tissue was homogenized with 1.5 ml of water using a Heidolph™ silent crusher M (26000 RPM). Free and phosphorylated [^{14}C]2-DG were separated by ion exchange chromatography using an anion exchange resin (AG1-X8, Bio-Rad laboratories, CA, USA). Biodegradable Counting Scintillant (16 ml) was added to each radioactive sample and radioactivity determined using a scintillation counter (Perkin Elmer Inc, Tri-Carb 2800TR, IL, USA). From this measurement and knowledge of plasma glucose and the time course of plasma 2-DG disappearance, glucose uptake into the muscle (R'g) was calculated as previously described by others (Kraegen 1985) and expressed as μg/g/min. The R'g for the combined muscle was calculated from the sum of R'g of each individual muscle multiplied by the wet weight of the individual muscle and divided by the sum of each individual muscle wet weight.

2.2.3.4 Whole Body Glucose Kinetics (Ra & Rd)

To determine the glucose turnover (rate of appearance and rate of disappearance of glucose), a prime (2 μCi), continuous infusion of 3-[^{3}H]-D-glucose (0.1 μCi/min, specific activity of 16.6 Ci/nmol, Sigma) was administered along with the insulin/saline infusion. Arterial samples were taken 15 min prior to, and on completion of the experiment, centrigugated and the plasma removed. The plasma was then deproteinised using 2 M PCA, evaporated to dryness to remove $^{3}H_2O$ and re-suspended in distilled water. Biodegradable Counting Scintillant was added to each sample and [^{3}H] glucose radioactivity was determined using a scintillation counter. The rate of appearance (Ra) and disappearance (Rd) of glucose were calculated using the isotope dilution equation:

$$Ra + GIR = Rd = F/SA$$

Where:

GIR = glucose infusion rate

F = rate of tracer infusion

SA = specific activity of glucose, calculated by dividing the plasma radioactivity by the glucose concentration.

The hepatic glucose production (Ra) was then calculated by subtracting the glucose infusion rate from the Rd as previously described (Burnol 1983).

2.2.3.5 1-MX Metabolism

For the assessment of the microvascular recruitment, a biochemical assay using an intrinsic property of the capillary beds was used (Rattigan 1997). Xanthine oxidase (XO) is an enzyme present at the luminal surface of capillaries and is practically absent from the bigger vessels (Jarasch 1986, Parks 1986). Thus, by using an infusion of a specific substrate of XO, 1-methylxanthine (1-MX) (Sigma, USA), the perfused capillary surface area can be assessed. In perfused capillaries, 1-MX will be converted by XO to 1-methylurate (1-MU). An increase in the microvascular recruitment will result in an increase conversion of 1-MX to 1-MU. Therefore, the 1-MX disappearance will be proportional to the surface area perfused.

Since 1-MX clearance is very rapid, it was necessary to partially inhibit the XO activity to obtain a constant arterial 1-MX concentration. Therefore, a bolus dose of allopurinol (ALP, 10μmol/kg) was administered via the carotid artery 5 min prior to commencing the 1-MX infusion (0.4 mg/min/kg). This allowed a constant arterial concentration of approximately 15-25 μM of 1-MX to be maintained throughout the experiment.

Perchloric acid-treated plasma samples collected at the end of the experiment were centrifuged for 10 min. The supernatants were used to determine 1-MX, 1-1-MU and oxypurinol concentrations by reverse-phase high-performance liquid chromatography (HPLC) (using Gemini 5 μm C18, 255 x 4.6 mm column (Phenomenex, USA)) as described previously (Rattigan 1997). The 1-MX metabolism in nmol/min was calculated from the following equation:

$$\textbf{1-MXD} = ([\text{1-MX}]a - [\text{1-MX}]v) * 0.871 * \textbf{FBF}$$

Where [1-MX]*a* and [1-MX]*v* are the plasma 1-MX concentration (μmol/L) obtained from arterial and venous blood samples respectively, 0.871 is the factor to convert the 1-MX concentration measured in plasma to that in whole blood, FBF is the femoral blood flow rate (ml/min) measured at the end of the experiment.

2.2.3.6 Xanthine Oxidase Activity Assay

XO activity was assessed from muscle homogenates as described previously (Rattigan 2001). 400 mg of muscle were homogenised in the 2 ml of Homogenising buffer (50 mM Na_2HPO_4, 0.1 mM EDTA, 4 mM dithiothreitol and 0.5 mg/ml Trypsin Inhibitor at pH of 7.4). Samples were centrifuged at 50000 ***g*** at 10 °C for 30 min (Sorvall WX Ultra 90 centrifuge, Thermo Electron Corporation, USA). Proteins were separated on a PD-10 desalting column (Amersham Pharmacia Biotec, USA) and fractions of 1 ml were sequentially collected. Fraction #5 contained the proteins and was then used for the assay. A 100μl sample of the protein fraction #5 was added to 900 μl of Assay buffer (Homogenising buffer with 0.1 mM Xanthine). Mixes were incubated for an hour at 37 °C, after which the reaction were stopped by adding 250 μl of the assay mix to 50 μl of 2 M PCA. Uric acid contents were then measured by HPLC (using Gemini 5 μm C18, 255 x 4.6 mm column (Phenomenex, USA) with 50 mM $NH_4H_2PO_4$ buffer (pH 3.5) at a flow of 1.2 ml/min)). The protein content of each of the reaction solution was measured by the Bradford assay (Bio Rad, USA). Activity was expressed as amount of uric acid from per mg of protein per minutes.

2.2.3.7 Contrast-Enhanced Ultrasound

Contrast Enhanced Ultrasound (CEU) imaging of the muscle microvasculature is a recently developed technique adapted from its use in cardiovascular imaging (Wei 1998). Gas filled phospholipid microbubbles (see section 2.2.3.7.1) were infused intravenously into systemic circulation at a constant rate of 45 μl/min

and visualised using a linear array transducer/probe (L7-4) interfaced with an ultrasound system (HDI-5000; Phillips Ultrasound, USA). The probe was positioned over the left hindleg of the rat to allow imaging of the proximal adductor muscle groups (adductor magnus and semimembranosus) (Armstrong 1983). The microbubbles have a similar rheology to erythrocytes, enabling them to stay in the microvasculature and act as a marker of microvascular space (Lindner 2002). The microbubbles are echogenic and as they pass under the ultrasound beam, they can be simultaneously imaged and destroyed. The velocity at which the microvasculature fills and the amount of volume perfused can be measured by controlling the amount of time between pulses. The mechanical index, a measure of acoustic power, was set to 0.8. The acoustic focus was set at the mid portion of the muscles and the gain settings were optimised and maintained through each separate experiment. The pulsing intervals were set at 0.2, 0.3, 0.5, 1, 2, 3, 5, 8, 12, 15, 20 and 25 sec. At each pulsing interval, 3 frames were captured and the signal/intensity from these frames was averaged. The signal from the larger vessels and background were subtracted and the pulsing interval curve was constructed by plotting pulsing intervals time versus acoustic intensity (Figure 7).

At the conclusion of the experiment, the data is analysed using Qlab advanced quantification software (Phillips Medical Systems, Netherlands). A region of interest was selected to include only proximal adductor muscle groups. This software gives a measure of the received ultrasound signal (in decibels) in the selected region of interest. This value is then converted to acoustic intensity (AI) by the equation: AI = 10^(decibels/10). Thus, using these values, we are able to subtract the signal intensity from the larger vessels and the background image, from the signal of the smaller vessels to gain a true measure of microvascular perfusion. Smaller time interval (0.07-0.5 s) represent the microbubble fill time of the larger vessels, while the longer pulsing intervals (20-25 s) represent the microvasculature volume. Subtraction of the shorter time interval, where only the bigger vessel would have had time to refill after the acoustic burst, enable the measurement of only the microvascular space. The vascular volume and the rate of filling can be determined by using the following equation:

$$Y = A\ (1 - \exp^{-\beta t})$$

Y is the acoustic intensity (AI), A is the microvascular blood volume, β is the microvascular flow rate. Microvascular blood flow can be calculated by multiplying the microvascular blood volume by the microvascular flow rate (A* β).

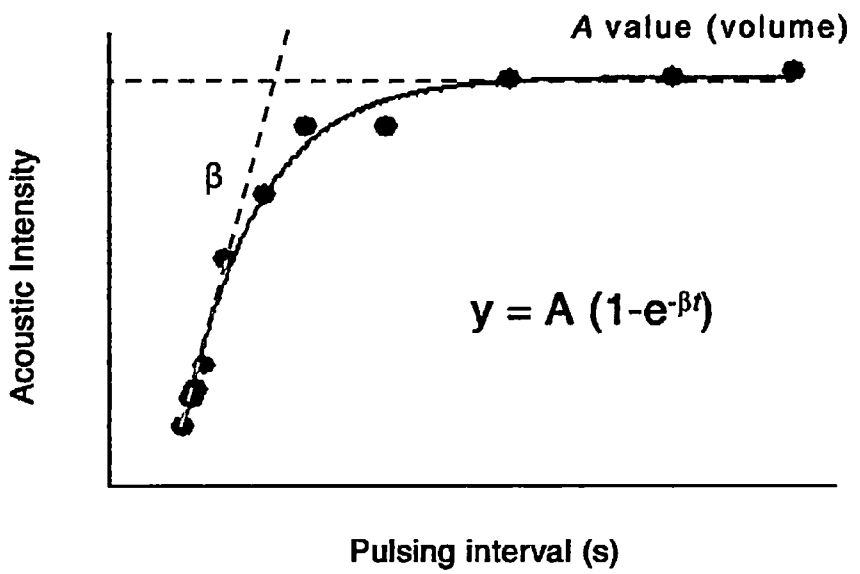

Figure 7: Microvascular blood volume and flow rate.
Once a pulsing interval curve has been constructed, the plateau position (A) represents a measure of microvascular blood volume, and the rate of increase (β) represents a measure of average filling rate of the microvasculature. By multiplying A and β, a measure of microvascular blood flow can be determined. Figure adapted from (Ross 2008).

2.2.3.7.1 Microbubbles Contrast Agents

The phospholipid microbubble solution was prepared in the laboratory.

Material per 100ml:
10.35 g Propylene glycol
12.62 g Glycerol
0.66 g NaCl
75 mg Lipid blend consisting of:

- 4.3 mg DPPA (1,2-dipalmitoyl-sn-glycero-3-phosphatidic acid, monosodium salt)
- 39 mg DPPC (1,2-dipalmitoyl-sn-glycero-3-phosphatidylcholine)
- 30.7 mg MPEG5000-DPPE (N-(methoxypholyethylene glycol 5000 carbomyl)- 1,2-dipalmitoyl-sn-glycero-3-phosphatidylanolamine, monosodium salt

The propylene glycol was heated in a 75 °C water bath in 200 ml beaker (covered with aluminium foil to prevent evaporation). The lipid blend was added to the propylene glycol when it has reached 75 °C (about 30 min). In a separate beaker, NaCl was dissolved in 60 ml of distilled water and added to glycerol before being heated to 75 °C. When dissolved, the lipid blend/propylene glycol was added to the NaCl/glycerol and dissolved in 75 °C water bath (about 60 min). The pH of the solution was adjusted to 6.5 using NaOH or HCl and filled to volume (100 ml) with distilled water. The solution was filtered through a sterilising filter (0.45μm) into sterile falcon tubes before 1.5 ml of solution was transferred into 5 ml vials. The head space was exchanged for octafluoropropane gas, the vials were sealed, and stored at 4 °C.

2.2.3.8 High-Energy Intermediates Determination by HPLC

Creatine compounds (Creatine and Creatine Phosphate) and adenine nucleotides (ATP, ADP, AMP) were determined by HPLC as previously described by Ye *et al.* (Ye 1996). Approximately 100 mg of muscle was added to 1.5 ml of ice cold 0.42 M of PCA. The samples were mixed by three quick vortex spin. Samples were then centrifugated for 5 min at 5000 RPM at 4 °C. One ml of the supernatant was removed and 220 μl of 1 M K_2CO_3 was added. Samples were kept on ice for 30 min to ensure the total neutralisation of the PCA. A final 5 min centrifugation at 5000 RPM was made to collect the supernatant, which was then used to measure the high-energy intermediates content by HPLC.

A Gemini 5 μm C18 column was used (Phenomenex, USA) for HPLC and peaks detected with ProStar 330 Photodiode Array Detector (Varian Analytical Instruments, USA). Compounds were eluted from the column using a

combination of two buffers, buffer A (174 mM of $NH_4H_2PO_4$, 1.76 mM of TBAHS) and buffer B (10% acetonitrile added to buffer A), in the following sequence:

- 0-3 min: 100% of buffer A
- 3-30 min: gradual increase of buffer B until it represented 80% of the buffer mix used at 30 min
- 30-40 min: 100% of buffer A.

Creatine compounds were detected by absorbance at 214 nm, and adenine based compounds by absorbance at 254 nm. Analysis of the peaks was done using the VarianStar programs suite (Varian Analytical Instruments, USA).

To measure the ratio of dry weight/wet weight, 100 mg of each muscle were dried in a 70 °C oven for 24 hours. The high-energy intermediates content was then expressed as μmol per gram of dry weight.

2.2.4 Hemodynamic Data Analysis

All data are expressed as means ± SEM. Mean arterial pressure, mean heart rate and mean femoral blood flow were calculated using five seconds sub-samples of WINDAQ data, which represented 501 flow and pressure measurements. These measurements were taken every 10 or 15 min during the experiment.

2.2.5 Statistical Analysis

Differences between basal and final values were assessed using a paired *t*-test. Comparisons were made between treatment groups over the course of the experiment using two-way repeated-measures ANOVA with Student-Newman-Keuls (SNK) *post hoc* test. The differences between treatment groups were examined using one-way ANOVA, repeated measures ANOVA or t-test as indicated in each chapter. All tests were performed using the SigmaStat statistical program (Systat Software Inc, CA, USA).

CHAPTER 3:

INSULIN-MEDIATED MICROVASCULAR RECRUITMENT IS IMPAIRED IN PRE-DIABETIC STATE

3.1 INTRODUCTION

The incidence of obesity and type 2 diabetes are on the rise in the western world (ABS 2008, ADA 2009, WHO 2009). Both pathologies are characterized by an impairment of insulin action (Jonk 2007). The skeletal muscle is an extremely important organ in insulin-mediated glucose disposal, as it accounts for about 80 % of the insulin-mediated glucose uptake after a meal (Defronzo 1988). In addition, muscle insulin resistance is a precursor to the hyperglycemia observed in patients with glucose intolerance or type 2 diabetes (Reaven 1988, Defronzo 1991) underscoring the contribution of the skeletal muscle to the insulin resistant phenotype. Therefore, skeletal muscle is a prime target for the early defects in the development of insulin resistance, although the exact mechanism remained largely unknown.

Nearly two decades ago, insulin was shown to possess vascular action during the euglycemic hyperinsulinaemic clamp (Laakso 1990). Since then, insulin was shown to increase the muscle microvascular recruitment (Rattigan 1997) and as such increase the delivery of hormones and nutrients to this tissue. Moreover, acute impairment of the vascular effect of insulin leads to a ~50% decrease in the insulin-mediated glucose disposal (Youd 2000). Studies have shown that insulin-mediated microvascular recruitment is impaired in type 2 diabetes (Wallis 2002) and obesity (Clerk 2006). What remains unknown is how the microvascular recruitment relates to the development of insulin resistance. Other groups have suggested that a defect in glucose delivery and/or transport is/are the major causes of dietary insulin resistance (Fueger 2007).

Animal models present a very interesting avenue to understand the pathogenesis of type 2 diabetes. Rodents can develop a state of insulin resistance and diabetes by many means: pharmacological intervention (Ziel 1988, Sato 1996, Roy 1998, Vincent 2003, Bradley 2006), genetic modifications (Araki 1994, Bruning 1997, Stenbit 1997, Kulkarni 1999, Mauvais-Jarvis 2000, Zisman 2000), and nutritional intervention (Kraegen 1986, Storlien 1991, Han 1997, Hansen 1998,

Kim 2000). When choosing a model, one must keep in mind how closely the pathogenesis resembles the human disease studied. Not only the phenotype must be as close as possible, but the induction process should be faithful to the human disease. In that context, nutritional intervention presents the most interesting method.

It has been known for years that a diet rich in fat, particularly in animal or saturated fat, can produce a state of insulin resistance (Masek 1959) and obesity over a prolonged period (Han 1997, Buettner 2007). The 4 week high-fat diet (HFD) fed rats has been repeatedly used in the literature as a pre-diabetic model of insulin resistance, characterized by a hyperinsulinemia with only mild changes in glucose homeostasis (Masek 1959, Kraegen 1986, Han 1997, Koshinaka 2004, Buettner 2007). HFD also induced an impairment of the insulin-mediated skeletal muscle glucose uptake (Han 1997) as well as an impairment of the insulin-mediated suppression of hepatic glucose output (Kraegen 1991). Furthermore, the HFD has been shown to induce vascular dysfunction within 1-2 weeks of the feeding (Youngren 2001, Kim 2008).

Thus, the aim of this study was to assess if the pre-diabetic state is characterized by an early impairment of the insulin-mediated microvascular recruitment. Such a decrease in nutrient and insulin delivery to the skeletal muscle may be responsible for the apparition of whole body insulin resistance in the later stage of type 2 diabetes.

3.2 MATERIALS AND METHODS

3.2.1 Animal Care

Hooded Wistar rats were raised as described in section 2.1. They were divided into two groups: one group received the normal diet (ND), while the other group

received the HFD. Table 1 shows the content of the different diets. Rats were fasted overnight before experimentation to enable the determination of whole body glucose kinetics as described in section 2.2.3.4.

3.2.2 *In vivo* Experiments

In vivo experiments were carried out in anaesthetised rats as described in section 2.2.1. Briefly, 1-hour after the surgery procedure, saline or insulin (10 mU/min/kg) was infused into the rat and continued for 2 hours (Figure 6). During experiments involving insulin infusion, a glucose solution (30 % w/v) was also infused at variable rates to maintain blood glucose levels around basal levels. Femoral artery blood flow (FBF) was continuously measured using a Transonic® flow probe positioned around the femoral artery of the right leg. 1-MX metabolism was used as an indicator of perfused capillary surface area as described in section 2.2.3.5. A bolus dose of [^{3}H]2-DG (50 μCi) was given 45 min before the end of the experiment. Calf muscles were excised at the completion of the experiment and freeze clamped in liquid nitrogen to assess the 2-DG uptake as described in section 2.2.3.3. Enzyme immunoassay ELISA was used to assess the plasma level of insulin (Mercodia AB, Sweden) and TNF-α (Thermo Scientific, USA).

3.2.3 Xanthine Oxidase Activity

Xanthine oxidase activity was assessed in muscle homogenates as described in section 2.2.3.6.

3.2.4 Data Analysis

All data are expressed as means ± SEM. Data were calculated as described in section 2.2.4. Differences between basal and final values were assessed using a paired *t*-test. Comparisons were made between treatment groups over the course of the experiment using two-way non-repeated or repeated-measures ANOVA

with Student-Newman-Keuls *post hoc* test as indicated in the figure legends. All tests were performed using the SigmaStat statistical program (Systat Software Inc, CA, USA)

3.3 RESULTS

3.3.1 Characteristics of the High-Fat Diet Fed Rats

Table 2 shows the characteristics of rats fed the ND or the HFD for 4 weeks. HFD fed animals showed an increase in total body mass and in epididymal adipose tissue mass, with a decrease in hindleg muscle mass (Table 2). As expected, HFD feeding induced a state of insulin resistance as seen by a significant increase in fasting plasma glucose (ND = 5.28 ± 0.14 mM vs. HFD = 5.91 ± 0.21 mM, $p<0.05$) and plasma insulin (ND = 66 ± 8 pmol/L vs. HFD = 112 ± 12 pmol/L, $p<0.01$). In the ND fed animal, plasma insulin levels were significantly higher after the insulin infusion (ND-Saline= 71 ± 12 pmol/l vs. ND-Insulin = 975 ± 81 pmol/l, $p<0.05$). Similarly, in the HFD fed animal, insulin was significantly increased following the insulin infusion (HFD-Saline= 114 ± 13 pmol/l vs. HFD-Insulin = 1280 ± 241 pmol/l, $p<0.05$). The magnitude of the increase in endpoint plasma insulin was similar in both diet groups (Figure 8).

Plasma TNF-α in samples from both groups were assayed but levels were below the detection range of the ELISA assay. Other studies have also failed to observe an increase in systemic level of TNF-α after 4 weeks of HFD feeding (Kim 2008, Chatterjee 2009).

Table 2: Characteristics of Normal Diet or High-Fat Diet Fed Rats.

	Normal Diet	High-Fat Diet
Body weight (g)	231 ± 1	241 ± 3 *
Epididymal fat pad (g)	0.92 ± 0.04	2.45 ± 0.16 **
Leg muscle mass (g)	2.04 ± 0.02	1.93 ± 0.03 **
Fasting plasma glucose (mmol/l)	5.28 ± 0.14	5.91 ± 0.21 *
Fasting plasma insulin (pmol/l)	66 ± 8	112 ± 12 **
Mean blood pressure (mmHg)	105 ± 2	107 ± 2
Heart rate (BPM)	336 ± 10	332 ± 8
Femoral blood flow (ml/min)	0.92 ± 0.04	0.87 ± 0.05

Data are means ± SE for n = 15-19 rats in each group. * $p<0.05$, ** $p<0.01$ vs. ND. Epididymal fat pad and leg muscles (Soleus, plantaris, grastrocnemius, EDL, tibialis) were removed from rats at the completion of the experiment. All other values were measured prior to the commencement of saline or insulin infusion.

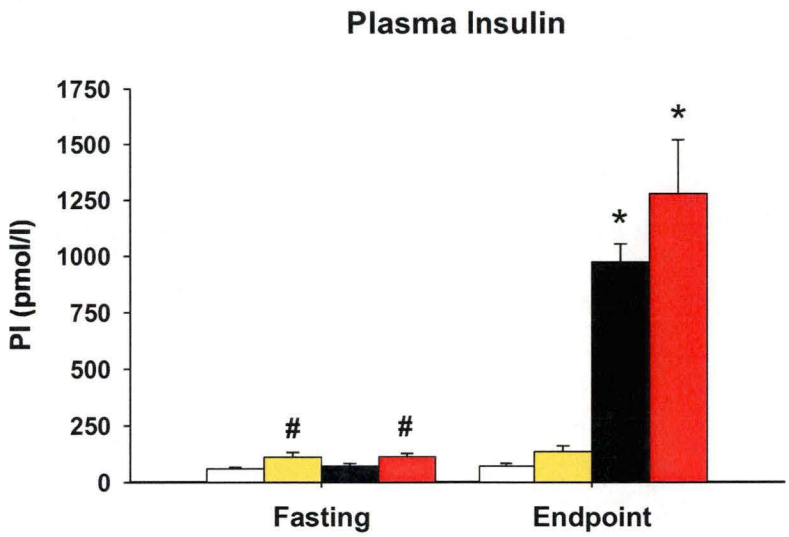

Figure 8: Plasma insulin before (Fasting) and at the completion of the experiment (Endpoint).
Data are means ± SEM for n = 6-10. * $p<0.05$ from saline of corresponding diet, # $p<0.05$ from ND.
□ ND-Saline, ■ HFD-Saline, ■ ND-Insulin, ■ HFD-Insulin.

3.3.2 Hemodynamic Parameters

HFD feeding had no effect on the basal blood pressure, heart rate or FBF (Table 2). Mean arterial pressure and heart rate were constant and unaffected by the different treatments (Figure 9). HFD fed rats had a significant impairment of the insulin-mediated increase in FBF (Figure 10). FBF in the ND was significantly increased from basal levels after 30 min of insulin infusion, while significant increases in FBF only occurred in the HFD animals after 50 min. Although a significant fold change in FBF still occurred with the HFD animals (Figure 10B) at the later stage of the insulin clamp, the increase was significantly less than in the ND (ND = 0.75 ± 0.06 ml/min vs. HFD = 0.43 ± 0.11 ml/min, $p<0.05$).

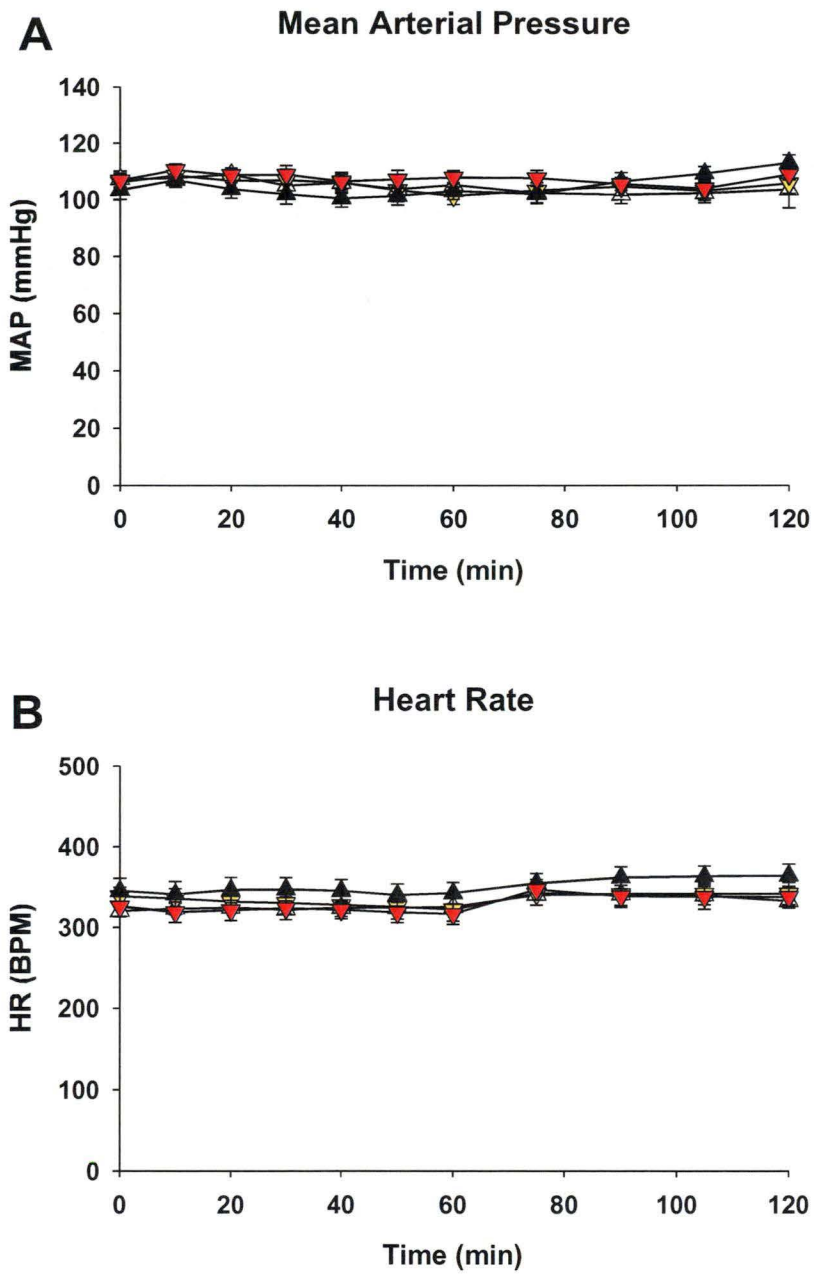

Figure 9: Mean arterial blood pressure and heart rate.
Time course for mean arterial pressure (A) and heart rate (B) as a result of a saline or insulin infusion in rats fed a ND or HFD for 4 weeks. Data are means ± SEM for n = 6-10.
Δ ND-Saline, ▲ ND-Insulin, ▼ HFD-Saline, ▼ HFD-Insulin

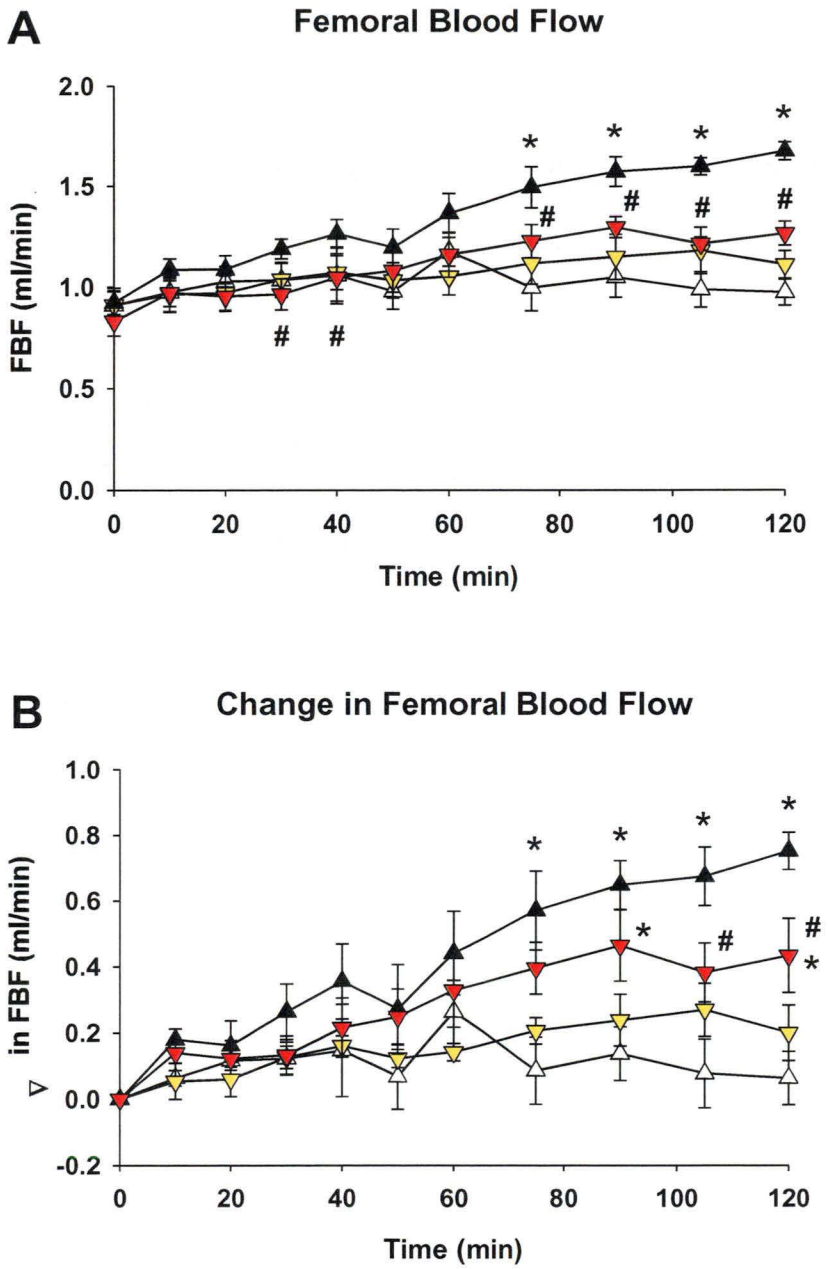

Figure 10: Femoral blood flow and change in femoral blood flow.
Time course for femoral blood flow (A) and change in femoral blood flow (B) as a result of a saline or insulin infusion in rats fed a ND or HFD for 4 weeks. Data are means ± SEM for n = 6-10. * $p<0.05$ from saline of corresponding diet, # $p<0.05$ from ND-insulin.
Δ ND-Saline, ▲ ND-Insulin, ▼ HFD-Saline, ▼ HFD-Insulin

3.3.3 Metabolic Parameters

Fasting blood glucose was significantly elevated in HFD fed rats compared to the ND and since the clamps were performed to maintain initial blood glucose levels, the blood glucose for the HFD animals were significantly higher at all times (Figure 11A). Whole body insulin sensitivity, reflected by the glucose infusion rate during the clamps, was significantly lower in HFD (Δ -31 % at 120 min, $p<0.01$) in comparison to ND (Figure 11B). Hindleg glucose uptake (Figure 12A) and 2-DG uptake (Figure 12B) was blunted with high-fat feeding (Δ -43 % $p<0.01$ and Δ -21 % $p=0.05$, respectively) and there was no fibre type preference to the impairment (Figure 13).

Assessment of the whole body glucose kinetics revealed that after a HFD insulin had blunted effects on both the decrease in Ra (ND-Insulin = 0.89 ± 0.51 mg/min/kg vs. HFD-Insulin = 2.83 ± 0.34, $p<0.01$) (Figure 14A) and the increase in Rd (ND-Insulin = 18.29 ± 1.22 mg/min/kg vs. HFD-Insulin = 14.37 ± 0.45, $p<0.01$) (Figure 14B). This is consistent with insulin resistance in both skeletal muscle and liver.

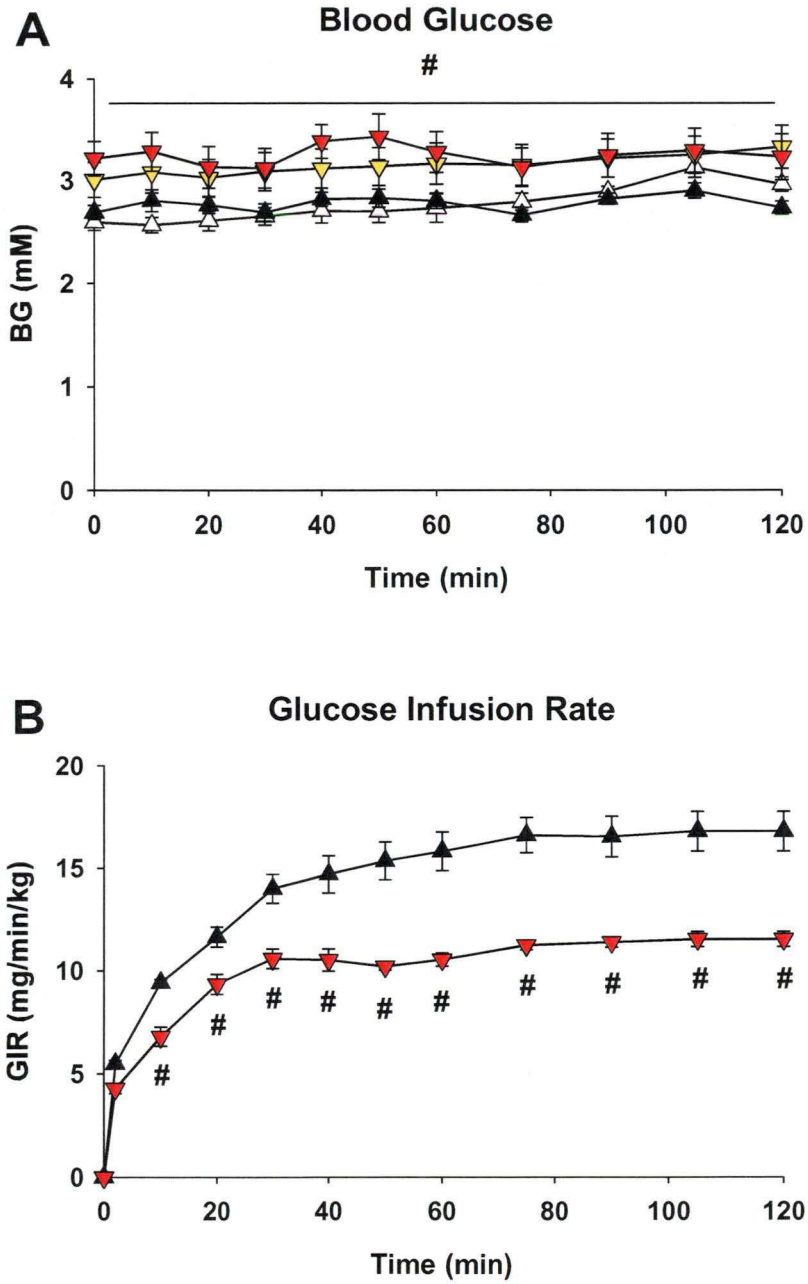

Figure 11: Blood glucose and glucose infusion rate.
Time course for the glucose infusion rate (A) and the blood glucose concentration (B) as a result of a saline or insulin infusion in rats fed a ND or HFD for 4 weeks. Blood glucose levels were maintained at basal level (time 0 min). Data are means ± SEM for n = 6-10. # $p<0.05$ from ND, two-way RM ANOVA with *post-hoc* analysis using SNK method.
Δ ND-Saline, ▲ ND-Insulin, ▼ HFD-Saline, ▼ HFD-Insulin

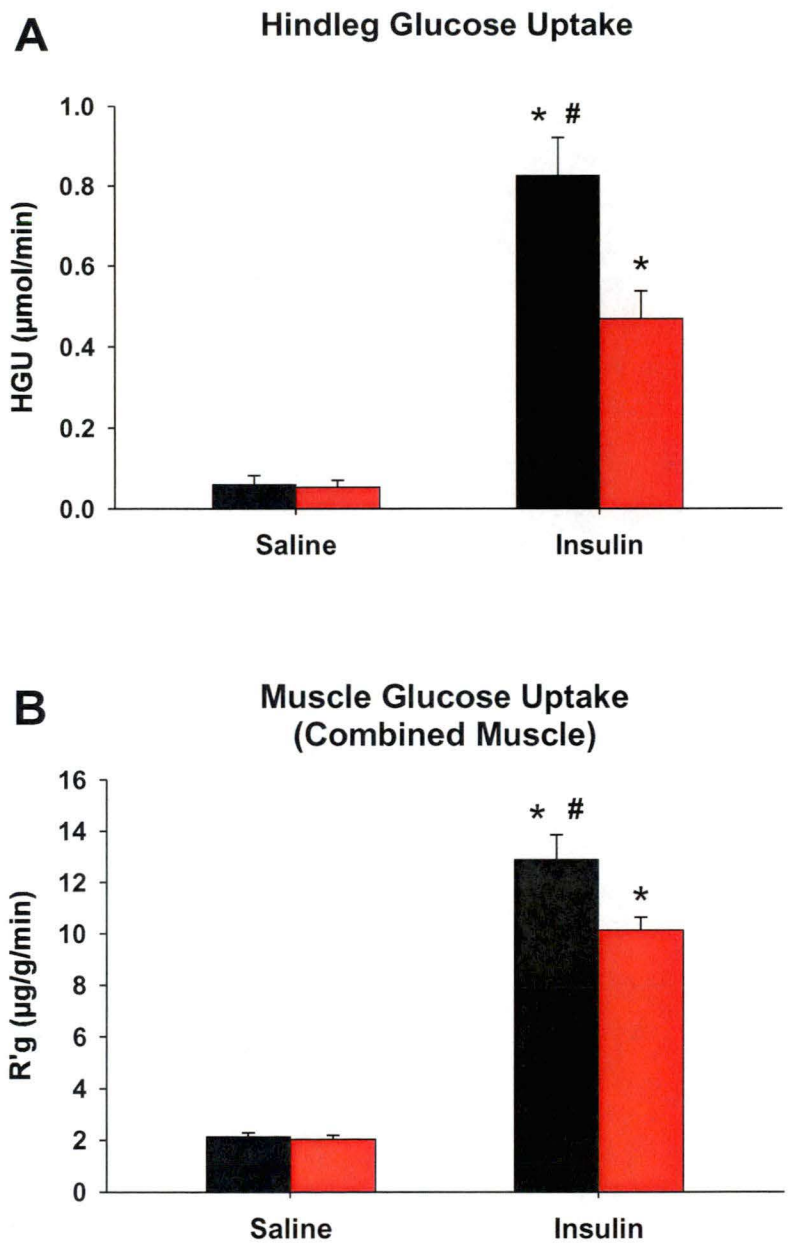

Figure 12: Hindleg glucose uptake and muscle 2-deoxy-glucose uptake. Hindleg glucose uptake (HGU) (A) and muscle radioactive 2-DG uptake (R'g) (B) for the combined calf muscle as a result of a saline or insulin infusion in rats fed a ND (■) or HFD (■) for 4 weeks. Data are means ± SEM for n = 6-10. * $p<0.05$ from saline of corresponding diet, # $p<0.05$ from ND-insulin, using two-way RM ANOVA with *post-hoc* analysis using SNK method.

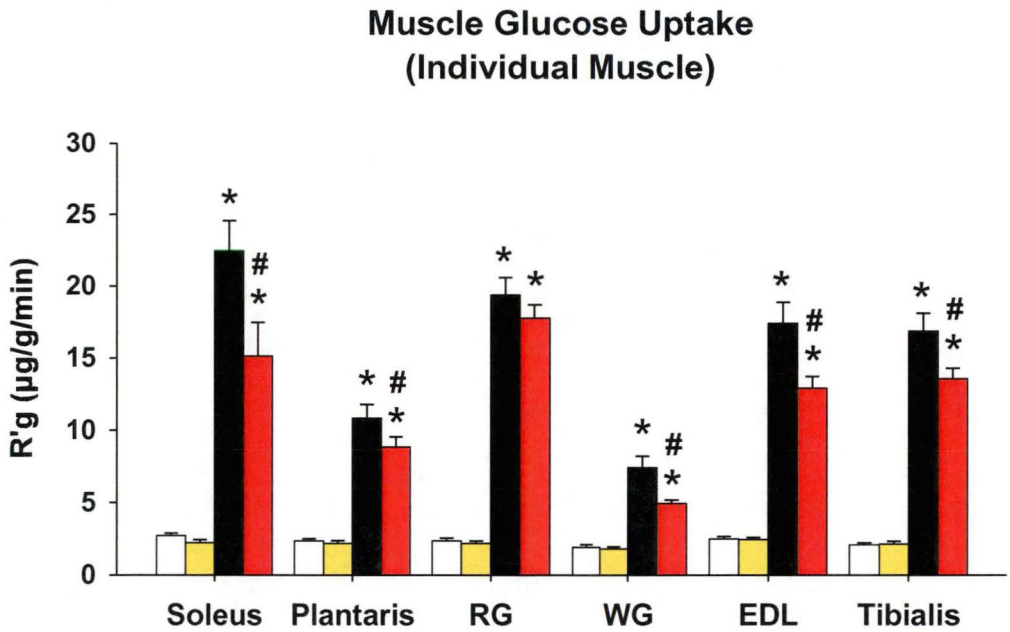

Figure 13: Muscle glucose uptake in individual muscles.
Muscle radioactive 2-DG uptake (R'g) for individual muscles of the lower leg as a result of a saline or insulin infusion in rats fed a ND or HFD for 4 weeks. Data are means ± SEM for n = 6-10. * $p<0.05$ from saline of corresponding diet, # $p<0.05$ from ND-insulin, using two-way RM ANOVA with *post-hoc* analysis using SNK method. (RG: red gastrocnemius, WG: white gastrocnemius, EDL: extensor digitorum longus)
□ ND-Saline, ■ HFD-Saline, ■ ND-Insulin, ■ HFD-Insulin.

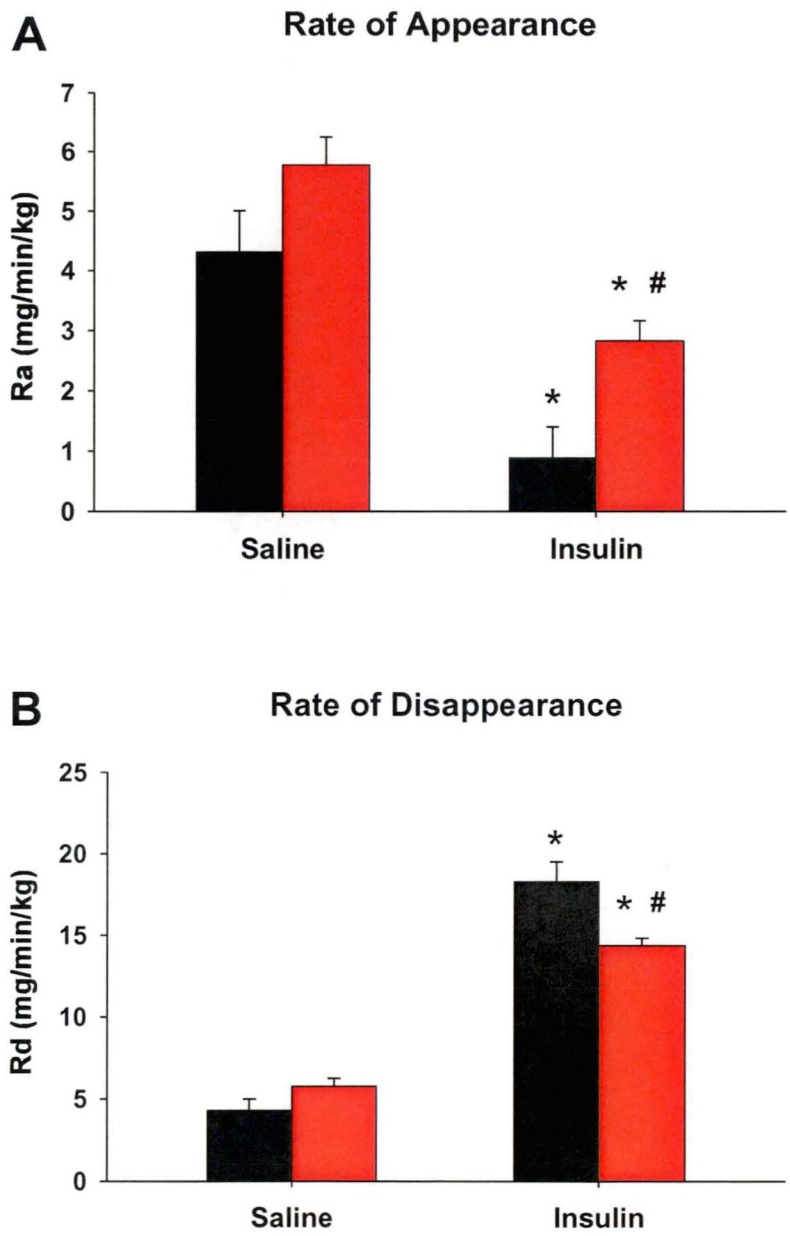

Figure 14: Rate of appearance and disappearance.
The rate of glucose appearance (hepatic glucose production (A)) and glucose disappearance (glucose uptake (B)) as a result of a saline or insulin infusion in rats fed a ND (■) or HFD (■) for 4 weeks. Data are means ± SEM for n = 6-10. * $p<0.05$ from saline of corresponding diet, # $p<0.05$ from ND-insulin, using two-way RM ANOVA with *post-hoc* analysis using SNK method.

3.3.4 Microvascular Recruitment

Arterial level of oxypurinol was similar in all groups (NS). Arterial 1-MX tended to be higher in the HFD fed rats, and this increase was significantly in the HFD-Insulin group (Figure 15A). ND fed rats had the expected insulin-mediated increase in microvascular recruitment (ND-Saline = 5.83 ± 0.69 nmol/min vs. ND-Insulin = 9.98 ± 0.78 nmol/min, $p<0.01$) while this effect of insulin was lost in the HFD fed rats (HFD-Saline = 5.76 ± 0.77 nmol/min vs. HFD-Insulin = 7.34 ± 0.98 nmol/min, $p=0.16$) (Figure 15B). Moreover, the insulin-mediated increase in the ND was significantly different from the level in the insulin clamp HFD rats (ND-Insulin = 9.98 ± 0.78 nmol/min vs. HFD-Insulin = 7.34 ± 0.98 nmol/min, $p<0.05$).

3.3.5 Xanthine Oxidase Activity

The level of xanthine oxidase activity measured in tissue homogenates from the calf muscles was unaffected by the HFD (ND = 45.5 ± 2.8, HFD = 46.9 ± 8.3 pmol/mg/min, $p=0.86$).

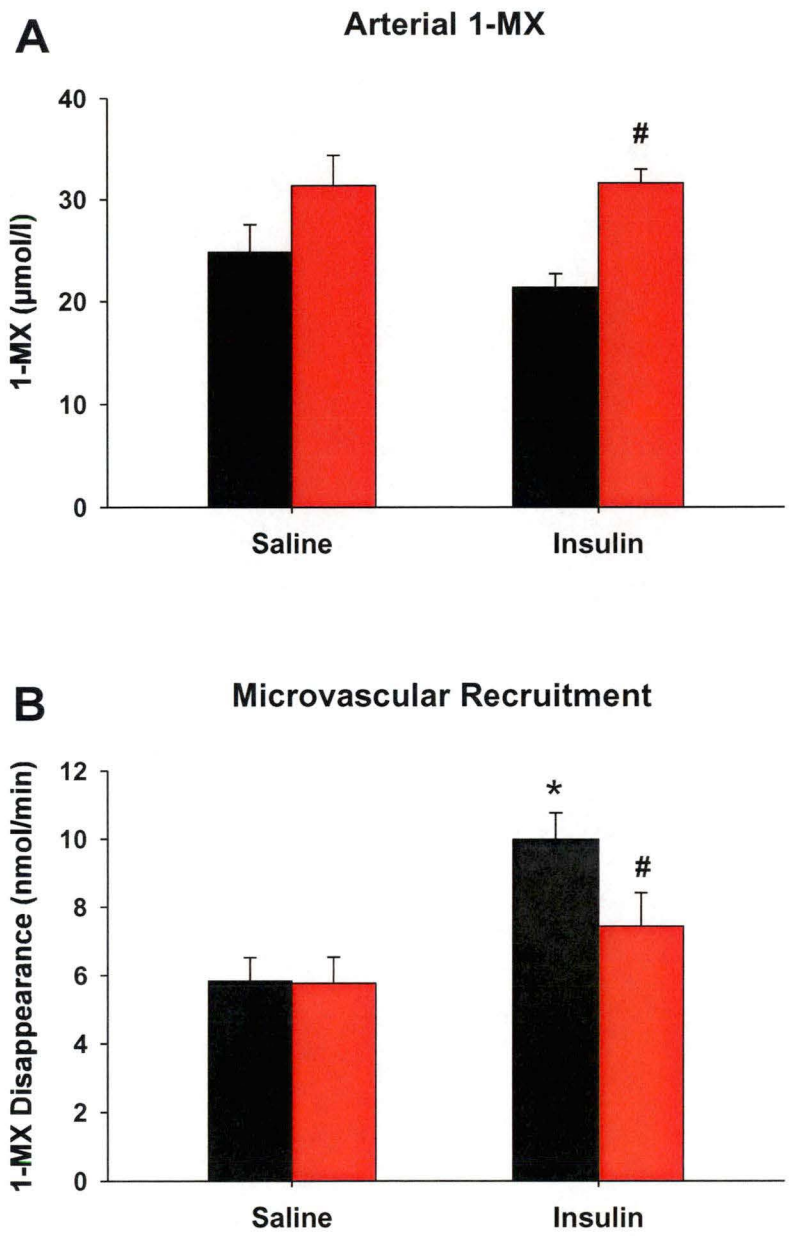

Figure 15: 1-MX arterial levels and disappearance.
Arterial level of 1-MX (A) and 1-MX metabolism (B) as a result of a saline or insulin infusion in rats fed a ND (■) or HFD (■) for 4 weeks. Data are means ± SEM for n = 6-10. * $p<0.05$ from saline of corresponding diet, # $p<0.05$ from ND-insulin, using two-way RM ANOVA with *post-hoc* analysis using SNK method.

3.4 DISCUSSION

The present study indicates that insulin-mediated microvascular recruitment is impaired in the pre-diabetic state and this is accompanied by a reduction in sensitivity to the insulin-mediated metabolic and macrovascular actions. These findings add important knowledge to the aetiology of the development of type 2 diabetes, as this is the first time that the microvascular recruitment has been implicated in the early stage of the development of insulin resistance. These data suggest that impaired insulin-mediated microvascular recruitment could be an early event that in due course, could worsen the muscle insulin resistance.

In the present study, the 4 week HFD induced a pre-diabetic state of insulin resistance, with a marked decrease in GIR (-31 %) associated with decrease hindleg (-21 %) and muscle specific (-43 %) glucose uptake. These results are consistent with other experiments using the HFD feeding model (Masek 1959, Kraegen 1986, Han 1997, Koshinaka 2004, Buettner 2007). The impairment of glucose metabolism was also accompanied with impairment of the vascular action of insulin on FBF and microvascular recruitment. The 4 weeks HFD has not only induced insulin resistance in the muscle, but also in the liver. Indeed, insulin inhibitory effect on the HGO is blunted following the high-fat diet. This is consistent with a previous study by Kraegen and colleagues, where 3 day of HFD feeding was shown to be sufficient to induced hepatic insulin resistance (Kraegen 1991).

The main finding of the present study is that the insulin-mediated microvascular recruitment was blocked with the HFD. As such, delivery of hormones and nutrients to muscle in response to insulin is impaired early in the progression of the disease. This impairment is likely to worsen the insulin resistance in the long term (Clark 2008) and agrees with studies suggesting that vascular insulin resistance precedes the peripheral insulin resistance (Youngren 2001, Kim 2008).

Two main hypotheses are present in the literature to explain the mechanisms leading to insulin resistance and ultimately to type 2 diabetes. The first states that an increase in circulating FFA is the culprit (Boden 2002). FFA will then accumulate in non-adipose tissues such as muscle and liver. At the molecular level, fatty acid interferes with the intracellular insulin signalling by increasing intracellular concentration of fatty acid metabolites, fatty acyl Co-A, ceramides and diacylglycerol (DAG) (Shulman 2000, Machann 2004, Summers 2006). Interestingly, this impairment of the insulin signalling is similar in skeletal muscle and endothelium (Kim 2005). In accordance with this theory, microvascular recruitment has been shown to be blunted with increase circulation FFA (Clerk 2002), due to a decrease in NO production (Steinberg 2000). Increase in FFA is unlikely to be the only signal responsible for the development of insulin resistance. Indeed, mice with adipocyte specific KO of GLUT-4 develops insulin resistance even though the circulating levels of FFA are decreased (Abel 2001).

Secondly, the vasocrine hypothesis (Yudkin 2005) states that the development of insulin resistance results from an increase secretion of cytokine by the adipose tissue, either by the adipocytes *per se* or by infiltrated macrophages (Hotamisligil 2006). TNF-α, an inflammatory cytokine, has been shown to be elevated in obesity and type 2 diabetes and to interfere with the insulin signalling. This cytokine is known to impair insulin-mediated NO production from eNOS (Valerio 2006), which has been shown to be implicated in the microvascular perfusion (Vincent 2003). The insulin resistance present with the HFD resembles the conditions observed during an acute infusion of TNF-α (Youd 2000). Indeed, similar responses to a 10 mU insulin infusion on the GIR, HGU, R'g, FBF and 1-MX disappearance were obtained. However, systemic levels of TNF-α after 4 weeks HFD were not elevated. This is not unexpected, as evidence from the literature place impairment of the vascular action of insulin before the increase in circulating inflammatory cytokine (Kim 2008 20791). Although not increased systemically, local increase in TNF-α may still be responsible for the impairment of capillary recruitment following a high-fat

feeding. Bakker and colleagues (Bakker 2009) recently showed that in db/db obese mice there is an increase in the size of the perivascular adipocytes of the feeding arteries. Adipocytes of bigger size have been shown to produce high level of TNF-α (Chatterjee 2009) that could affect the response to insulin at the level of feeding and terminal arterioles. Therefore, a paracrine secretion might prevent the insulin-mediated microvascular recruitment without a remarkable increase in systemic level. TNF-α infusion was shown impair insulin-mediated FBF (Youd 2000). However, this was not the case with the HFD model. This would also support a paracrine secretion, as local TNF-α would not be able to act on the total blood flow to the leg.

A recent study has shown that the muscle xanthine oxidase protein levels are increased after 10 weeks of high-fat feeding (Erdei 2006). Since the assessment of microvascular recruitment by the 1-MX technique relies on the activity of the xanthine oxidase, it was important to verify the activity in the present model. Xanthine oxidase activity was identical in both groups. Furthermore, an increase in the xanthine oxidase activity would have resulted in a decrease arterial level of 1-MX, which is not the case in the 4 week HFD. Another indication of preserved activity in the HFD is the level of 1-MX disappearance in the basal state. As 1-MX disappearance in the saline infusion groups was not different, it is also supportive of similar level of xanthine oxidase activity. Therefore, as the level of xanthine oxidase in muscle was not affected by the 4 week HFD, the use of the 1-MX technique was justified in these experiments. Explanation for the difference in xanthine oxidase activity may relate to the feeding time (10 weeks vs. 4 weeks) and/or type of fat composing the diet. Furthermore, 10 week HFD fed animals showed an increase in pressure, which was not the case in the 4 week HFD.

Another factor that could have influenced the 1-MX disappearance is a change in the capillary density. Although not investigated in the present study, previous studies have shown that the capillary density is unchanged following a HFD

(Zou 2003, Fueger 2007). Furthermore, as the 1-MX disappearance during the saline infusion does not present any change following the HFD, it is unlikely that the impairment in microvascular recruitment could be explained by a decrease in the number of capillaries. Thus, it is unlikely the insulin-mediated capillary recruitment impairment is due to any anatomical change by the dietary intervention.

In summary, insulin-mediated microvascular recruitment is impaired in a pre-diabetic model of insulin resistance. This finding may be important in linking the impairment of nutrient and insulin delivery and the development of insulin resistance. It places the defects in vascular action of insulin as an early event in the aetiology of type 2 diabetes. By preventing the access of glucose and insulin to the myocyte, this may contribute to the myocytes insulin resistance.

CHAPTER 4: CONTRACTION-MEDIATED EFFECTS ON MICROVASCULAR RECRUITMENT IN THE PRE-DIABETIC STATE

4.1 INTRODUCTION

Muscle contraction is another physiological process that regulates glucose uptake (Hayashi 1997). The mechanisms by which exercise and insulin increase glucose disposal are independent of each other and, interestingly, both are additive (Kennedy 1999). Moreover, contraction has been show to increase glucose uptake in models of insulin resistance and type 2 diabetes (Wallberg-Henriksson 1984, Kennedy 1999, Wallis 2002). As exercise has long been the cornerstone in the management of diabetes (Weltman 2009), a better understanding of the mechanism involved in exercise-mediated glucose disposal may lead to improved treatment of this disease.

For more than a decade studies have shown the physiological importance of microvascular recruitment in both insulin- and contraction-mediated glucose uptake (Dawson 2002, Rattigan 2005). Microvascular recruitment can be measured using different techniques, the most frequently used are the 1-MX technique and contrast-enhanced ultrasound (CEU) (Clark 2008). Using these techniques it was shown that insulin-mediated microvascular recruitment is impaired in type 2 diabetes (Wallis 2002, Clerk 2006, Clerk 2007). However, contraction-mediated microvascular recruitment may or may not be impaired in type 2 diabetes. In one animal model, the obese Zucker rat, contraction-mediated microvascular recruitment responses are preserved as assessed by the 1-MX technique (Wheatley 2004). Studies of the microvascular response to exercise in humans are not consistent. Experiments using CEU have shown that exercise-mediated microvascular perfusion is unaffected in type 2 diabetes patients (Womack 2009). In contrast, a slight level of impairment of the microvascular perfusion during submaximal exercise was observed in type 2 diabetes patients using estimated microvascular blood flow kinetics (Qm) (Bauer 2007). It is not clear whether the inconsistencies are related to difference in exercise intensity or the techniques used to measure microvascular recruitment. Therefore, assessment of microvascular recruitment in the same model of insulin resistance

using varying intensities of contraction as well as different techniques to measure microvascular recruitment could help explained these inconsistencies.

The aims of the present study were to assess in a pre-diabetic model of insulin resistance: 1) the effect of contraction on muscle glucose uptake and microvascular recruitment, 2) directly compare two microvascular recruitment measurement techniques (1-MX and CEU) during contraction.

4.2 MATERIALS AND METHODS

4.2.1 Animal Care

Hooded Wistar rats were raised as described in section 2.1. They were divided into two groups: one group received the normal diet (ND), while the other group received the high-fat diet (HFD).

4.2.2 *In vivo* Surgery

In vivo surgery was carried out in anaesthetised rats as described in section 2.2.1. For the contraction studies, an incision was made through the skin at the lateral side of the hip. Electrodes were attached to the muscle of the hindleg and the Achilles tendon (using a curved needle to pierce the skin of the ankle). The foot was secured to minimise movement. Twitch stimulation was performed with 0.1 ms pulses of 30 V current. Animals were subject to contractions at 0.05, 0.1 and 2 Hz in 15 min stepwise increments. The contralateral leg was used for comparison.

Three different experimental protocols were used to evaluate the effect of HFD feeding on muscle contraction (Figure 16, Figure 17 and Figure 19).

4.2.2.1 Contraction Protocol #1: Force Development and Glucose Uptake

This protocol was designed to assess the effect of contraction on muscle glucose uptake in the HFD fed model (Figure 16). The contractile force developed by the soleus, plantaris and gastrocnemius muscle group during each frequency was measured by a Harvard Apparatus isometric transducer. The right leg was stabilised in a jig with a pin securing the knee to prevent any movement. A hooked wire was placed around the Achilles tendon. This hook was attached to the isometric transducer, which was interfaced to a computer to allow continuous measure of force development via the WINDAQ software program. Voltage across the leg was measured using an oscilloscope (Model BWD 506, BWD Electronics, Victoria, Australia).

Glucose uptake following the 2 Hz contraction was measured using the 10 min 2-DG uptake method (Ross 2007). A bolus of 50 µl 2-deoxy-d-[2,6-^{3}H]glucose (1 mCi/ml, Sigma) was injected 10 min before the end of the experiment. Immediately after this bolus injection, arterial blood was continuously withdrawn at a rate of 50 µl/min over 10 min. This blood sample was used to measure the plasma concentrations of 2-DG. At the end of the protocol, the leg was rapidly skinned and the calf muscles were freeze-clamped *in situ* using liquid nitrogen cooled tongs. After 5 s, the frozen calf was excised from the surrounding tissue and placed in liquid nitrogen. Muscle samples were stored at -80 °C. Ion-exchange chromatography was used to determine 2-DG uptake, as described in section 2.2.3.3.

Of note, high-fat feeding has previously been shown to increase blood coagulation (Olsen 2002). To ensure a continuous arterial withdraw during the 10 min sampling, a 250 U heparin bolus was arterially injected 5 min prior to the arterial withdrawal (Figure 16). Furthermore, frequency of contraction was used instead of force of contraction as the later could be altered with voltage, but this

changes the amount of contracting fibres that are recruited. By keeping the voltage/force constant this variable is removed.

4.2.2.1.1 High-Energy Intermediates Determination

High-energy intermediates were extracted from powdered muscle as describe in section 2.2.3.7. All the high-energy phosphates intermediates are expressed as µmol/g of wet weight.

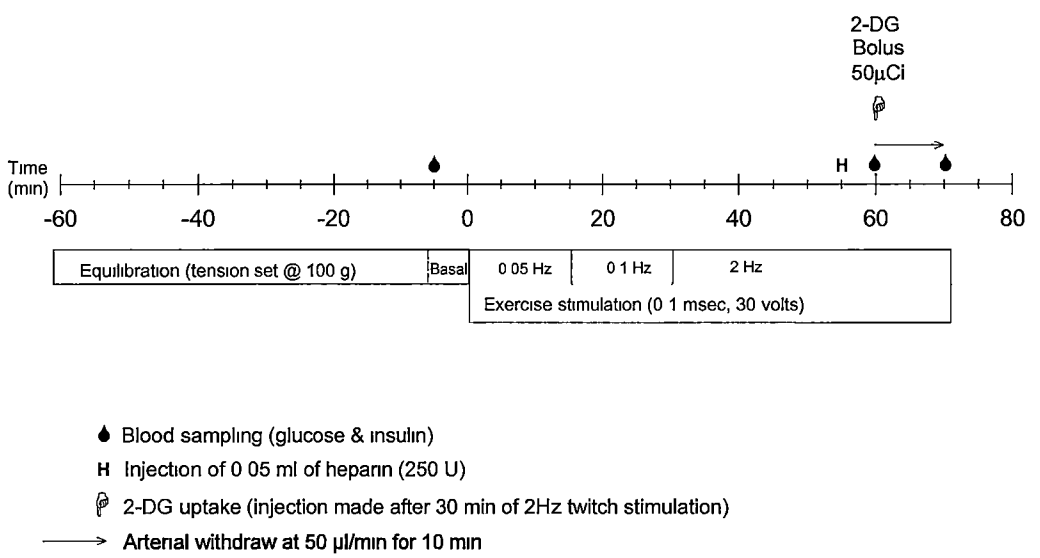

Figure 16: Contraction protocol #1: Force development and glucose uptake. Contraction treatments are indicated by the bars. Bolus injection is shown by ☟. Blood glucose was measured in arterial samples at the times indicated by ♦. Arterial sampling for the determination of radioactivity is indicated by the arrow.

4.2.2.2 Contraction Protocol #2: Capillary Surface Area Perfusion

The second protocol was designed to measure the effect of contraction on perfused capillary surface area in the HFD fed model (Figure 17). 1-MX was continuously infused for 60 min, during which a stepwise increase in contraction frequency was applied. Femoral artery blood flow in both legs was measured

using a Transonic® flow probe positioned around each femoral artery. At the completion of the experiment three blood samples were taken, one arterial and one venous from each femoral vein. Plasma glucose was measured on each sample to allow the calculation of hindleg glucose uptake, as describe in 2.2.3.2. The concentrations of 1-MX, 1-MU and OXY were determined from PCA treated plasma samples by HPLC as described in section 2.2.3.5.

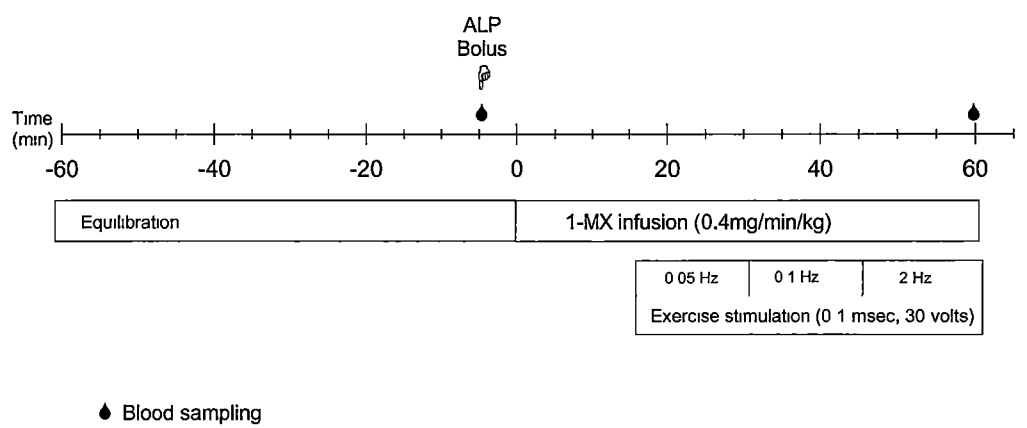

Figure 17: Contraction protocol #2: Capillary surface area perfusion. Contraction treatments and 1-MX infusion are indicated by the bars. Bolus injection is shown by ℙ. Blood glucose was measured in arterial samples at the times indicated by ♦.

4.2.2.3 Contraction Protocol #3: Microvascular Volume

In the third procedure, contrast-enhanced ultrasound (CEU) was used to assess the microvascular volume as describe in section 2.2.3.7. Linear-array transducer/probe (L7-4) was placed on the shaved left leg to allow the imagining of the hindleg muscle. Initial trials have determined that the dose curve of acoustic intensity as function of microbubble concentration was identical in both diets (Figure 18).

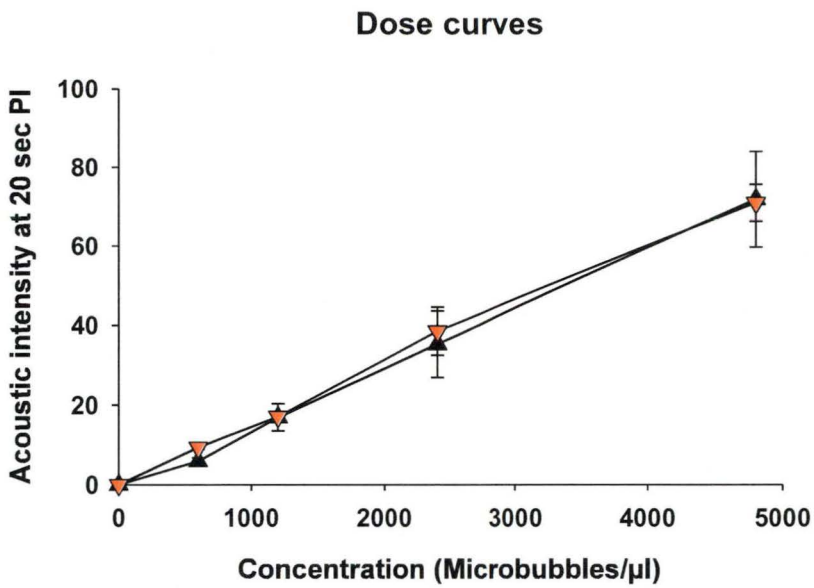

Figure 18: Plot of acoustic intensity as a function of microbubble (MB) concentration.
Increasing dilutions of microbubbles were infused at a rate of 45 µl/min into rats fed either the ND (▲) or the HFD (▼) and the acoustic intensity at a pulsing interval of 20 sec recorded. Data are means ± SEM for n = 2-4.

Animals were electrically stimulated (contraction) for 5 min at each frequency before the ultrasound imaging was initiated. Each PI curve required 10 min of imaging during contraction. PI curves, AI vs. ultrasound pulsing interval (ranging for 0.2-25 seconds) was used to determine the microvascular blood volume (A value), microvascular fill rate (β value) and the microvascular blood flow (A*β) (see Figure 7). Background subtraction was made by using the 0.5 sec frames for 0.05 and 0.1 Hz, and 0.2 sec frames for 2 Hz. This enabled the assessment of only the microvasculature, as the 0.2/0.5 sec background subtraction will remove the signal from larger vessels.

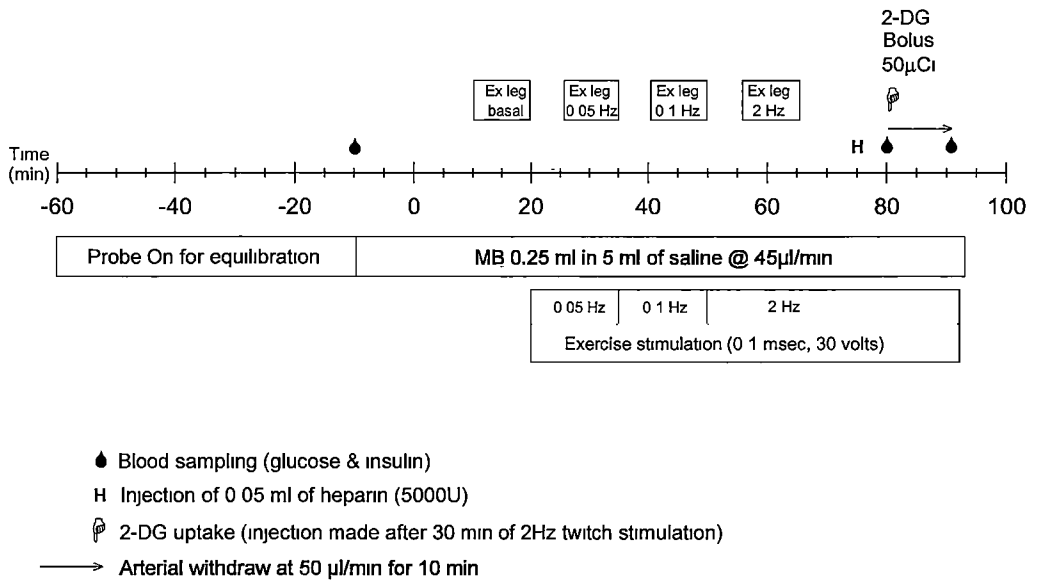

Figure 19: Contraction protocol #3: Microvascular volume.
Contraction treatments and microbubble (MB) infusion are indicated by the bars under the timeline. CEU measurements are indicated by the boxes on top of the timeline. Bolus injection is shown by ☞. Blood glucose was measured from arterial samples at the times indicated by ♦. Arterial sampling for the determination of radioactivity is indicated by the arrow.

4.2.3 Data Analysis

All data are expressed as means ± SEM. Data were calculated as described in section 2.2.4. Comparisons between basal value for each diet, and differences between basal and final values were assessed using a paired *t*-test, unless stated otherwise in the figure legend. Comparisons were made between treatment groups over the course of the experiment using two-way repeated-measures ANOVA with Student-Newman-Keuls *post hoc* test as mentioned in the corresponding figure legend. All tests were performed using the SigmaStat statistical program (Systat Software Inc, CA, USA).

4.3 RESULTS

4.3.1 Characteristics of the High-Fat Diet Fed Rats

Table 3 summarises the difference between the ND and the HFD fed subgroups for body weight, epididymal fat pad weight, and plasma glucose and insulin. Duplicate plasma measurements were taken at the end of the contraction period. As seen in chapter 3, HFD rats developed a pre-diabetic state of insulin resistance. HFD feeding resulted in increase body weight, larger epididymal fat pads, higher plasma glucose and plasma insulin in compared with the ND.

Following contraction, the ND rats had a significant increase in plasma glucose (Fasting = 5.22 ± 0.13 mmol/l vs. Endpoint = 5.75 ± 0.16 mmol/l, $p<0.05$) (Table 3). This can be explained by feed-forward regulation of hepatic glucose production occurring during exercise (Sonne 1985, Suh 2007). Interestingly, this hepatic feed-forward mechanism was absent in the HFD groups, where there was no significant difference in plasma glucose before and after contraction.

Table 3: Characteristics of rats fed normal diet or high-fat diet for 4 weeks used for the contraction protocols.

	Normal Diet	High-Fat Diet
Body weight (g)	235 ± 2	243 ± 3 *
Epididymal fat pad (g)	1.05 ± 0.04	2.15 ± 0.15 **
Fasting plasma glucose (mmol/l)	5.22 ± 0.13	6.27 ± 0.14 **
Fasting plasma insulin (pmol/l)	61 ± 7	154 ± 18 **
Endpoint (2Hz) plasma glucose (mmol/l)	5.75 ± 0.16 #	6.45 ± 0.17 **
Endpoint (2Hz) plasma insulin (pmol/l)	83 ± 10	180 ± 18 **

Data are means ± SE for n = 18-23 rats in each group. * $p<0.05$ and ** $p<0.01$ vs. ND, # $p<0.05$ vs. fasting level, paired student *t-test*. Epididymal fat pads were removed from rats at the completion of each experiment.

4.3.2 Contraction Protocol #1: Force Development and Glucose Uptake

4.3.2.1 Evaluation of the Contraction in the HFD

The voltage during the electrical stimulation was measured across the contracting leg (Figure 20A) and was identical in both treatment groups (ND = 7.7 ± 0.3 volts vs. HFD = 7.7 ± 0.9 volts, $p<0.05$). The force of the contraction during the field stimulation was also similar in both ND and HFD rats (Figure 20B). During the 2 Hz contraction, a two-phase force development occurred where the first 5 min was characterised by a sharp increase in force development followed by a slow decrease overtime (Figure 20B).

4.3.2.2 Hemodynamic Measurements

Mean arterial pressure was similar between ND and HFD fed groups (Figure 21A). An increase in MAP occurred after 2 Hz contraction, but did not reach significance. MAP for the last 10 min could not be obtained due to the arterial withdraws needed for the determination of 2-DG uptake. Heart rate increased

after 10 min of 2Hz contraction and this effect was similar in both treatment groups (Figure 21B).

4.3.2.3 Skeletal Muscle Glucose Metabolism

The basal level of the calf muscle glucose uptake, as seen in the resting leg, was unchanged with HFD (ND = 3.6 ± 0.1 μg/g/min vs. HFD = 3.8 ± 0.3 μg/g/min, NS) (Figure 22). The glucose uptake induced by contraction increased by 11 fold and this effect was similar in both groups (ND = 42.7 ± 4.3 μg/g/min vs. HFD = 43.7 ± 4.3 μg/g/min, NS).

4.3.2.4 High-Energy Intermediates

Table 4 shows that calf muscles isolated from the HFD rats have an increased ratio of dry weight/wet weight (ND = 0.201 ± 0.004 vs. HFD = 0.217 ± 0.006, $p<0.05$). This is a consequence of an increase in dry weight, due to an increase accumulation of intramuscular triglycerides (Kraegen 1991). However, beside a small decrease in ADP content of the HFD calf muscle, there were no differences in high-energy phosphates (Table 4).

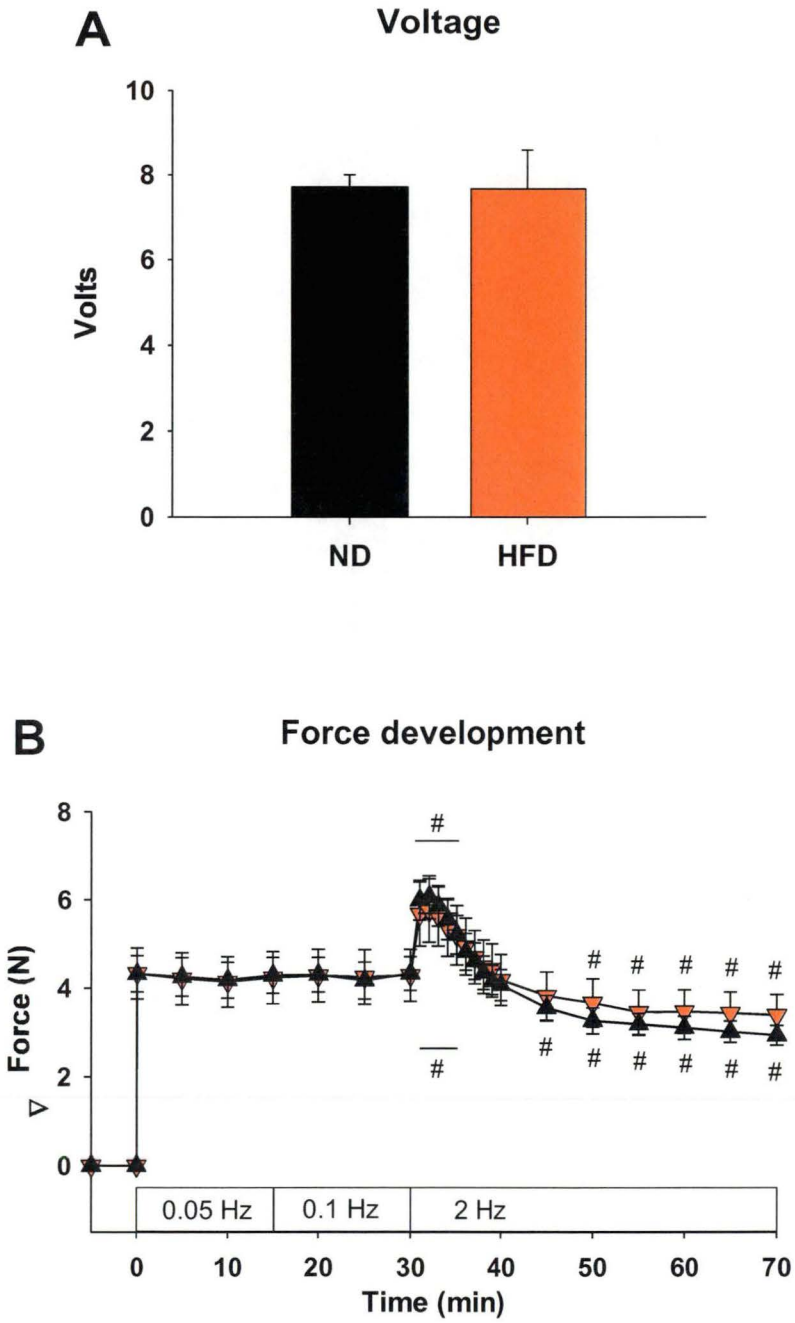

Figure 20: Contraction protocol #1: Voltage and force development during leg contraction.
Electrical stimulation-mediated (A) voltage and (B) force development in lower leg muscles of test leg in rats fed a ND (▲) or HFD (▼) for 4 weeks. Voltage across the leg was measured using an oscilloscope and force was determined by an isometric force transducer attached to the Achilles tendon. Data are means ± SEM for n = 8. # $p<0.05$ from contraction at 0.05 Hz, using two-way RM ANOVA with *post-hoc* analysis using SNK method.

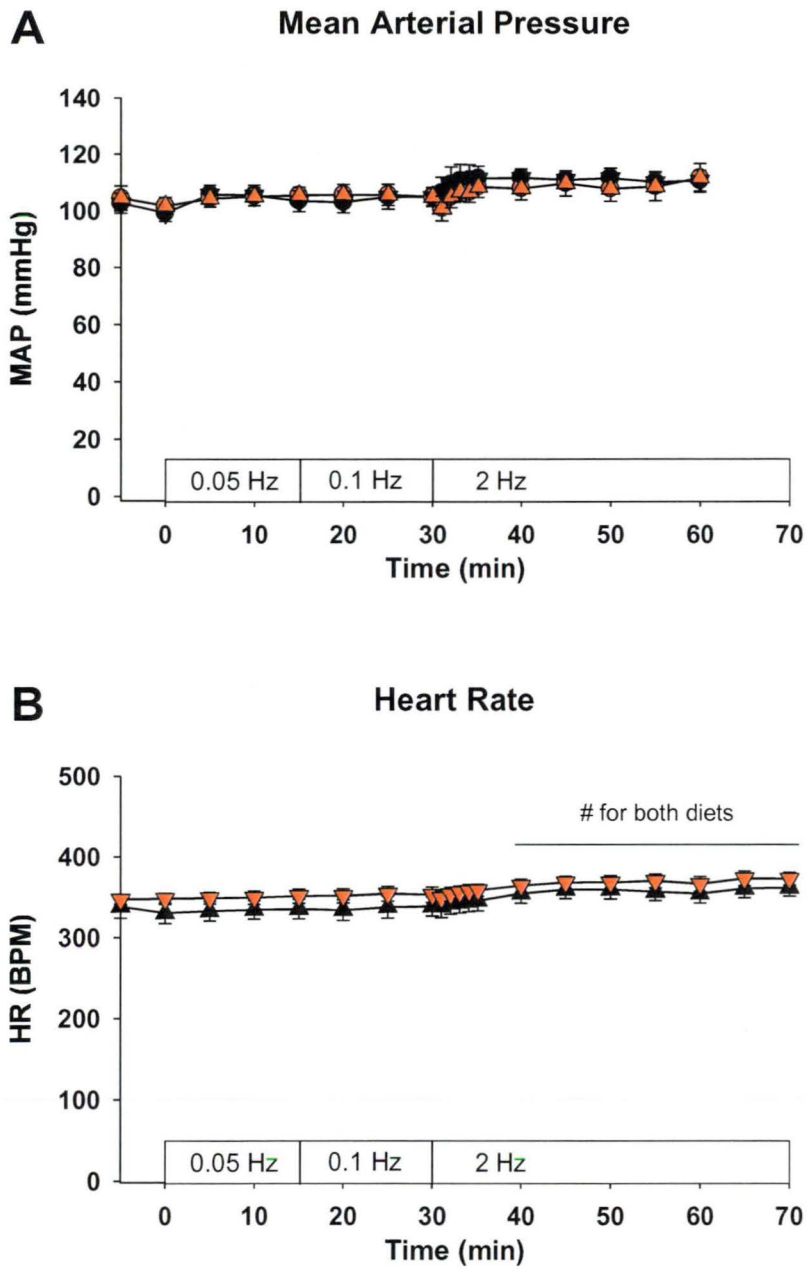

Figure 21: Contraction protocol #1: Mean arterial pressure and heart rate. Time course for mean arterial pressure (A) and heart rate (B) as a result of electrical stimulation in rats fed a ND (▲) or HFD (▼) for 4 weeks. Data are means ± SEM for n = 8. # $p<0.05$ from basal, using two-way RM ANOVA with *post-hoc* analysis using SNK method. Last 10 min of MAP could not be obtained due to the arterial withdraws needed for the 2-DG uptake measurement.

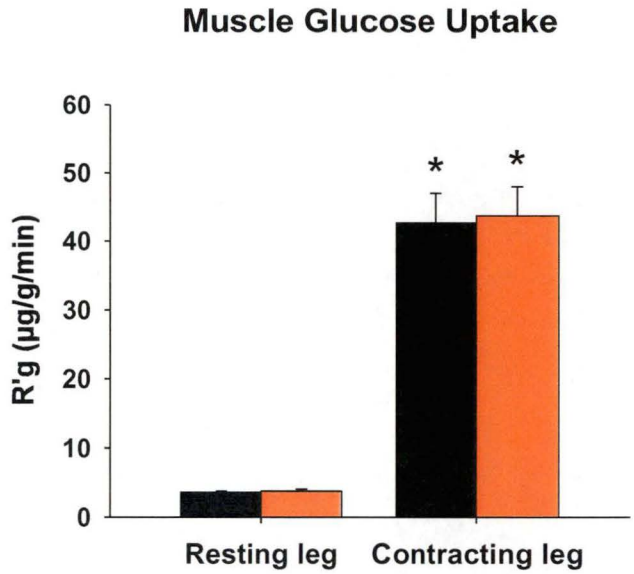

Figure 22: Contraction protocol #1: Calf muscle 2-DG uptake.
Muscle radioactive 2-DG uptake (R'g) for both resting and contracting legs as a result of electrical stimulation in rats fed a ND (■) or HFD (■) for 4 weeks. 2-DG was administered as a bolus after 30 min of 2 Hz contraction (Figure 16) and calf muscles were excised 10 min later. Data are means ± SEM for n = 8. * $p<0.05$ from resting leg of same diets, using two-way RM ANOVA with *post-hoc* analysis using SNK method.

Table 4: Contraction protocol #1: High-energy intermediates content of calf muscles after 2 Hz contraction.

	Normal Diet	High-Fat Diet
Dry wt/Wet wt	0.201 ± 0.004	0.217 ± 0.006 *
Creatine (μmol/g wet weight)	18.93 ± 0.88	17.96 ± 0.88
Phospho-Creatine (μmol/g wet weight)	23.99 ± 0.52	22.84 ± 0.87
PCr/Cr	1.28 ± 0.05	1.28 ± 0.05
ATP (μmol/g wet weight)	6.41 ± 0.14	5.95 ± 0.32
ADP (μmol/g wet weight)	0.53 ± 0.03	0.44 ± 0.02 *
AMP (μmol/g wet weight)	0.069 ± 0.006	0.065 ± 0.005
NAD (μmol/g wet weight)	0.66 ± 0.03	0.61 ± 0.03
Energy Charge	0.952 ± 0.002	0.955 ± 0.002

Data are means ± SEM for n = 8 rats in each group. * $p<0.05$, vs. ND, paired student *t-test*. Calf muscles were freeze clamped then removed from rats at the completion of each experiment.

4.3.3 Contraction Protocol #2: Microvascular Recruitment

4.3.3.1 Hemodynamic Measurements

Mean arterial pressure was similar between ND and HFD fed groups (Figure 23A). A significant increase in MAP occurred after 5 min of 2 Hz contraction, however MAP for the last 10 min could not be obtained due to the arterial withdraws needed for the determination of 2-DG uptake. Heart rate was similar in both group and was not affected by the contractions (Figure 23B).

4.3.3.2 Femoral Blood Flow

FBF showed a similar response to contraction in both ND and HFD fed groups. FBF significantly increased 15 min after 0.1 Hz frequency and throughout the 2 Hz contraction (Figure 24A). There was a 2.5 fold increase in the FBF of the contracting leg after 5 min of 2 Hz, with no difference in the amplitude of the increase between treatment groups (ND = 2.71 ± 0.19 ml/min vs. HFD = 2.52 ± 0.15 ml/min, NS). Although there was a trend for a decrease in FBF in the non-contracted leg during the contraction of the contralateral leg, this was not significant (Figure 24B).

4.3.3.3 1-MX Metabolism Assessment of the Perfused Capillary Surface Area

Increase in perfused capillary surface area, a marker of microvascular recruitment, was unaffected by the diets (ND = 9.61 ± 0.99 nmol/min vs. HFD = 11.20 ± 1.60 nmol/min, NS) (Figure 25A). Of note, the microvascular recruitment observed in the resting leg was also unaffected by the dietary modification (ND = 4.13 ± 0.59 nmol/min vs. HFD = 4.97 ± 1.01 nmol/min, NS), indicative of similar basal level of capillary surface area perfusion in both groups.

4.3.3.4 Skeletal Muscle Glucose Metabolism

Basal level of muscle glucose uptake, as seen in the resting leg, was unchanged with HFD (ND = 0.06 ± 0.03 μmol/min vs. HFD = 0.03 ± 0.03 μmol/min, NS). Electrical stimulation increased HGU to a similar extend in both groups (ND = 0.75 ± 0.08 μmol/min vs. HFD = 0.74 ± 0.10 μmol/min, NS), representing a ~12 fold increase from resting levels, consistent with the 2-DG uptake in contraction protocol #1.

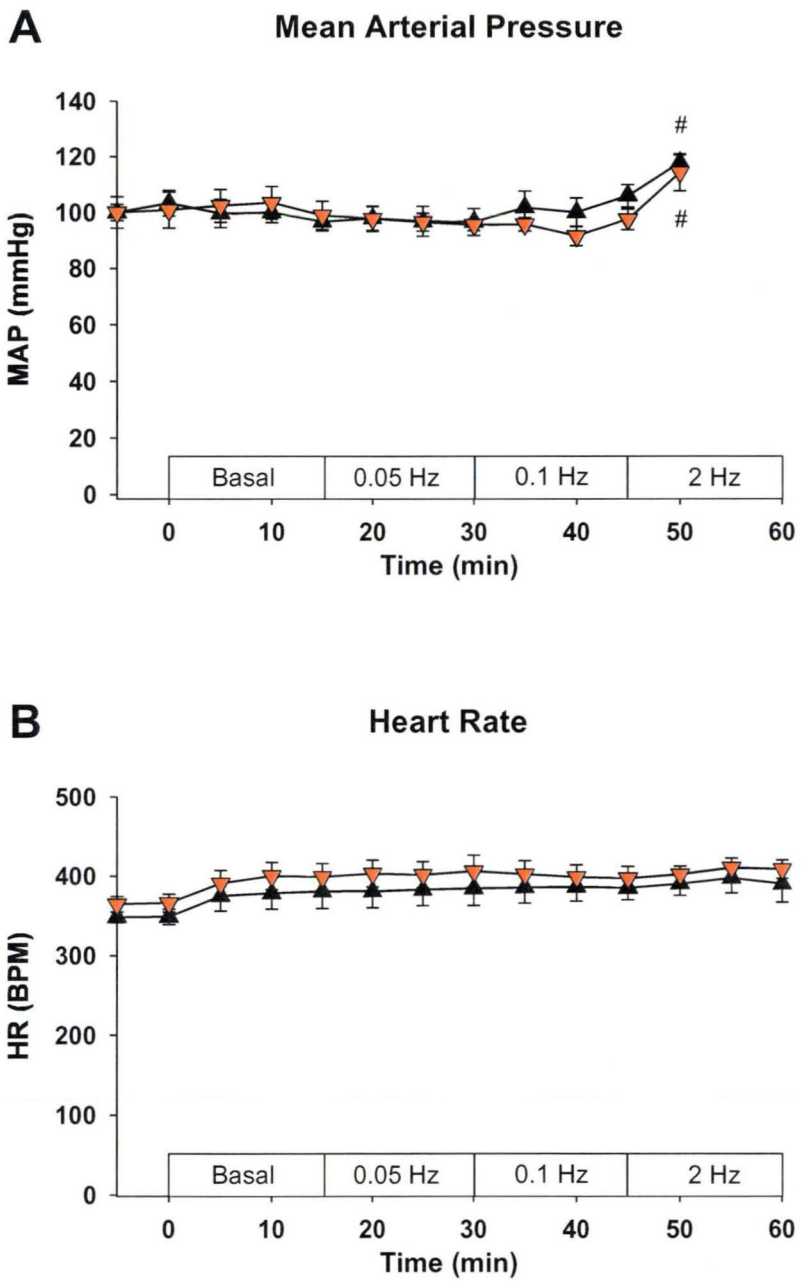

Figure 23: Contraction protocol #2: Mean arterial pressure and heart rate. Time course for mean arterial pressure (A) and heart rate (B) as a result of electrical stimulation in rats fed a ND (▲) or HFD (▼) for 4 weeks. Data are means ± SEM for n = 5-6. # $p<0.05$ from basal, using two-way RM ANOVA with *post-hoc* analysis using SNK method.

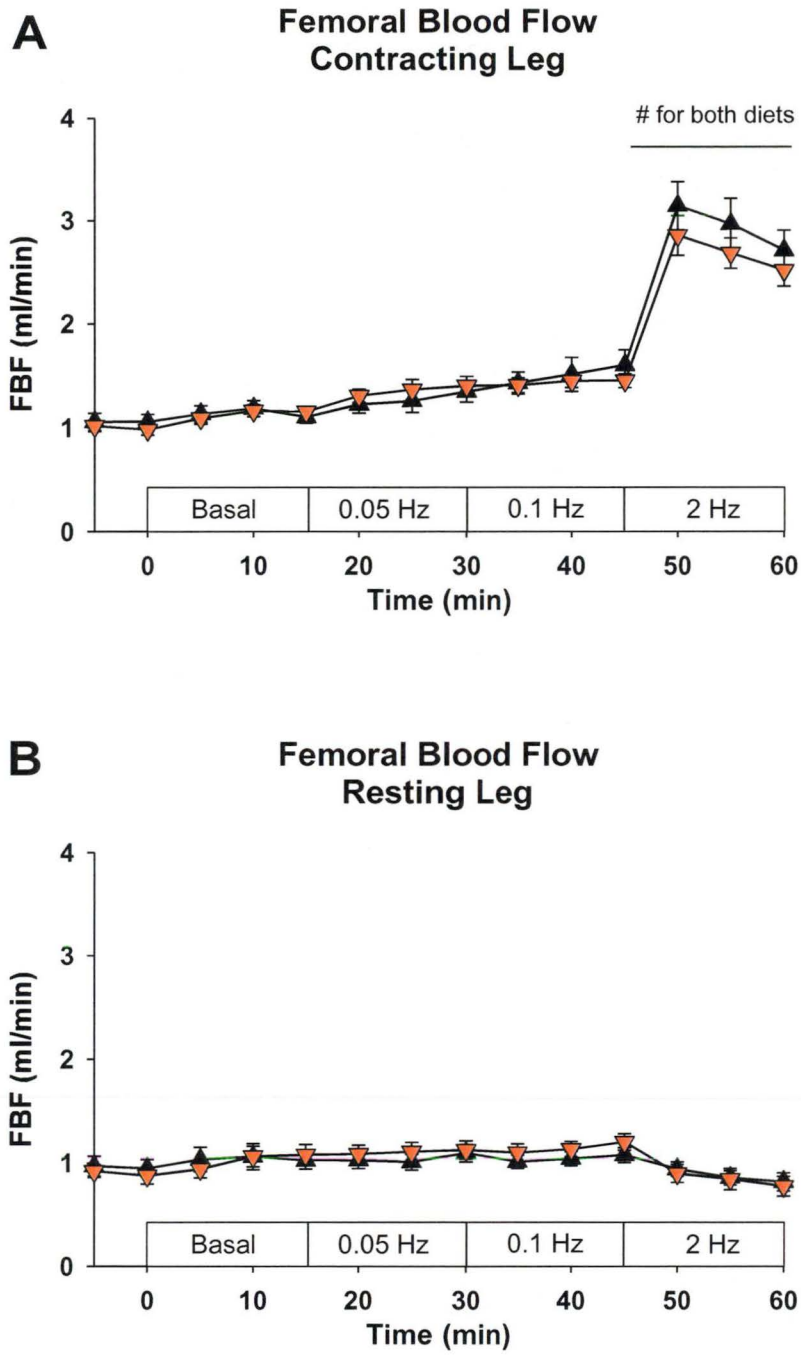

Figure 24: Contraction protocol #2: Femoral blood flow in contracting and resting leg.
Time course for the femoral blood flow for both contracting (A) and resting (B) legs as a result of electrical stimulation in rats fed a ND (▲) or HFD (▼) for 4 weeks. Data are means ± SEM for n = 5-6. # $p<0.05$ from basal, using two-way RM ANOVA with *post-hoc* analysis using SNK method.

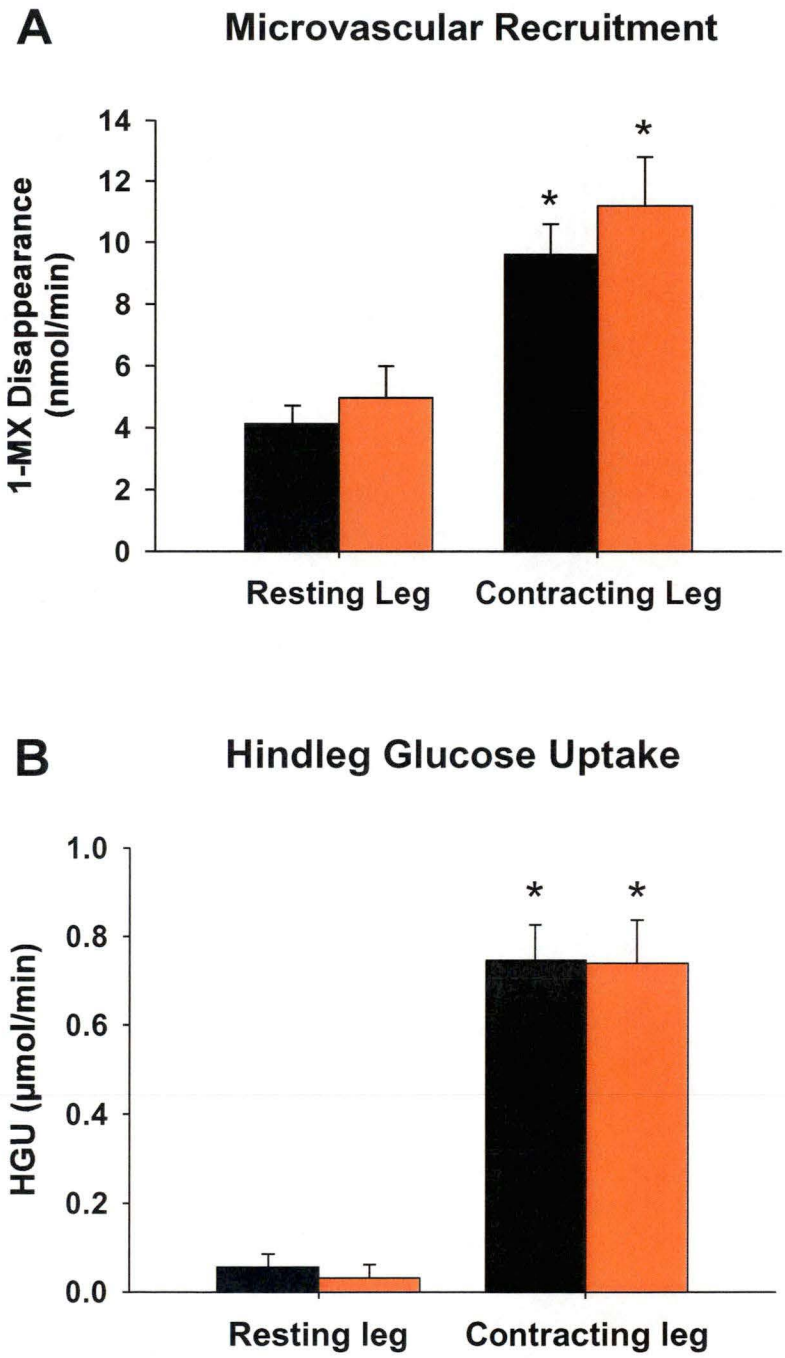

Figure 25: Contraction protocol #2: Capillary surface area perfused and hindleg glucose uptake.
Hindleg glucose uptake measurements (A) and 1-MX metabolism (B) as a result of 2 Hz electrical stimulation in rats fed a ND (■) or HFD (■) for 4 weeks. Hindleg glucose uptake was measured by the blood glucose arterio-venous difference multiplied by the femoral blood flow. Data are means ± SEM for n = 5-6. * $p<0.05$ from resting leg of same diets, using two-way RM ANOVA with *post-hoc* analysis using SNK method.

4.3.4 Contraction Protocol #3: Microvascular Volume

4.3.4.1 Hemodynamic Measurements

As seen in Figure 26, MAP and HR were similar between diets, and remained unchanged at 0.05 and 0.1 Hz contractions. During the 2 Hz contraction, an increase in MAP and HR occurred, with significantly greater increase in the HFD compared to the ND (Figure 26A).

4.3.4.2 CEU Assessment of the Microvascular Volume

Microvascular blood volume (MBV) significantly increased from resting level during 2 Hz contraction for both diets, and at 0.1 Hz in ND (Figure 27A). Although it did not reach significance, the increase in MBV during 2 Hz contraction was smaller in the HFD rats compared to the ND level (ND = 22.5 ± 4.5 AI vs. HFD = 15.3 ± 2.6 AI, p=0.07). Furthermore, microvascular flow rate (MFR) and microvascular blood flow (MBF) showed similar pattern with each diet, where 0.05 and 0.1 Hz contractions did not have an effect on either MFR (Figure 27B) or MBF (Figure 27C). On the other hand, 2 Hz contraction induced a significant increase in MFR and MBF, which was significantly less in the HFD fed animals.

4.3.4.3 Skeletal Muscle Glucose Metabolism

Basal level of muscle glucose uptake, as seen in the resting leg, was unchanged with HFD (ND = 2.0 ± 0.2 μg/g/min vs. HFD = 2.32 ± 0.2 μg/g/min, NS) (Figure 28). The glucose uptake induced by contraction increased significantly during 2 Hz contraction, and levels were similar in both groups (ND = 43 ± 13 μg/g/min vs. HFD = 27 ± 12 μg/g/min, NS).

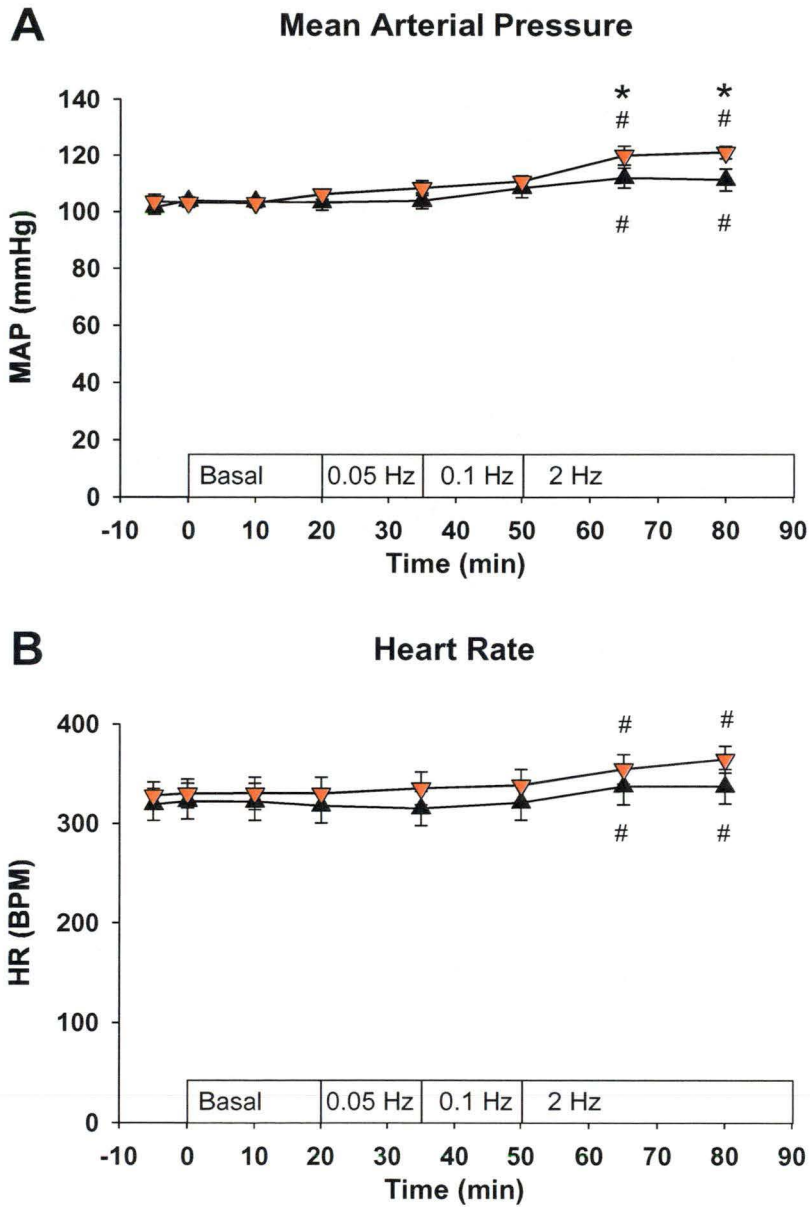

Figure 26: Contraction protocol #3: Mean arterial pressure and heart rate. Time course for mean arterial pressure (A) and heart rate (B) as a result of electrical stimulation in rats fed a ND (▲) or HFD (▼) for 4 weeks. Data are means ± SEM for n = 9. # $p<0.05$ from Basal, * $p<0.05$ from ND, using two-way RM ANOVA with *post-hoc* analysis using SNK method.

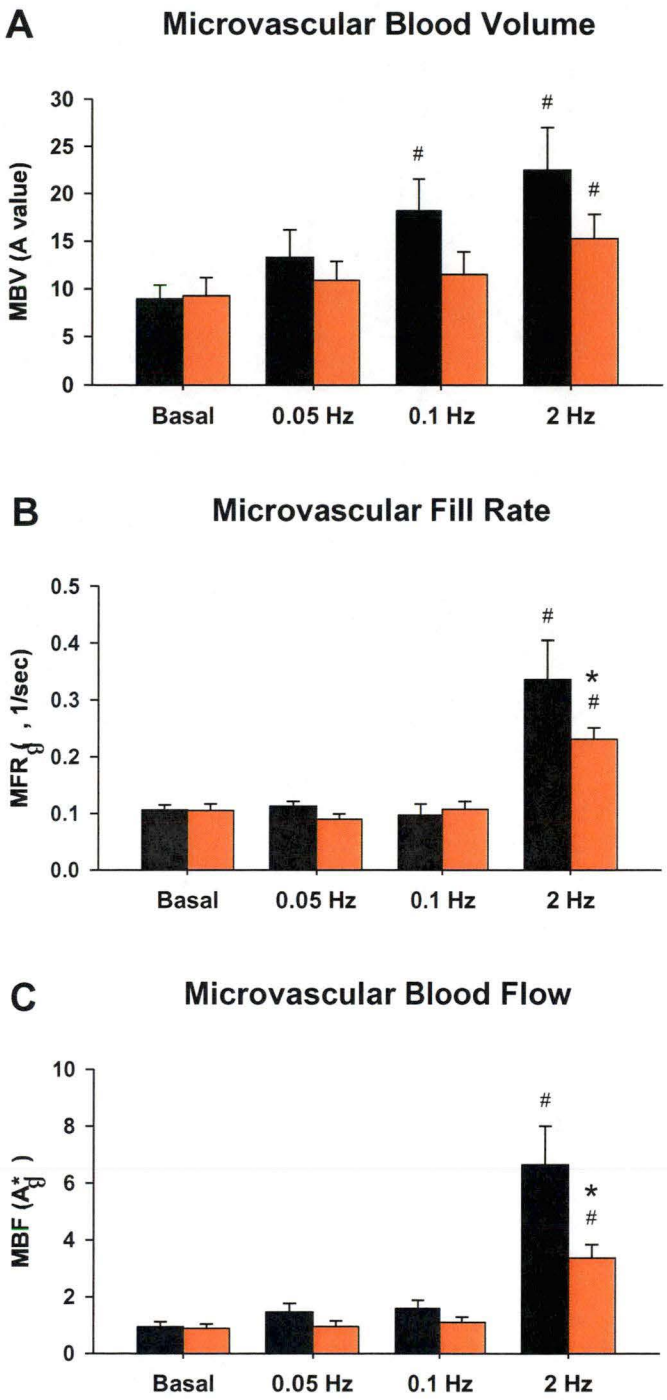

Figure 27: Contraction protocol #3: CEU imaging of the microvascular space.
Effects of different frequencies of electrical stimulation on microvascular blood volume (A), flow rate (B) and blood flow (C) in rats fed a ND (■) or HFD (■) for 4 weeks. Measurements were made by contrast enhanced ultrasound using phospholipid microbubbles before commencement of contraction (Basal) and after 5 min of contraction at each frequency. Data are means ± SEM for n = 9. # $p<0.05$ from Basal, * $p<0.05$ from ND of same frequency, using two-way RM ANOVA with *post-hoc* analysis using SNK method.

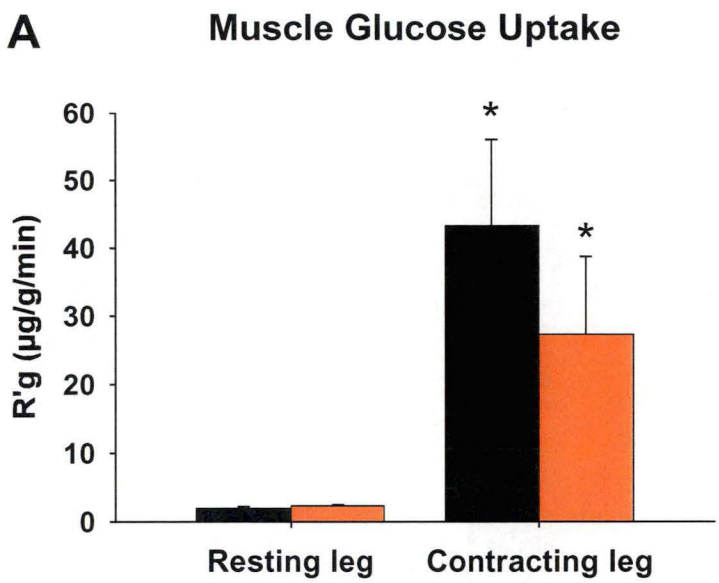

Figure 28: Contraction protocol #3: Muscle glucose uptake.
Muscle radioactive 2-DG uptake (R'g) for both resting and contracting legs as a result of electrical stimulation in rats fed a ND (■) or HFD (■) for 4 weeks. 2-DG was administered as a bolus after 30 min of 2 Hz contraction (Figure 19) and calf muscles were excised 10 min later. Data are means ± SEM for n = 5-6. # $p<0.05$ from Basal, * $p<0.05$ from ND of same frequency, using two-way RM ANOVA with *post-hoc* analysis using SNK method.

4.4 DISCUSSION

Two main findings resulted from the present study. The first finding was that metabolic responses to contraction after 4 weeks HFD fed rat was preserved in the skeletal muscle. Electrical stimulations induced similar force development, high-energy intermediates profile, and glucose uptake regardless of the diets. This data is consistent with contraction experiments in the obese Zucker rat (Wheatley 2004) showing essentially normal contraction-mediated glucose uptake response in this model of type 2 diabetes.

Measurements of skeletal muscle glucose uptake were made using different techniques (R'g and HGU) and after different periods of 2 Hz contraction (15 min and 40 min). In all these procedures, contraction elicited similar muscle glucose uptake in both the ND and HFD groups. This was important to verify as controversy exist in the literature as to whether contraction-mediated glucose disposal is impaired after a HFD. Several reports found exercise-mediated glucose uptake to be normal following an HFD (Kusunoki 1993, Liu 1996), while others showed a decrease (Rosholt 1994, Han 1997, Hansen 1998, Tanaka 2007). The reason for this inconsistency may reside in experimental procedure. Studies where the exercise-mediated glucose uptake was assessed *in vivo* reported no effect of the HFD on glucose disposal. On the other hand, decreases in glucose uptake were observed after an HFD when the glucose uptake was assess using the incubated muscle preparation. As this procedure required excision of the muscle after exercise, this technique may not be indicative of the glucose uptake occurring during exercise, but instead represent the glucose uptake post-exercise. Furthermore, the contribution of the microvasculature is non-existent in the incubated muscle preparation. As the microvascular component has been shown to be crucial for glucose uptake, this component should be considered when studying muscle glucose uptake.

Intramyocellular lipids (IMCL) have been shown to be increased after a HFD (Tanaka 2007). Although not assessed directly in the present study, the increase

in dry weight/wet weight ratio would support an increase in IMCL in the present model (Table 4). As the putative physiological function of IMCL is to serve as an energy source for muscular fatty acid oxidation (Krssak 2000, Schrauwen-Hinderling 2006), increases in IMCL content in the HFD could have modified the fuel usage during contraction. However, similar high-energy intermediates profiles and glucose uptake after contraction found in the present study indicates that the metabolic usage of the contracting muscle was similar in both diets. This is consistent with a study showing that consumption of a high-fat diet for one week is accompanied by molecular changes favouring fat storage in skeletal muscle rather than oxidation (Schrauwen-Hinderling 2005).

The second significant finding from the present study was that different techniques of assessment of the microvascular recruitment resulted in discordant results. 1-MX assessment of the microvascular recruitment showed no difference between ND and HFD. Both have similar level of 1-MX metabolism during contraction (ND = 9.61 ± 0.99 nmol/min vs. HFD = 11.20 ± 1.60 nmol/min, NS). However, CEU assessment of the microvascular volume showed an impairment of the contraction-mediated microvascular recruitment. Indeed, microvascular blood volume ($p=0.07$), microvascular flow rate and microvascular blood flow were all blunted in the HFD fed animal during the 2 Hz contraction (Figure 27). This was surprising, as 1-MX and CEU assessment of microvascular recruitment have always yielded similar outcomes in the past (Dawson 2002, Clark 2008). It is also the first time that CEU was used to assess contraction-mediated microvascular recruitment in a model of insulin resistance. Studies in humans with CEU have showed that type 2 diabetes patients without microvascular complication have preserved exercise-mediated microvascular recruitment (Womack 2009). However, in type 2 diabetic patients having other microvascular complications (defined by a proteinuria or a diagnosis of neuropathy), exercise-mediated microvascular recruitment was decreased. 4 weeks HFD is unlikely to have induced these other microvascular complications, which only become apparent in later stage of type 2 diabetes. Future experiments are needed to assess contraction-mediated microvascular recruitment with CEU

in the obese Zucker rats. Microvascular recruitment was previously assessed in this model by the 1-MX technique and was shown to respond normally to contraction (Wheatley 2004), therefore it would be interesting to verify if the CEU technique of assessing the microvascular recruitment during contraction reproduces the results observed in the HFD model.

The metabolic effects of contraction and force development in the current study were not affected by HFD, indicative of a preserved response of the microvasculature to contraction. Therefore, assessment of the microvascular recruitment during contraction with 1-MX is a more reliable method than CEU. Indeed, decreases in delivery of blood during exercise would have affected the muscle contraction, glucose uptake, and high-energy intermediates. Thus, difference between the two techniques for measuring microvascular recruitment may account for the observed decrease in microvascular volume in the HFD.

Results from the current study have demonstrated that measurements of microvascular recruitment using 1-MX and CEU techniques provide different information about microvascular recruitment, which could be responsible for the inconstancy of the results. 1-MX metabolism is a biochemical measure that relies on the presence of xanthine oxidase at the surface of capillaries and thus the values of 1-MX metabolism reflect the perfused capillary surface area. As describe in section 2.2.3.5, 1-MX technique utilises the infusion of a soluble molecule (1-methylxanthine) to assess microvascular recruitment. On the other hand, CEU utilises a contrast agent consisting of gas filed lipid-shell microbubbles to obtain an image of the perfused microvascular space. Measurements obtained from this technique reflect microvascular red blood cells volume (see section 2.2.3.7). Therefore, a difference in the access of the 1-MX and the microbubbles to the microvasculature could explain the inconsistencies in the present study. One factor that could affect the access of the microbubbles is an increased presence of the glycocalyx on the capillaries surface after 4 weeks HFD (Reitsma 2007). 1-MX may diffuse freely through the glycocalyx to

reach the xanthine oxidase at the surface of the vessels while the increase in the thickness of the glycocalyx could limit the accessibility of the microbubbles to the microvascular space. This could explain the decrease in volume seen in Figure 27A. Since total blood flow was not significantly different between diets, a decrease in microvascular blood volume would perhaps be expected to be matched by a increase in the microvascular flow rate. The CEU measurements indicated that no increase in microvascular flow rate was associated with the decreased microvascular volume. However, as has been observed previously, total blood flow and microvascular blood flow do not always correlate as blood flow can be redistributed between high flow non-nutritive routes and nutritive routes (Rattigan 1997, Zhang 2004). Therefore, an exclusion of the microbubbles from the microvasculature (by an increase in glycocalyx or other) combined with blood flow going to the high-flow non-nutritive vessels, undetectable by CEU, may explain the unexpected findings using this technique. However, it should be mentioned that glycocalyx have been shown to be decreased during experimental hyperglycaemia (Nieuwdorp 2006) and type 1 diabetes (Nieuwdorp 2006). Glycocalyx levels of the microvasculature have not been assess after an HFD and may have been affected differently in this model. However, the glycocalyx level will need to be directly assess in the HFD model before any definitive conclusion can be drawn.

Another possible explanation for differences in CEU findings may lie in the spatial resolution of CEU. Indeed, tens to hundreds of capillaries can be in a single pixel area, therefore changes in signal within a pixel may be not be properly detected. Furthermore, CEU technique cannot discriminate between different flow patterns within muscle (Ross 2008), and the present data may have been affected by changes in the non-nutritive route.

In conclusion, contraction-mediated metabolic and FBF response are preserved in a pre-diabetic state of insulin resistance. As contraction-mediated glucose disposal is preserved after a 4 weeks HFD, even though the insulin-mediated

response is impaired, it supports the hypothesis of different mechanisms for insulin and contraction effects. On the other hand, conflicting data were obtained with the measurement of microvascular recruitment, where 1-MX assessment of the microvascular recruitment was intact while the CEU showed an impairment. As glucose uptake was unchanged after HFD feeding, this would indicate that capillary surface area is more important for the disposal of glucose than the microvascular volume. Further experiments in models of insulin resistance and type 2 diabetes need to be done to confirm these results, as it would cast doubt on the effectiveness of measuring microvascular recruitment with CEU during contraction. On the other hand if confirmed then it would indicate that the HFD has subtly altered the microvasculature that affects microvascular volume but not surface area changes during contraction.

CHAPTER 5:

ACUTE MICROSPHERE OCCLUSION INDUCED VASCULAR INSULIN RESISTANCE

5.1 INTRODUCTION

The diabetic state is characterised by a lack of insulin action in different organs, including the liver (Kraegen 1991, Bergman 2001), the adipose tissue (Bergman 2001) and the skeletal muscle (Crettaz 1981, Baron 1991, Krook 2000). Decreased insulin action has been observed in skeletal muscle during the initial stage of insulin resistance (Rothman 1995) and before the appearance of systemic insulin resistance (Kraegen 1991). Furthermore, improvements to skeletal muscle insulin sensitivity either by exercise training (Schneider 1984, Ivy 1997, Goodyear 1998, Pauli 2008) or by drug intervention (Hallsten 2002, Meyer 2002) enhance systemic insulin sensitivity, demonstrating the importance of the skeletal muscle in the pathogenesis of type 2 diabetes.

Endothelial dysfunction is defined as a state where there is a decrease in the NO mediated vasodilatation (Vanhoutte 2009), primarily of the resistance arterioles. Associated with this dysfunction is an impairment of the insulin-mediated increase in blood flow and glucose disposal in skeletal muscles (Baron 1997). Thus, endothelial dysfunction has also been implicated in the insulin resistant state, where it could lead to a decrease in insulin-mediated glucose uptake (Kim 2006, Jansson 2007).

In vivo studies in anaesthetised rats showed that the muscle microvasculature, and its response to insulin stimulation, is essential for optimal insulin-mediated glucose uptake. As shown in chapter 3 of the present thesis, insulin-mediated microvascular recruitment is inhibited in the early stage of insulin resistance and is accompanied by a ~40 % decrease in insulin-mediated glucose uptake. Furthermore, pharmacological treatments using infusions of TNF-α (Youd 2000), α-methylserotonin (Rattigan 1999) or intralipids (Clerk 2002) results in the prevention of insulin-mediated microvascular recruitment and approximately 50 % decrease in insulin-mediated skeletal muscle glucose uptake. Thus, all of these treatments lead to an acute vascular state of insulin resistance by limiting insulin

and glucose access to skeletal muscle. These studies confirm the importance of the microvasculature in glycaemic control as insulin-mediated glucose uptake is impaired by the lack of insulin's vascular actions. While these pharmacological treatments support the idea that muscle microcirculation is involved in insulin-mediated glucose uptake, they do not rule out the effect of other tissues. Indeed, infusions of TNF-α, α-methylserotonin and intralipids were conducted systemically, therefore the effects of the liver and the adipose tissue cannot be ruled out.

Additional evidence of a role for microvasculature in insulin-mediated glucose uptake came from isolated hindleg perfusion experiments. Using this preparation, partial occlusion of the rat hindlimb vasculature (with 15μm diameter latex microspheres (MS)) was shown to impair insulin-mediated activation of Akt and decrease glucose uptake by 46% (Vollus 2007). This study provided evidence that a decrease in the delivery of insulin to the myocytes is sufficient to prevent the insulin-mediated glucose uptake *in situ*. The MS occlusion is a more advantageous approach than pharmacological treatments, as physical occlusion directly limits the perfusion to the muscle while pharmacological treatments may have other cells and tissues effects.

The aim of the present study was to evaluate the involvement of microvascular delivery in insulin-mediated skeletal muscle glucose uptake *in vivo*. The hypothesis was that prevention of insulin-mediated microvascular recruitment would decrease the insulin-mediated glucose disposal. Therefore, insulin-mediated glucose uptake was studied in the isoglycaemic hyperinsulinaemic clamp following partial occlusion of the microvascular beds with 15μm diameter latex MS.

5.2 MATERIAL AND METHODS

5.2.1 Animal Care

Hooded Wistar rats weighing 252 ± 2 grams were used during this experiment. The rats were raised as described in section 2.1. Rats were not fasted prior to the experiments, as the determination of whole body glucose kinetics was not required.

5.2.2 Surgery

Experiments were conducted using the anaesthetised rat model, with surgery as described in section 2.2.1.

5.2.3 Epigastric Cannulation for Microsphere Injection

After careful separation of the epigastric vessels from the overlying connective tissue, an incision was made in the epigastric artery using an insulin syringe needle. The artery was then cannulated using a homemade cannula comprising a blunted 27G needle (Terumo, Tokyo, Japan) connected to PE50 size tubing (Microtube Extrusions, NSW, Australia). A successful cannulation resulted in arterial blood pulsing into the tubing. Once the cannula was firmly secured with 7-0 size silk tie, flow probes were positioned on the femoral arteries of both legs as previously described. Prior to the MS injection, LDF probe (Laser Doppler Perfusion Monitor moorLAB server, Moor Instruments, USA) was positioned on the sole of the cannulated foot. The LDF probe was used to assess the blood flow going through the foot. A haemostatic clamp, applied at the Achilles region, was used to restrict blood flow to the large shunt vessels of the foot. A injection of 250 µl of the MS mix (or saline in sham experiments) comprising a predetermined amount of MS (Fluka, Germany) and 50,000 fluorescent MS (Molecular Probe, USA) was then injected retrogradely via the epigastric artery over a period of 10 sec. This was immediately followed by flushing the cannula with 200 µl of saline. The entire injection procedure lasted about 90 sec.

Following the injection, both epigastric vessels were ligated and the animal was left to equilibrate for 1-hour before commencing the isoglycaemic hyperinsulinaemic clamp. In addition to sham treated rats, the contralateral leg in each experiment was used to compare the effects of occlusion within each group.

The stock solution of MS was counted on a haemocytometer at regular intervals to ensure than the same amount of MS was injected in each procedure.

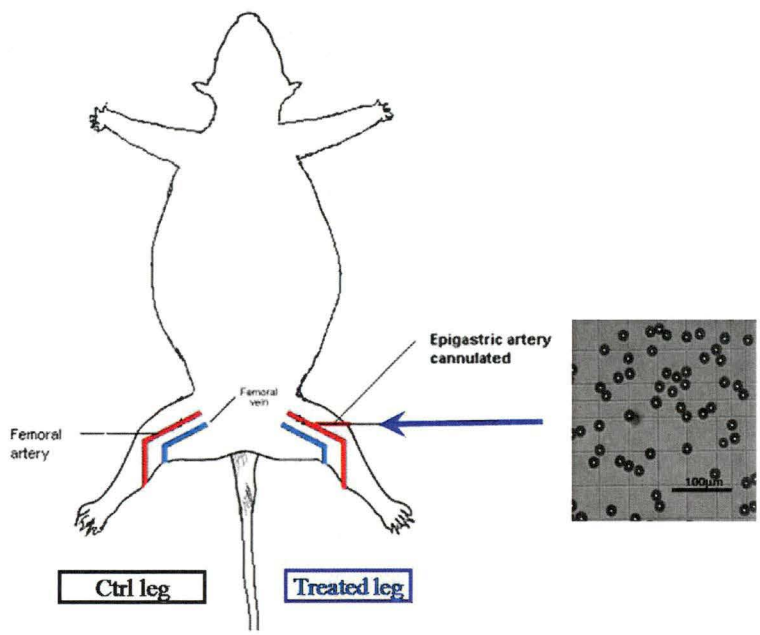

Figure 29: Epigastric Cannulation for Microsphere Injection
Surgery details are given in section 5.2.3. Briefly, the epigatric artery of one leg (Treated leg) was cannulated using a homemade cannula to enable the local injection of either a mix of microsphere or a bolus of saline. The contralateral leg in each experiment (Ctrl leg) was used to compare the effects of occlusion within each group. Diagram adapted from Mahajan *et al.* (Mahajan 2004).

5.2.4 Experimental Procedure

The local effects of MS occlusion on the skeletal muscle microvasculature were assessed during an isoglycaemic hyperinsulinaemic clamp as described in section 2.2.2. Briefly, 1-hour after the injection of the MS/saline bolus into the epigastric artery on the treated leg, saline or insulin (10 mU/min/kg) was initiated and continued for 2 hours (Figure 6). During experiments involving insulin infusion, a glucose solution (30 % w/v) was also infused at variable rates to maintain blood glucose levels around at basal. Femoral artery blood flow was continuously measured using Transonic® flow probes positioned around the femoral arteries of both legs. The 1-MX disappearance was used as an indicator of perfused capillary surface area as described in section 2.2.3.5. A bolus dose of [^{3}H] 2-DG (50 μCi) was given 45 min before the end of the experiment. Calf muscles were excised at the completion of the experiment and freeze clamped in liquid nitrogen to assess the 2-DG uptake as described in section 2.2.3.3. Selected tissues (tibialis anterior, lung, heart, quadrate lobe of the liver) were excised from rats and kept at -20 °C until the fluorescence could be assessed.

5.2.4.1 High-Energy Intermediates Determination

Calf muscles were ground under liquid nitrogen and used to assess the high-energy intermediate content. Extraction and measurement techniques are described in section 2.2.3.7.

5.2.4.2 Fluorescence

All tissue samples were weighed in 50 ml centrifuge tubes and digested using previously published methods (Rattigan 1997). Each tissue was incubated in a volume of 10 ml of tissue solubilising solution (2 M KOH in 95 % ethanol with 0.5 % Tween 80) per gram of tissue. Tubes were left overnight at room temperature to allow dissolving, after which the supernatant was discarded following 20 min centrifugation at 2500 RPM (Damon/IEC). The formed pellet was resuspended in 15 ml of water. After another centrifugation (20 min at 2500

RPM), the supernatant was again removed (leaving 0.5 ml on pellet) before adding 5 ml of 2-epoxy ethylacetate (MS dissolving solvent). Over the course of an hour, the solution was vortexed several times to ensure the complete dissolution of the fluorescent MS. The dissolving solution was then centrifuged at 2500 RPM for 20 min. The fluorescence intensity of the supernatant was determined by spectrophotofluorometry (Aminco-Bowan, USA) at an excitation wavelength of 505 nm and an emission wavelength of 515 nm.

For each experiment, fluorescence intensity of 10 µl of the MS mix injected in each animal (dissolved in 5 ml of 2-epoxy ethylacetate) was assessed. This allowed the expression of tissue fluorescence as a percentage of the total injected fluorescence.

5.2.5 Data Analysis

All data are expressed as means ± SEM. Data were calculated as described in section 2.2.4. The effect of different doses MS on high-energy intermediates was assessed with one-way ANOVA with *post-hoc* analysis using Bonferroni's method to compare with the sham (0 MS) treated group. Comparisons were made between treatment groups over the course of the experiment using two-way non-repeated or repeated-measures ANOVA with Student-Newman-Keuls *post hoc* test as indicated in the figure legends. All tests were performed using the SigmaStat statistical program (Systat Software Inc, CA, USA).

5.3 RESULTS

5.3.1 Tissue Localisation of MS

Initial studies were made to assess the tissue distribution of the injected MS. These studies showed that after a retrograde epigastric arterial injection, less than

10 % of the MS were located within the lower leg muscles and 44 % were located in the lung. In subsequent studies, the blood flow to the large shunt vessels in the feet was restricted before and during MS injection by clamping the ankle region with a haemostatic clamp to ensure a redirection of the MS into the lower leg muscles. Following this procedure, 84 % of the locally injected fluorescent MS were recovered in the treated leg, 18 % of which were within the calf muscles (soleus, EDL, red and white gastrocnemius). Meanwhile, fluorescence in the tibialis anterior accounted for approximately 4 % of the injected MS.

5.3.2 Determination of the MS Dose Required for the Occlusion of the Muscle Microvasculature

Initial trials were conducted to determine the number of MS that were required to impair the microvascular delivery to skeletal muscle. This was assessed by measuring the calf muscles high-energy intermediates content after an injection of 0, 1.5, 3 or 7 $x10^6$ MS. Two parameters were closely monitored: the PCr/Cr ratio (a marker of adequate microvascular blood delivery) and the energy charge (EC) (a marker of cellular damage). As seen in Table 5, 1.5 $x10^6$ MS did not affect the PCr/Cr ratio or the EC. 3 $x10^6$ MS induced a decrease in PCr/Cr ratio without affecting the EC while 7 $x10^6$ MS induced a decrease in both PCr/Cr ratio and EC. Therefore, only 3 $x10^6$ MS impaired the microvascular delivery of blood without inducing cellular damage.

During these initial trials, insulin-mediated microvascular recruitment was also assessed to determine the appropriate dose of MS to impair this process. As seen in Figure 30, 1.5 $x10^6$ MS did not significantly affect the insulin-mediated microvascular recruitment. In contrast, a significant impairment occurred at the higher doses of 3 and 7 $x10^6$ MS.

The 3 $x10^6$ MS dose was the only one that decreased the PCr/Cr ratio and prevented insulin-mediated microvascular recruitment without affecting the EC.

Prior studies using the perfused hindlimb (Vollus 2007) also indicated that 3 $x10^6$ MS prevented the insulin-mediated glucose uptake. As a result, an injection of 3 $x10^6$ MS was judged to represent the most suitable dose of MS for the partial occlusion of the microvasculature. Therefore, this dose was used in subsequent experiments to determine the effect of MS occlusion on the insulin-mediated glucose uptake during an isoglycaemic hyperinsulinaemic clamp *in vivo*. It should be noted that incorrect values were provided for the dose of MS used in the hindlimb perfusion paper (Vollus 2007). The MS doses of 9, 15 and 30 $x10^6$ MS should have been labelled 1.5, 3 and 7 $x10^6$ MS (personal communication with S. Rattigan).

Table 5: Effects of different doses of MS on high-energy intermediates of the calf muscle group.

Microspheres ($x10^6$)	0	1.5	3	7
Dry wt/Wet wt	0.212 ± 0.004	0.223 ± 0.005	0.192 ± 0.010	0.178 ± 0.007*
Creatine (μmol/g dry weight)	86 ± 5	68 ± 11	100 ± 5	126 ± 6*
Phospho-Creatine (μmol/g dry weight)	124 ± 3	84 ± 8	82 ± 9	60 ± 26*
PCr/Cr	1.46 ± 0.09	1.33 ± 0.15	0.82 ± 0.06*	0.48 ± 0.20*
ATP (μmol/g dry weight)	30.96 ± 0.65	24.45 ± 2.86	27.43 ± 2.12	21.52 ± 5.93
ADP (μmol/g dry weight)	3.33 ± 0.32	1.75 ± 0.16*	1.80 ± 0.41*	1.97 ± 0.26*
AMP (μmol/g dry weight)	0.24 ± 0.04	0.35 ± 0.09	0.49 ± 0.09	1.21 ± 0.37*
NAD (μmol/g dry weight)	3.01 ± 0.11	2.55 ± 0.26	2.55 ± 0.28	2.30 ± 0.45
Energy Charge	0.945 ± 0.005	0.954 ± 0.001	0.954 ± 0.008	0.903 ± 0.020*

Data are means ± SEM for n = 3-5 rats in each group. * $p<0.05$ relative to 0 MS, one-way ANOVA with *post-hoc* analysis using Bonferroni's method. 3hr post-injection, calf muscles were freeze clamped then excised from rats.

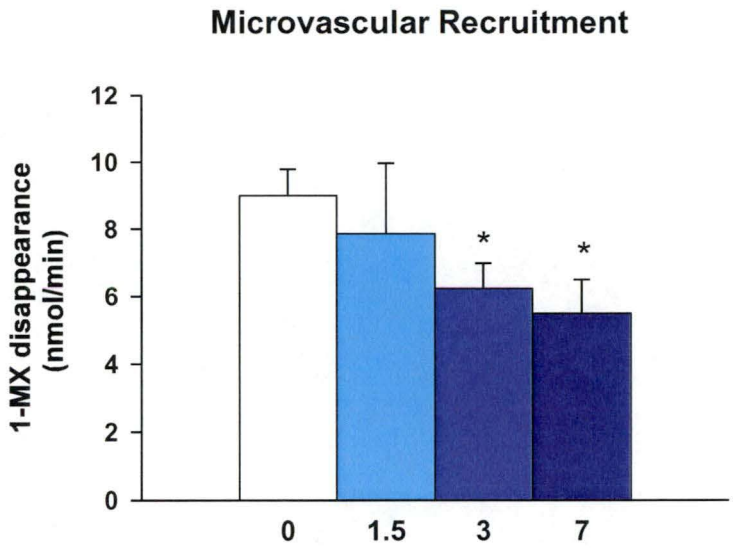

Figure 30: Effects of different doses of microspheres (x 10^6 MS) on insulin-mediated microvascular recruitment.

1-MX metabolism of the treated leg as a result of different doses of MS. Animals were left to equilibrate for one hour after the retrograde epigastric artery MS injection. Measurements were made at the end of a 2 hrs insulin infusion. Data are means ± SEM for n = 5-7 in each group. * $p<0.05$ relative to 0 MS, unpaired student *t-test*.

□ 0 MS, ■ 1.5 x10^6 MS, ■ 3 x10^6 MS, ■ 7 x10^6 MS.

5.3.3 Effects of MS Occlusion on Insulin-Mediated Glucose Disposal

Four experimental groups were used to assess the effects of MS occlusion on insulin-mediated glucose uptake. The first two groups received the sham operation followed by a saline infusion (□ Sham-Saline) or a 10 mU/kg/min insulin infusion (■ Sham-Insulin). The final two groups received an epigastric injection of 3 x10^6 MS followed by either a saline (◦ MS-Saline) or a 10 mU/kg/min insulin infusion (• MS-Insulin). As such, the sham groups were used as controls for the effects of the MS occlusion.

5.3.3.1 Hemodynamic Parameters

Figure 31 shows the MAP and HR after saline or insulin infusions in both sham and MS treated groups. In all groups, no significant change in MAP or HR was observed.

5.3.3.1.1 FBF in the Treated Legs

FBF of the treated leg is shown in Figure 32A. The two sham groups yielded expected results with no observed change in FBF in the saline infusion and an increase in the FBF 40 min after the insulin infusion was begun. The difference between Sham-Saline and Sham-Insulin reached significance from 50 min onward.

MS occlusion affected the FBF in two ways. First, MS occlusion itself produced an increase in basal FBF when compared to the sham group (at 0 min, Sham = 0.82 ± 0.04 ml/min, MS = 1.34 ±0.05 ml/min, $p<0.001$). This effect was maintained and increased throughout the procedure, resulting in a significant increase in FBF at all time points during the MS-Saline compared to Sham-Saline experiments. This was also evident when comparing MS-Insulin and Sham-Insulin, although the difference was no longer significant at 120 min (Sham-Insulin = 1.89 ± 0.26 ml/min, MS-Insulin = 2.24 ± 0.24 ml/min, $p=0.12$). Second,

the slight continual increase in FBF in MS-Saline group resulted in significant changes over basal levels from 75 min onward. During MS-Insulin experiments, the increase in FBF was apparent from 30 min onward. Higher FBF compared to sham in both MS groups meant that there was no significant difference between the MS-Saline and the MS-Insulin at any time points.

5.3.3.1.2 FBF in the Contralateral Leg

FBF in the contralateral leg is shown in Figure 32B. Insulin infusion elicited an increase in FBF at 40 min onward in the contralateral leg (both sham and MS) while saline infusion did not (both sham and MS). While FBF in Sham-Insulin was significantly different from Sham-Saline from 50 min onward, this was not the case in the MS groups. Unexpectedly, the insulin-mediated increase in FBF in the MS-Insulin group was not significantly different from MS-Saline group ($p=0.08$).

5.3.3.2 Microvascular Recruitment

Figure 33 depicts the microvascular recruitment at the end of the 2 h experiment in all four groups, for both the contralateral and the treated legs. The expected insulin-mediated increase in microvascular recruitment was observed in the contralateral leg when compared to the corresponding saline group. In the treated legs, sham treatment did not affect the insulin-mediated microvascular recruitment as seen from the conserved increase with insulin (Sham-Saline = 5.13 ± 0.34 nmol/min, Sham-Insulin = 8.99 ± 0.79 nmol/min, $p<0.01$). On the other hand, MS injection prevented the insulin-mediated increase in microvascular recruitment (Sham-Insulin = 8.99 ± 0.79 nmol/min, MS-Insulin = 6.23 ± 0.75 nmol/min, $p<0.05$). Of note, the MS occlusion did not affect the basal recruitment as 1-MX metabolism was similar in both saline infusion groups of the treated leg (Sham-Saline = 5.13 ± 0.34 nmol/min, MS-Saline = 4.64 ± 1.04 nmol/min, $p=0.65$).

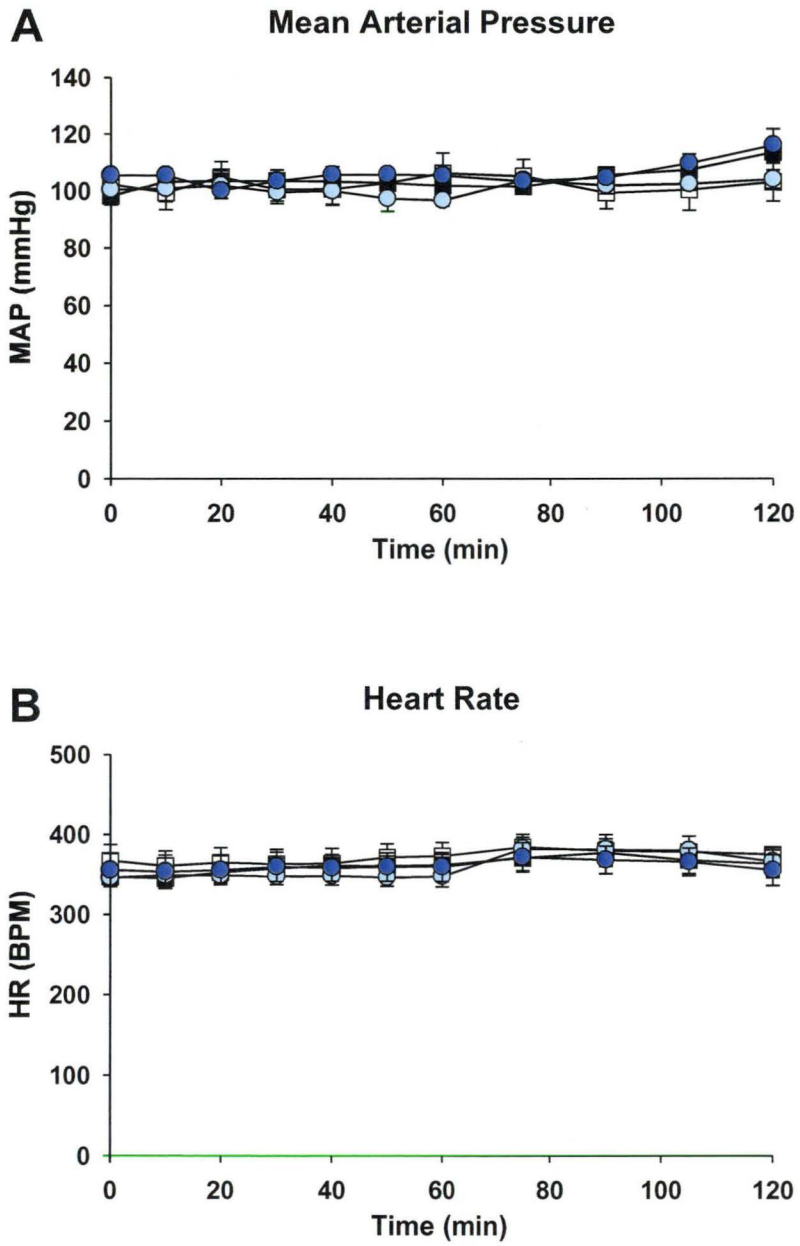

Figure 31: Mean arterial pressure and heart rate during acute MS occlusion. Time course for mean arterial pressure (A) and heart rate (B) as a result of an acute MS occlusion. Mean arterial pressure and heart rate were measured by a catheter placed in the carotid artery. Data are means ± SEM for n = 6-7. Comparisons were made using two-way RM ANOVA.
□ Sham-Saline, ■ Sham-Insulin, ◦ MS-Saline, • MS-Insulin.

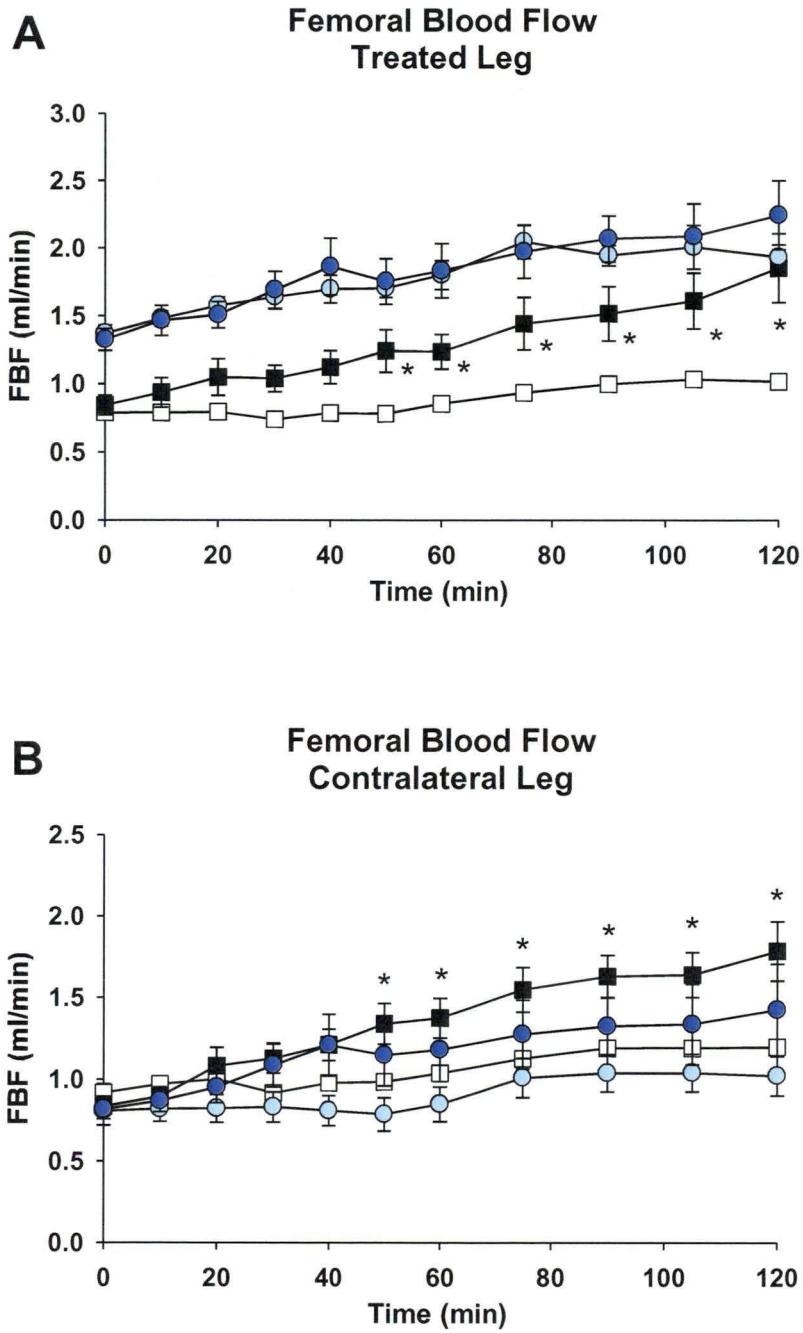

Figure 32: Femoral blood flow in both legs of rats during acute MS occlusion.

Time course of femoral blood flow in the treated leg (A) and the contralateral leg (B) as a result of an acute MS occlusion. Flow probes were positioned around the femoral arteries of each leg. Data are means ± SEM for n = 6-7. * $p<0.05$ from saline of same treatment, two-way RM ANOVA with *post-hoc* analysis using SNK method.

□ Sham-Saline, ■ Sham-Insulin, ○ MS-Saline, ● MS-Insulin

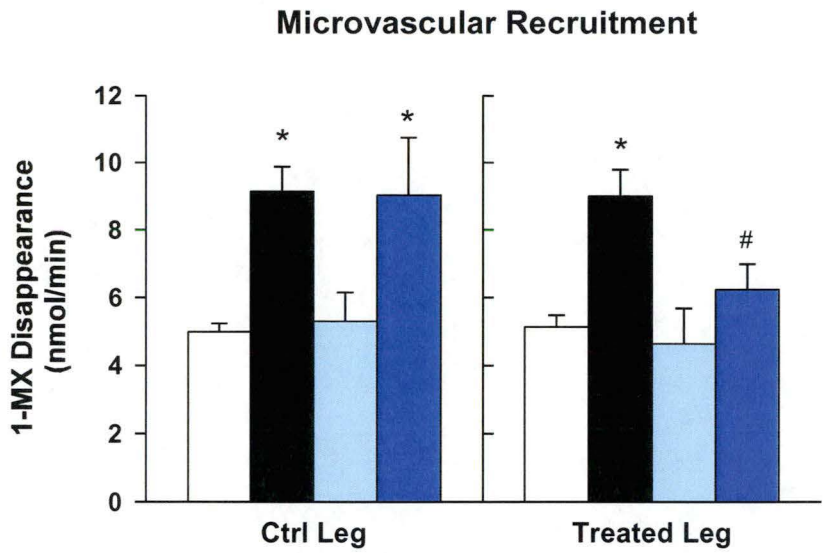

Figure 33: 1-MX disappearance during acute MS occlusion.
1-MX metabolism of the contralateral leg (left panel) and the treated leg (right panel) after an acute MS occlusion. Measurements were made at the end of a 2 hrs insulin or saline infusion. Data are means ± SEM for n = 5-6. * $p<0.05$ from saline of same treatment, # $p<0.05$ from Sham-Insulin, two-way ANOVA with *post-hoc* analysis using SNK method.
□ Sham-Saline, ■ Sham-Insulin, ■ MS-Saline, ■ MS-Insulin.

5.3.3.3 Glucose Infusion Rate and Blood Glucose

There was no significant difference in GIR between the Sham-Insulin and MS-Insulin in response to the 10 mU/kg/min insulin infusion (23.5 ± 0.9 mg/kg/min and 22.8 ± 0.7 mg/kg/min, p=0.51 respectively) (Figure 34A). Additionally, the blood glucose did not change significantly at any time point for any of the four groups (Figure 34B).

5.3.3.4 Muscle Glucose Uptake

As expected, insulin elicited an increase in the disposal of glucose into the calf muscles of the contralateral leg (Figure 35A) in both the sham and the MS groups as seen by the increased disposal of radiolabeled 2-DG.

In the treated leg, Sham-Insulin showed increased glucose uptake when compared to the Sham-Saline (Sham-Saline = 3.55 ± 0.14 μg/g/min, Sham-Insulin = 12.79 ± 1.02 μg/g/min, $p<0.001$) (Figure 35A). However, MS occlusion by itself also increased glucose disposal as seen from the significant increase in the MS-Saline when compared to the Sham-Saline (Sham-Saline = 3.55 ± 0.14 μg/g/min, MS-Saline = 11.01 ± 1.60 μg/g/min, $p<0.001$). Nevertheless, insulin still significantly increased glucose uptake in the MS-Insulin when compared to MS-Saline (MS-Saline = 11.01 ± 1.60 μg/g/min, MS-Insulin = 16.07 ± 1.00, $p<0.01$). Assessment of the insulin-mediated increase in R'g (obtained by subtraction of saline R'g from the insulin R'g), a 46 % reduction was observed in the MS treated legs when compared to the sham (5.06 ± 1.31 μg/g/min and 9.24 ± 0.76 μg/g/min, $p<0.01$ respectively) (Figure 35B).

5.3.3.5 Venous Plasma Lactate

Figure 36 shows the plasma lactate of the venous samples in the treated legs of each of the four experimental groups. In the sham experiments, insulin induced

the expected increase in lactate release. Interestingly, MS occlusion itself induced an increase in venous lactate as seen in the MS-Saline treated leg.

5.3.3.6 High-Energy Intermediates

Table 6 shows the high-energy intermediates assessed in the treated calf muscles of each group. Two results stand out. Firstly, decreases in the PCr/Cr ratio and in the total level of PCr occurred during MS occlusion, consistent with a decrease in blood delivery. Secondly, the EC was unaffected with a $3x10^6$ MS occlusion, as observed in the previous study of the dose effect of MS occlusion (Table 5).

5.3.3.7 Tibialis Anterior Muscle Fluorescence

MS entrapment was assessed by measuring the fluorescence of MS in both legs of the MS treated rats. Similar levels of fluorescence were observed in the tibialis anterior muscle extracted from the MS-Saline and MS-Insulin treated legs (MS-Saline = 4.05 ± 0.55 % of expected, MS-Insulin = 4.19 ± 1.00 % of expected, p = 0.91). No significant fluorescence was observed in the contralateral leg.

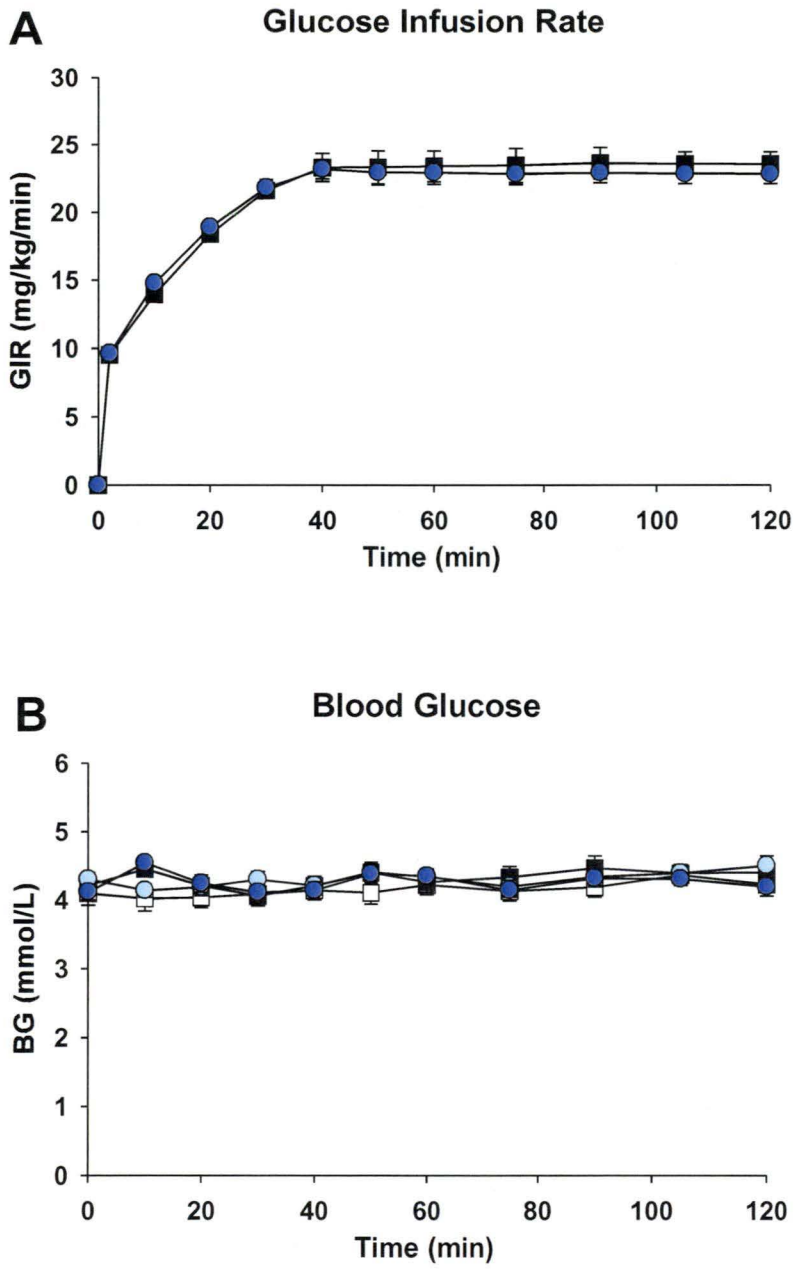

Figure 34: Glucose infusion rate and blood glucose during acute MS occlusion.

Time course for the glucose infusion rate (A) and the blood glucose concentration (B) as a result of an acute MS occlusion. Blood glucose levels were maintained at basal level (time 0 min). Data are means ± SEM for n = 6-7. Comparisons were made by a two-way RM ANOVA.

□ Sham-Saline, ■ Sham-Insulin, ● MS-Saline, ● MS-Insulin

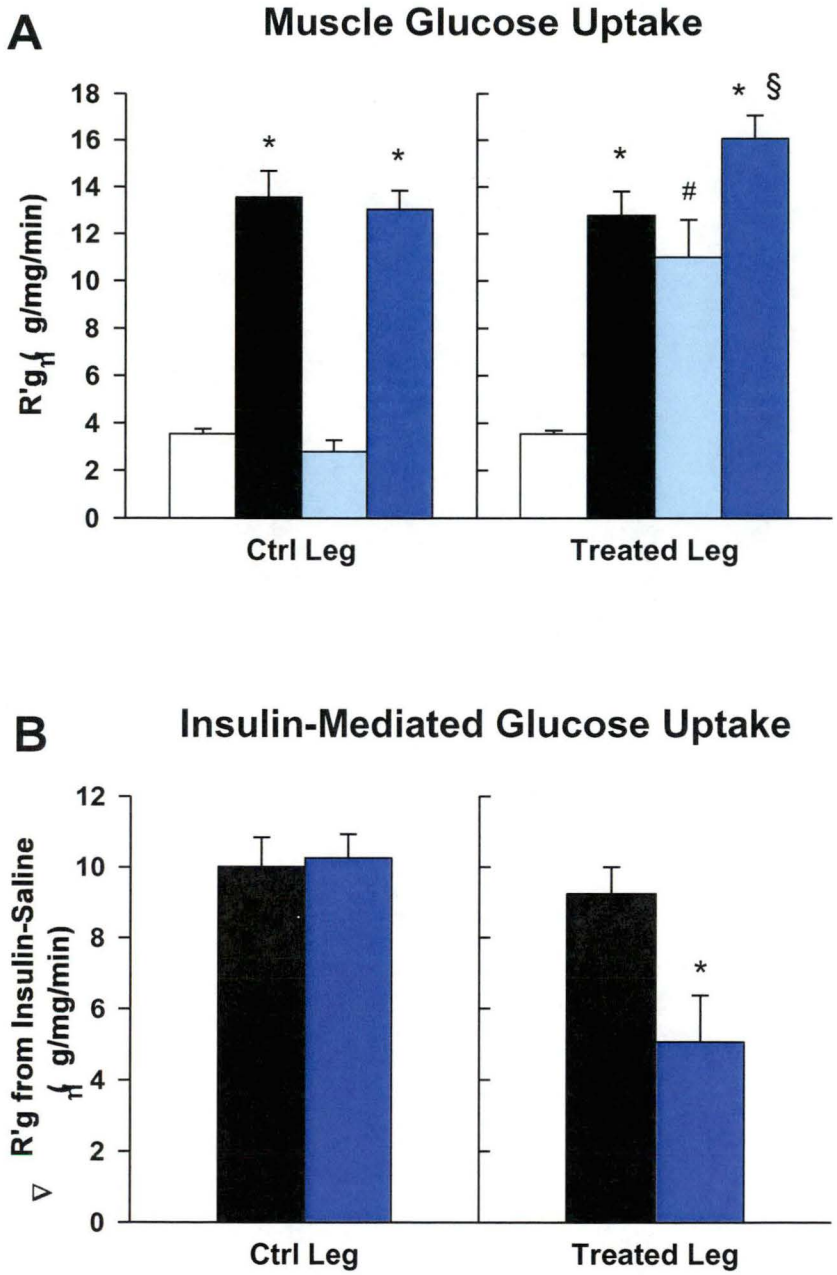

Figure 35: Muscle glucose uptake during acute MS occlusion.
(A) Muscle radioactive 2-DG uptake (R'g) for both legs of each group as a result of an acute MS occlusion. 2-DG was administered as a bolus at 75 min (Figure 6) and calf muscles were excised at the completion of the experiment. □ Sham-Saline, ■ Sham-Insulin, ■ MS-Saline, ■ MS-Insulin. (B) Insulin-mediated glucose uptake was calculated from the difference between Insulin and Saline 2-DG uptake in each treatment group. ■ Sham-Insulin minus Sham-Saline, ■ MS-Insulin minus MS-Saline. Data are means ± SEM for n = 6-7. * $p<0.05$ from saline of same treatment, # $p<0.05$ from Sham-Saline, § $p<0.05$ from Sham-Insulin, two-way ANOVA with *post-hoc* analysis using SNK method.

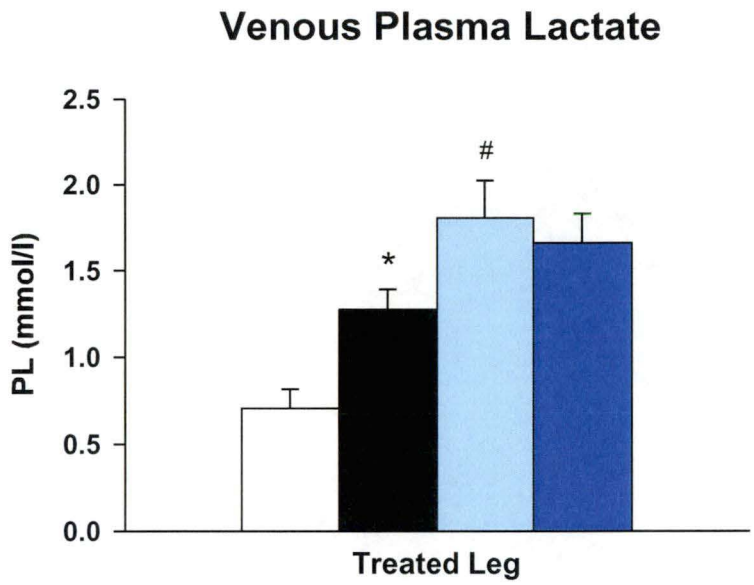

Figure 36: Venous plasma lactate in the treated leg during acute MS occlusion.

Venous plasma lactate for the treated leg in response to an acute MS occlusion. Data are means ± SEM for n = 6. * $p<0.05$ from saline of same treatment. # $p<0.05$ from Sham-Saline, two-way ANOVA with *post-hoc* analysis using SNK method.

□ Sham-Saline, ■ Sham-Insulin, ■ MS-Saline, ■ MS-Insulin.

Table 6: High-energy intermediate content of calf muscles from treated legs during acute MS occlusion.

	Sham-Saline	Sham-Insulin	MS-Saline	MS-Insulin
Dry wt/Wet wt	0.203 ± 0.007	0.211 ± 0.004	0.185 ± 0.007*	0.187 ± 0.004*
Creatine (μmol/g dry weight)	83 ± 3	83 ± 4	91 ± 9	94 ± 5
Phospho-Creatine (μmol/g dry weight)	121 ± 5	117 ± 5	92 ± 4*	91 ± 5*
PCr/Cr	1.46 ± 0.07	1.42 ± 0.07	1.06 ± 0.13*	0.97 ± 0.05*
ATP (μmol/g dry weight)	29.27 ±0.95	29.45 ± 1.04	26.85 ± 1.63	25.58 ± 1.75
ADP (μmol/g dry weight)	3.38 ± 0.06	3.28 ± 0.23	3.04 ± 0.19	2.66 ± 0.15
AMP (μmol/g dry weight)	0.49 ± 0.11	0.27 ± 0.03#	0.28 ± 0.06	0.56 ± 0.07*#
NAD (μmol/g dry weight)	3.06 ± 0.10	2.80 ± 0.09	2.67 ± 0.14	2.56 ± 0.17
Energy Charge	0.934 ± 0.004	0.942 ± 0.004	0.940 ± 0.003	0.933 ± 0.005

Data are means ± SEM for n = 6-7 rats in each group. * $p<0.05$, vs. corresponding Sham. # $p<0.05$, vs. corresponding Saline, two-way ANOVA with *post-hoc* analysis using SNK method. Calf muscles were freeze clamped then excised at the completion of each experiment.

5.4 DISCUSSION

Results of the present study indicate that physical blockage of the microvasculature can prevent both hemodynamic and metabolic actions of insulin in skeletal muscle. One of the most significant discoveries was the 46 % decrease in insulin-mediated glucose uptake resulting from the impairment of the insulin-mediated microvascular recruitment.

The MS occlusion is a more advantageous approach than pharmacological treatments as it limits the skeletal muscle microvascular recruitment directly. Pharmacological blockage of the insulin-mediated microvascular recruitment required prolonged systemic infusions (Rattigan 1999, Youd 2000, Clerk 2002, Wallis 2005), thus extra-muscular effects cannot be excluded. MS occlusion effects are limited to the skeletal muscle, as the local injection would only block the microvasculature of the lower leg muscles. Therefore, MS occlusion is the only treatment that directly and specifically targets the microvasculature of the skeletal muscle.

5.4.1 Effects of MS Occlusion on Hemodynamic Parameters

The aim of the present experimental procedure was to assess if physical occlusion of the skeletal muscle microvasculature by MS can affect the insulin actions in this tissue. As such, the first aim was to show that the insulin-mediated microvascular recruitment was indeed impaired with the presence of MS. As shown in Figure 33, insulin-mediated microvascular recruitment was prevented by the MS occlusion (MS-Saline = 4.64 ± 1.04 nmol/min, MS-Insulin = 6.23 ± 0.75 nmol/min, NS). Therefore, MS occlusion is akin to the impaired vascular actions of insulin at the terminal arterioles as seen in endothelial dysfunctional (Bakker 2009, Vanhoutte 2009). The arterioles of the fifth order, considered to be the terminal arterioles, would be the most likely to be blocked with 15μm MS (Murrant 2000). The acute physical occlusion of the terminal arterioles would mimic a functional rarefaction usually associated with impaired vasodilatory

response (Clerk 2004). Endothelial dysfunction prevents the insulin-mediated microvascular recruitment and the glucose disposal in the skeletal muscle (Baron 1997) and has been implicated in the insulin resistant state (Kim 2006, Jansson 2007). The partial occlusion of the microvasculature in the present study reduced the access of insulin to the myocyte and therefore decreases its effects to promote glucose uptake, in a similar manner to endothelial dysfunction.

The similar basal level of 1-MX metabolism (Sham-Saline = 5.13 ± 0.34 nmol/min, MS-Saline = 4.64 ± 1.04 nmol/min, p=0.65) may seem surprising given the fact that the MS occlusion will have blocked parts of the microvasculature. The explanation for this relies on the ischemic state that has been induced by the MS occlusion. Ischemia is known to increase microvascular recruitment (Parthasarathi 1999). Blocked capillary beds may cause the tissues to become ischemic and secrete factors that promote microvascular blood flow (Noon 1997, Bertuglia 2005). These secreted factors can migrate to the surrounding tissue and could act on the non-occluded terminal arterioles. These may then open, and allow previously closed capillary beds to be perfused. Therefore, the basal level of microvascular recruitment after the MS occlusion will be similar to the basal level of the sham treated leg.

Basal FBF was increased by the presence of MS (Sham = 0.82 ± 0.04 ml/min, MS = 1.34 ±0.05 ml/min, $p<0.001$) (Figure 32A). This increase in FBF may be due to an ischemic state resulting from the MS occlusion. Additionally, FBF in both the MS-Saline and MS-Insulin groups increased over time and no significant difference was evident between these two groups. Therefore, the expected insulin-mediated increase in FBF was prevented by the MS occlusion. FBF was also affected in the contralateral legs by the MS occlusion of the treated legs (Figure 32B). Insulin-mediated increase in FBF was still present in the MS-Insulin group, with a tendency of the MS-Insulin group to be increase when compared to the MS-Saline group (p=0.08 at 120 min). Hence, insulin may have failed to induce a significant increase in FBF when the microvasculature was occluded.

5.4.2 Effects of MS Occlusion on Metabolic Parameters

The most significant finding from the present study is that prevention of the insulin-mediated microvascular recruitment led to a 46 % decrease in insulin-mediated glucose uptake (Figure 35B). It is important to acknowledge that an increased glucose disposal was observed during the MS occlusion itself, as showed by a significant increase in R'g in MS-Saline compared to Sham-Saline (Sham-Saline = 3.55 ± 0.14 μg/g/min, MS-Saline = 11.01 ± 1.60 μg/g/min, $p<0.001$). This effect can be attributed to ischemia. As the muscle begins to rely more on anaerobic metabolism, an increase in glucose uptake occurs in order to sustain the metabolic needs of the muscle. As a consequence, the level of glucose uptake in the MS-Saline increases to a similar extent as the insulin response in the sham group (Sham-Insulin = 12.79 ± 1.02 μg/g/min, MS-Saline = 11.01 ± 1.60 μg/g/min, NS). Insulin and ischemia have been reported to have an additive effect on glucose uptake (Azevedo 1995). Therefore, the effect of insulin alone can be calculated by subtracting the glucose uptake of the MS-Saline (ischemia-mediated glucose uptake) from the glucose disposal of the MS-Insulin (ischemia- and insulin-mediated glucose uptake). Thus, levels of insulin-mediated glucose uptake were decreased during MS occlusion (Figure 35B). Therefore, occlusion of the microvasculature reduced the insulin-mediated glucose uptake, creating an acute state of vascular-derived insulin resistance.

The unchanged basal blood glucose and the normal GIR (Figure 34) indicate that whole body insulin sensitivity was unaffected. This was not surprising as only a portion of the muscle mass of the treated leg would be affected by local MS occlusion, leaving the remainder of the muscle mass available for the actions of insulin.

5.4.3 MS Occlusion and Other Acute States of Vascular Derived Insulin Resistance

It is interesting to compare data of the present study to the effects of acute infusion of TNF-α. The levels of this cytokine have been observed to increase in the insulin resistant state (Hotamisligil 1995, Hotamisligil 1999, Xu 2002, Torres 2004) and have been shown to prevent insulin's intracellular signalling at different levels (Plomgaard 2005, Li 2007). Studies using a one hour pre-infusion of TNF-α before a hyperinsulinaemic clamp have impaired the insulin-mediated microvascular recruitment (Youd 2000). It was also observed that the insulin-mediated increase in FBF and microvascular recruitment was fully blunted, with a concomitant decrease of approximately 50 % of the insulin-mediated glucose uptake. Comparison between TNF-α infusion and MS occlusion revealed that only the GIR was different. Interestingly, TNF-α infusion induced a 21 % decrease of the GIR while MS occlusion did not have significant effect on the GIR. As the TNF-α infusion was systemic it would have affected the entire muscle mass, while the MS occlusion was local and limited to the muscles of one leg. Moreover, extra-muscular systemic effects of TNF-α cannot be excluded. TNF-α effects on liver (Lang 1992) and/or adipose tissue (Hotamisligil 1994) could have occurred, resulting in a decrease in the GIR. MS occlusion effects would be limited to the skeletal muscle, as the local injection would restrict the blockage to the microvasculature of the lower leg muscles. Therefore, the MS occlusion provides a novel and more direct model for determining the microvascular contribution to muscle insulin resistance.

The similarities between MS occlusion and TNF-α infusion are also reflected in other acute states of vascular derived insulin resistance. Indeed, α-methylserotonin (Rattigan 1999), increased circulating FFA (Clerk 2002), and glucosamine (Wallis 2005) have all been shown to block the insulin-mediated microvascular recruitment and as much as 50 % of the insulin-mediated glucose disposal. Similar to the TNF-α infusion, these treatments also impaired the systemic action of insulin, as evidenced by decrease in the GIR during the insulin

clamp procedure. MS occlusion is then the only treatment that directly and specifically targets the microvasculature of the skeletal muscle.

5.4.4 MS Occlusion Induced Ischemia

As described above, it was also apparent that a mild ischemic state had been created by the MS occlusion of the muscle microcirculation. Ischemia occurs when the supply of arterial blood is insufficient to maintain the metabolic needs of the tissue. This results in a shift toward anaerobic metabolism to maintain the ATP levels required for normal function of the skeletal muscle. Three parameters clearly indicate that an ischemic state was induced by the MS occlusion. First, there was a decrease in the PCr/Cr ratio (Table 6). This parameter is frequently used as an indicator of blood delivery to the skeletal muscle (Ye 1996). Myocytes utilize their PCr store to maintain a constant ATP level (Boron 2003). As the selection for the dose of MS was made based on a decrease in PCr/Cr ratio, this decrease was anticipated (Table 5). The second marker of ischemia is the presence of oedema, as seen by a slight but significant decrease in the dry weight/wet weight ratio (Table 6). Accumulation of water in the interstitial space is a known consequence of ischemia, resulting from a change of hydrostatic pressure and increased permeability of capillaries (Kasner 1997). The third indicator of ischemia is the increase in lactate production (Figure 36). As the basic metabolic needs of the ischemic muscle shift from oxidative phosphorylation to glycogen metabolism, there is an increase in the amount of lactate released. Overall, these parameters indicate that an ischemic state resulted from MS occlusion. Insulin action during the MS occlusion must then be analysed with regard to the effect of the ischemia *per se*. Correspondingly, comparisons with the MS-Saline were made in order to assess the effect of insulin alone during the partial occlusion of the skeletal muscle microvasculature.

5.4.5 MS Occlusion: *In vivo* vs. Perfused Hindlimb

Previous studies of hindlimb perfusion preparations established the effect of MS occlusion on insulin-mediated glucose uptake (Vollus 2007). In this preparation, MS occlusion prevented the insulin-mediated glucose uptake. While hindlimb perfusion generated very interesting data, it still represents an *in situ* preparation where the vasculature is fully dilated, and as such, may not accurately represent the normal *in vivo* blood flow distribution. Therefore, the assessment the MS occlusion in an *in vivo* model was critical to our understanding of the physiological importance of the microvasculature in insulin-mediated glucose disposal.

In the *in vivo* model, similarly to the hindlimb perfusion, presence of MS in the skeletal muscle microvasculature prevented the insulin-mediated glucose uptake (Figure 35). Thus, both models provide support for a role of the microvasculature in insulin-mediated glucose uptake. However, the hindlimb perfusion differs from the *in vivo* in its effect of the occlusion on basal glucose uptake. The basal level of glucose uptake in the hindlimb perfusion was unaffected (Vollus 2007) whereas an increase in glucose uptake occurs in the *in vivo* model in response to the ischemic state (Figure 35A). As there was an increase in phosphorylation of AMPK in the perfused hindlimb, this is indicative of a degree of ischemia. One explanation for the difference in basal glucose uptake could the lower temperature of the perfusion setting (32°C). Temperature would affect the rate of metabolism, while the delivery of insulin is only important in insulin-mediated glucose uptake. However, it is more likely that the difference results from different microvascular distribution of the MS in the two systems. In the hindlimb perfusion, MS were injected over 2 sec in the descending aorta while in the *in vivo* model a retrograde injection over 10 sec was made in the epigastric artery. This means that MS would have lodged in a much larger muscle mass in the hindlimb perfusion and than in the *in vivo* model, where the MS would be localised in the lower leg muscle. This divergence in the muscle localisation of the MS could be responsible for the difference in basal glucose uptake.

Differences were also observed between the models in the high-energy intermediates content. In the perfused hindlimb, all doses of MS decreased the PCr/Cr ratio in a dose dependent fashion (Vollus 2007), while in the *in vivo* model the PCr/Cr ratio was affected only at the higher doses of 3 and 7 $x10^6$ MS (Table 5). Furthermore, the EC remained unchanged in the hindlimb perfusion while a significant decrease was observed *in vivo* at the highest dose of 7 $x10^6$ MS. A plausible explanation might reside in the time of the muscle excision. In the perfused hindlimb experiments, the high-energy intermediate determinations were made 10 min post-occlusion, while 3 hours had passed in the *in vivo* model. 10 min is unlikely to affect the EC. However, the increases in AMPK phosphorylation in the perfused muscle indicate that an ischemic state may have been created. In addition, distinctions in the high-energy intermediate may also results from the perfusion states of each model. The vasculature in the hindlimb perfusion preparation represents a fully perfused state while only a third of the microvasculature is perfused at the basal level in the *in vivo* model (Honig 1982). This means that even with the occlusion of some of the vessels in the hindlimb perfusion, the majority of vessels still received glucose preventing a decrease in the EC. The *in vivo* occlusion may prove more important in terms of microvascular delivery than in the hindlimb perfusion. Furthermore, as discussed above, the divergence in injection site and the subsequent difference in muscle leg localisation may also be responsible for the difference in the high-energy intermediates content. All of these factors could explain the different high-energy intermediates results. Nevertheless, both preparations showed an impairment of insulin-mediated glucose uptake during MS occlusion of the microvasculature.

5.4.6 Study Design and Future Experiments

Limitations of the present study design need to be acknowledged. One of these is how the dose of MS to be injected was determined. While the determination was based on many parameters (high-energy intermediate profile, microvascular recruitment, impaired insulin-mediated glucose uptake in the hindlimb perfusion),

the effect on the basal blood flow should have been considered more. The ideal dose of MS would have been one that would have eliminated the insulin-mediated microvascular recruitment without affecting the resting blood flow. However, the lower dose of $1.5x10^6$ MS failed to prevent the insulin-mediated microvascular recruitment. Further experiments using higher doses of MS (2.0 and $2.5x10^6$ MS) should be done to assess if the insulin-mediated microvascular recruitment can be blocked without affecting the basal FBF. Another limitation of the present study is the lack of information about the spatial distribution of the injected MS. This limitation could be resolved by observing the three-dimensional distribution of individual MS in representative muscles using a Fluorescent Imaging CryoMicrotome (Vincent 2001). This would also enable the assessment of the histological effects of the MS occlusion on the surrounding tissue (i.e. inflammatory response, necrosis, etc).

The question of the route occluded (nutritive vs. non-nutritive) by the MS is a critical component of the present study. Another limitation of the study design is that the injection of the MS was done in the basal state when mostly the non-nutritive route is considered to be perfused (Clark 2000). As the insulin-mediated glucose uptake occurs principally in the nutritive route, injection of MS at rest may not have sufficiently blocked this route. This issue was partly addressed by preventing the access of blood to the foot during the MS injection. Preliminary experiments have shown that epigastric artery injection of MS in the unrestrained state failed to localise the MS within the lower leg muscles. Using a haemostatic clamp, blood flow passing through the large shunt vessels in the foot was prevented. Therefore, the MS were redirected toward the leg muscles. Although the actual route that the blood flow is redirected to is unknown, an increased proportion of the nutritive route of the skeletal muscle would likely have been perfused, and subsequently blocked by the MS injection.

Since in the present design it is unknown which flow route was blocked, future studies targeting the occlusion of the nutritive route could be undertaken. This

could be achieved in two ways. First, by stimulating an increase in microvascular recruitment with insulin prior to MS injection. This would have the advantage of blocking the vessels that are recruited by insulin. Another way would be to make the muscle contract using electrical stimulation as the nutritive route is known to be recruited during muscle contraction (Clark 2000). Overall, both stimuli would enable a more direct assessment of a blockage of the nutritive route on the insulin-mediated glucose uptake. More targeted blockage of the nutritive route may require less MS, and as such, decrease the ischemic response currently seen. This would allow for clearer interpretations of insulin-mediated muscle glucose disposal.

Overall, this study demonstrated the importance of the microvasculature as a target for insulin action. By preventing the insulin-mediated increase in skeletal muscle microvascular recruitment, insulin-mediated glucose uptake was decreased. Therefore, acute MS occlusion can be viewed as a functional defect, mimicking the initial stage of insulin resistance. This model provides a paradigm for examining the effects of long-term impairment of microvascular recruitment in relation to the development of metabolic insulin resistance within skeletal muscle and type 2 diabetes.

CHAPTER 6:

CHRONIC EFFECT OF MICROSPHERE OCCLUSION

6.1 INTRODUCTION

Skeletal muscle is a prime target for early defects in the development of insulin resistance (Reaven 1988, Defronzo 1991), although the exact mechanisms remain largely unknown. That myocyte insulin resistance occurs in fully established type 2 diabetes is without question (Defronzo 1985, Zierath 1998, Ryder 2001, Karlsson 2007). However it is not clear whether myocyte insulin-signalling defects are the sole cause of skeletal muscle insulin resistance (Karlsson 2007). There is evidence that vascular dysfunction precedes, and may contribute to the development of insulin resistance in the muscle (Jansson 2007, Serne 2007).

Impairment of insulin signalling in the vasculature has been shown to precede skeletal muscle insulin resistance (Youngren 2001, Kim 2008). Impairment in insulin-mediated Akt phosphorylation in endothelial cells occurs after two weeks of HFD feeding, while four weeks feeding is needed for this impairment to be present in the skeletal muscle. Furthermore, diminished NO signalling, responsible for the vasodilatation action of insulin in first-order arterioles from the gastrocnemius muscle, precede the development of diabetes and hypertension in ZDF rats (Lesniewski 2008). These findings indicate that loss of insulin action in vasculature precedes the muscle insulin resistance.

Decreased insulin action in the vasculature will affect the insulin-mediated microvascular recruitment. Impairment in insulin-mediated microvascular recruitment is present in animal models of type 2 diabetes (Wallis 2002, Clerk 2007) and in obese patients (Clerk 2006), as well as in the early stage of insulin resistance, as shown in chapter 3. Impairment of insulin-mediated microvascular recruitment as an early event may be responsible for the development of whole body insulin resistance in the later stage of type 2 diabetes (Defronzo 1985).

Pharmacological blockages of the insulin-mediated microvascular recruitment have also been shown to impair more than 50% of the insulin-mediated skeletal

muscle glucose uptake (Rattigan 1999, Youd 2000, Clerk 2002, Wallis 2005). These treatments required systemic infusion and have been shown to affect tissues other than the skeletal muscle, therefore they are not ideal for chronic study of the muscle microvasculature. A more appropriate model would be the MS occlusion of the skeletal muscle microvasculature. As shown in the previous chapter, physical blockage of the skeletal muscle microvasculature led to an acute vascular-derived state of insulin resistance. This model used chronically could help inform on the importance on the microvasculature in the development of muscle and myocyte insulin resistance.

Therefore, the present study aims to assess the effects of a chronic impairment of insulin-mediated microvascular recruitment on skeletal muscle insulin sensitivity. The hypothesis is that an impairment of the skeletal muscle microvasculature would lead to the myocyte insulin resistance seen in fully established type 2 diabetes.

6.2 MATERIAL AND METHODS

6.2.1 Recovery Surgery

Hooded Wistar rats weighing 250 grams were anesthetised using a Stinger apparatus (Advance Anaesthesia Specialist, Sydney, Australia). Rats were placed in a bucket with lid where the tube of the Stinger was inserted. The oxygen rate was at 4 l/min and the isoflurane vaporiser (1ml/ml, VCA, NSW, Australia) set at 4 %. Once the rat was unresponsive to touch, it was transferred to the preparation area. The nozzle of the anaesthetic apparatus was placed over the head of the rat and the oxygen rate was set at 0.8 l/min and the anaesthetic vaporiser at 2 % for the remainder of the procedure. The left leg was shaved and cleaned with the antiseptic solution Benamine (7.5 % w/v Povidone-Iodine, Faulding Pharmaceuticals, Australia). The animal was then transferred to the surgery table for the remaining of the procedure. A sterile cloth, containing a small window for leg access, was placed over the rat. A small incision of about 1

cm was made on the overlying skin of the femoral vessels. The epigastric artery cannulation for the $3x10^6$ MS injection was undertaken as described in section 5.2.3. Since this experiment required recovery surgery, special care was taken to ensure the sterility of the procedure and reduce the risk of post-surgery complications.

Once the MS injection procedure was completed, the wound was closed using a braided polyglycolic acid synthetic absorbable surgical suture (3-0 Dexon II, Sherwood Medidal, USA). The animal was then removed from the isoflurane inhalation apparatus, and allowed to recover in a 32°C heated cage. Thereafter, rats were housed two per cage for a period of 2 weeks and were monitored throughout the recovery process. Of note, no observable ill effects from the procedure, such as loss of mobility or necrosis, were observed in any of the animals used. They were kept as described in section 2.1.

At the end of the 2 weeks chronic occlusion, rats weighed 291 ± 3 g, with no significant difference between sham and MS treated animals. Rats used in these experiments were not fasted, as the determination of whole body glucose kinetics was not required.

6.2.2 *In vivo* Surgery

Two weeks post-injection, *in vivo* experiments were conducted using the anaesthetised rat model, with surgery as described in section 2.2.1.

6.2.3 Experimental Procedure

The chronic effect of MS embolism on the skeletal muscle microvasculature was assessed during an isoglycaemic hyperinsulinaemic clamp as described in section 2.2.2. Briefly, 1-hour after the surgical procedure, saline or insulin (10 mU/min/kg) was infused into the rat and continued for 2 hours (Figure 6). During experiments involving insulin infusion, a glucose solution (30 % w/v)

was also infused at variable rates to maintain blood glucose levels at around basal levels. Femoral artery blood flow was continuously measured with a Transonic® flow probe positioned around the femoral artery of both the treated and the contralateral legs. 1-MX disappearance was used as an indicator of perfused capillary surface area as described in section 2.2.3.5. A bolus dose of [^{3}H] 2-DG (50 μCi) was given 45 min before the end of the experiment. Calf muscles were excised at the completion of the experiment and freeze clamped in liquid nitrogen to assess the 2-DG uptake as described in section 2.2.3.3.

6.2.3.1 High-Energy Intermediates

Powdered calf muscles were used to assess the high-energy intermediates. Extraction and measurement were done as described in section 2.2.3.7.

6.2.3.2 Fluorescence

Tibialis anterior muscle from both legs were excised at the end of the experimental procedure and kept at -20 °C until the fluorescence was assessed as described in section 5.2.4.2.

6.2.4 Data Analysis

All data are expressed as means ± SEM. Data were calculated as described in section 2.2.4. Comparisons were made between treatment groups over the course of the experiment using two-way non-repeated or repeated-measures ANOVA with Student-Newman-Keuls *post hoc* test as mentioned in the corresponding figure legend. All tests were performed using the SigmaStat statistical program (Systat Software Inc, CA, USA).

6.3 RESULTS

Four experimental groups were used to assess the effects of MS occlusion on the insulin-mediated glucose uptake. The first two groups received the sham operation two weeks prior to either a saline infusion (□ Sham-Saline) or a 10 mU/kg/min insulin infusion (■ Sham-Insulin). The other two groups received an epigastric injection of 3 x10^6 MS two weeks prior to either a saline (○ MS-Saline) or a 10 mU/kg/min insulin infusion (● MS-Insulin). As such, the Sham groups were used as controls for the effects of the MS occlusion.

6.3.1 Hemodynamic Parameters

Figure 37 shows the MAP and HR after saline or insulin infusion in both the sham and MS treated groups. In all groups, no significant change in MAP or HR occurred, except for a slight significant increase from basal of MAP in the MS-Insulin group after 120 min of experiment (Figure 37A).

6.3.1.1 FBF in Treated Leg

FBF in the treated legs are shown in Figure 38A. In the sham animals, there was no change in FBF during the saline infusion. An increase in the FBF occurred after 40 min in the Sham-Insulin group, with a significant difference from Sham-Saline from that point onward.

Similar results were obtained in the chronically MS occluded legs, with an insulin-mediated increase in FBF at 30 min onward in the MS-Insulin group, which was significantly different from the MS-Saline group from 50 min onward.

6.3.1.2 FBF in Contralateral Legs

In the contralateral leg (Figure 38A), insulin induced increase in FBF in both Sham-Insulin and MS-Insulin groups from 30 min onward. These increases were

significantly increased from their respective saline group at 40 min onward for the Sham-Insulin and at 75 min onward for the MS-Insulin.

6.3.2 Microvascular Recruitment

Figure 39 depicts the microvascular recruitment at the end of the 2 h experiment in all four groups, for both the contralateral and the treated legs. In the contralateral leg of all groups, the expected insulin-mediated increase in microvascular recruitment was apparent when compared to the corresponding saline group. In the treated leg, Sham-Insulin had a significant increase in microvascular recruitment compared to the Sham-Saline (Sham-Saline = 5.02 ± 0.90 nmol/min, Sham-Insulin = 10.33 ± 1.33 nmol/min, $p<0.01$). Unexpectedly for a MS occlusion model, an insulin-mediated increase in microvascular recruitment was also observed in the MS treated leg (MS-Saline = 6.29 ± 0.60 nmol/min, MS-Insulin = 9.47 ± 1.57 nmol/min, $p<0.05$). This implies that the chronic presence of MS does not impair insulin-mediated microvascular recruitment, in contrast to what was observed in the acute occlusion (Figure 33).

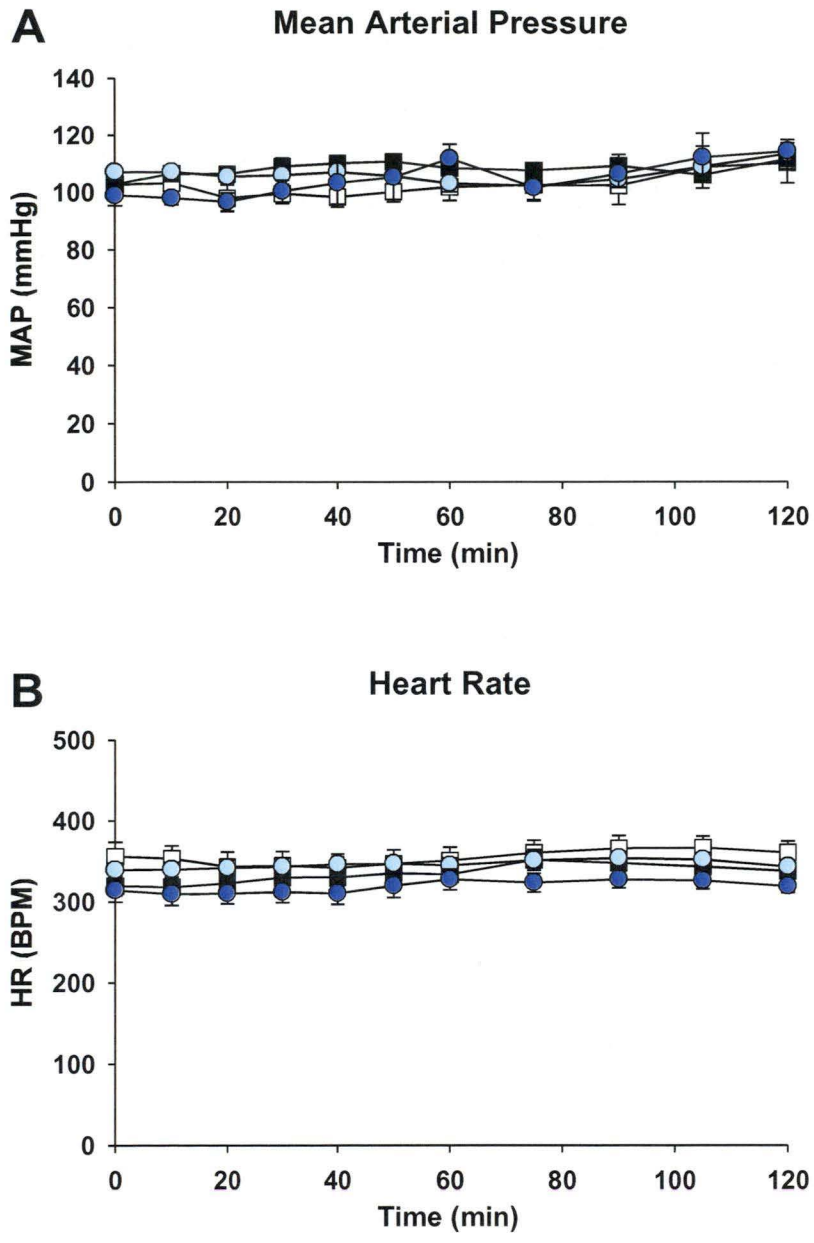

Figure 37: Mean arterial pressure and heart rate in chronic MS treated rats.

Time course for mean arterial pressure (A) and heart rate (B) as a result of a chronic MS occlusion. Data are means ± SEM for n = 6-8. Comparisons were made using two-way RM ANOVA.

□ Sham-Saline, ■ Sham-Insulin, ○ MS-Saline, ● MS-Insulin.

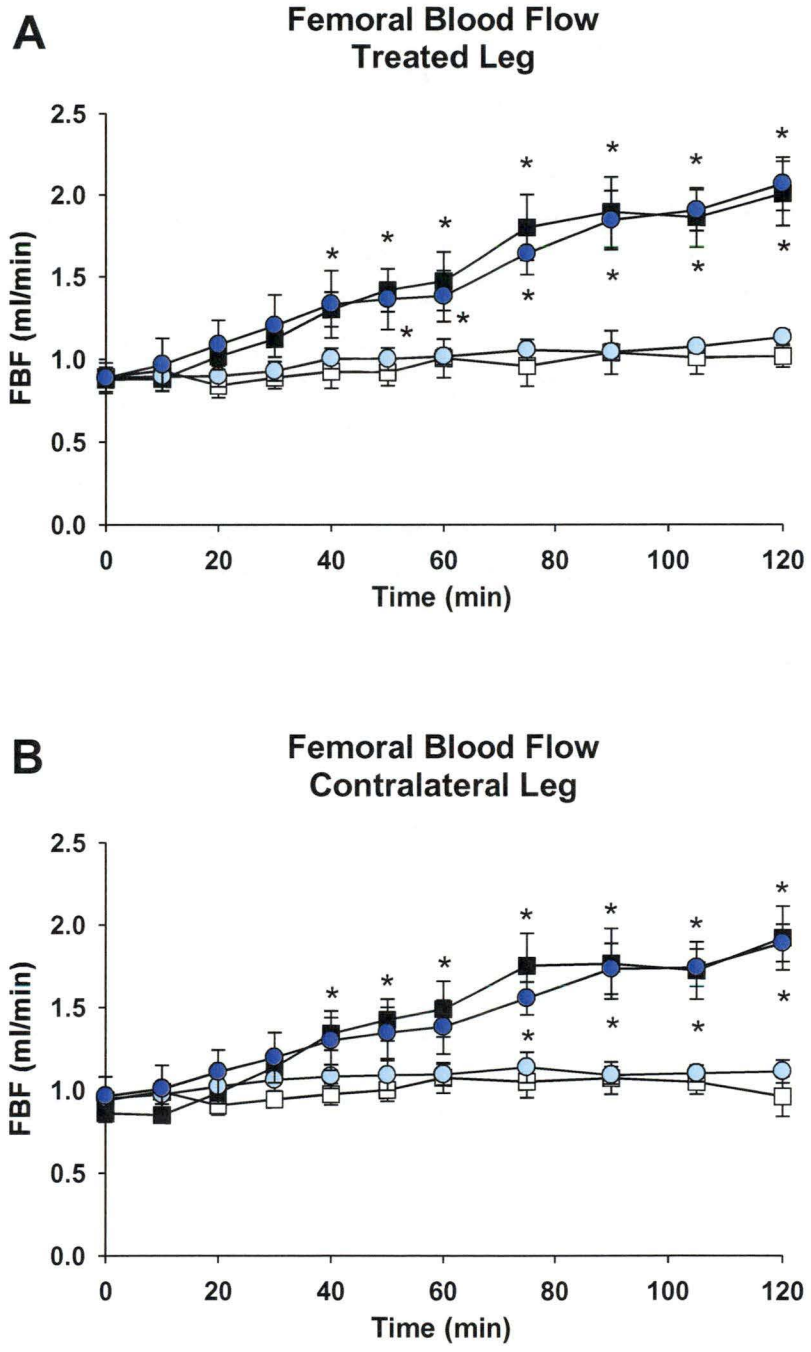

Figure 38: Femoral blood flow in chronic MS treated rats.
Time course of femoral blood flow in the treated leg (A) and the contralateral leg (B) as a result of a chronic MS occlusion. Data are means ± SEM for n = 6-8. * $p<0.05$ from saline of same treatment, two-way RM ANOVA with *post-hoc* analysis using SNK method.
□ Sham-Saline, ■ Sham-Insulin, ○ MS-Saline, ● MS-Insulin.

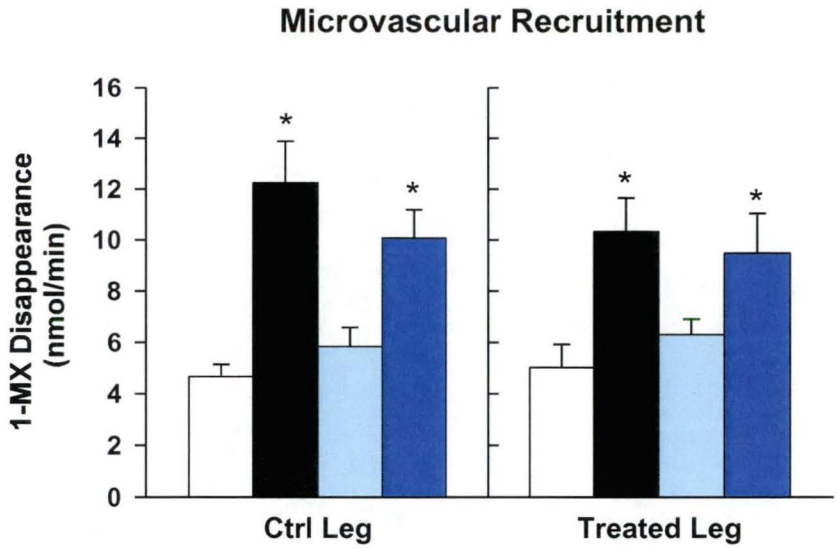

Figure 39: Microvascular recruitment in chronic MS treated rats.
1-MX metabolism of the contralateral leg (left panel) and the treated leg (right panel) after an chronic MS occlusion. Measurements were made at the end of a 2 hrs insulin or saline infusion. Data are means ± SEM for n = 6-8. * $p<0.05$ from saline of same treatment, two-way ANOVA with *post-hoc* analysis using SNK method.
□ Sham-Saline, ■ Sham-Insulin, ◦ MS-Saline, • MS-Insulin.

6.3.3 Glucose Infusion Rate and Blood Glucose

There was no significant difference in GIR between the Sham-Insulin and MS-Insulin groups in response to the 10mU/kg/min insulin infusion (20.6 ± 0.9 mg/kg/min and 21.9 ± 1.4 mg/kg/min, p=0.43 respectively) (Figure 40A). Blood glucose did not significantly change in any of the groups, except for a small increase from basal in the Sham-saline group from 90 min onward (Figure 40B).

6.3.4 Muscle Glucose Uptake

As expected in the contralateral leg, insulin elicited an increase in glucose uptake into the calf muscles (Figure 41) in both the sham and the MS groups, as seen by the increased disposal of radiolabeled 2-DG. In the treated leg, glucose uptake in both the sham and MS groups responded normally to the insulin infusion. While surprising in an occlusion setting, it is consistent with the preserved effect of the increased microvascular recruitment by insulin (Figure 39).

6.3.5 Plasma Lactate

No change in venous plasma lactate concentration was observed 14 days after the MS treatment (Figure 42). Insulin increased lactate release to the same extent in both sham and MS treated legs.

6.3.6 Tibialis Muscle Fluorescence

Fluorescence was assessed in the tibialis anterior muscle of both legs of MS treated rats. As seen in Figure 43, levels of fluorescence after 2 weeks occlusion were similar to those observed in the acute treatment (Acute MS = 4.12 ± 0.57 % of expected, Chronic MS = 3.30 ± 0.70% of expected, p = 0.37).

6.3.7 High-Energy Intermediates

As seen in Table 7, the high-energy intermediates were not affected by the chronic presence of MS. The decrease in PCr, PCr/Cr ratio and dry weight/wet weight ratio observed in the acute MS occlusion (Table 6) were absent in the chronic occlusion.

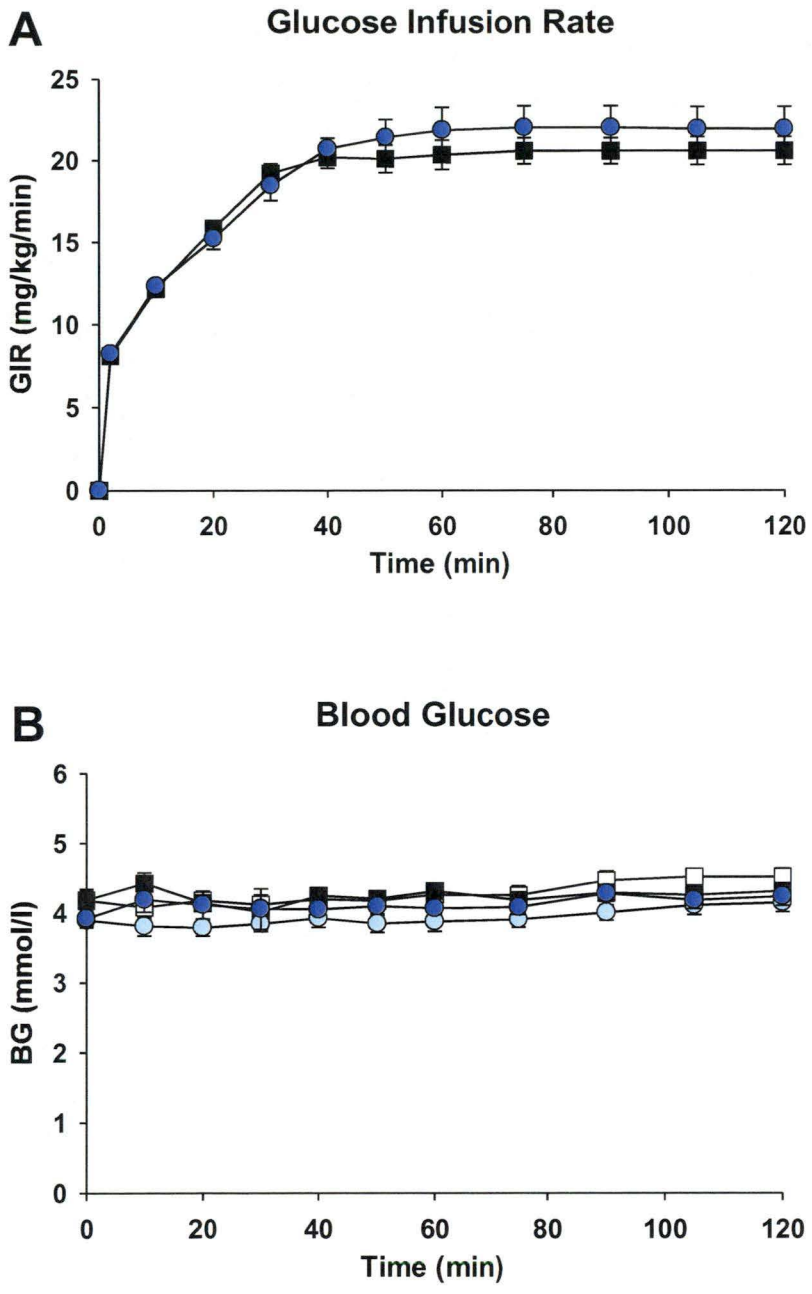

Figure 40: Glucose infusion rate and blood glucose in chronic MS treated rats.

Time course for the glucose infusion rate (A) and the blood glucose concentration (B) as a result of a chronic MS occlusion. Blood glucose levels were maintained at basal level (time 0 min). Data are means ± SEM for n = 6-8. Comparisons were made by a two-way RM ANOVA with *post-hoc* analysis using SNK method.

□ Sham-Saline, ■ Sham-Insulin, ○ MS-Saline, ● MS-Insulin.

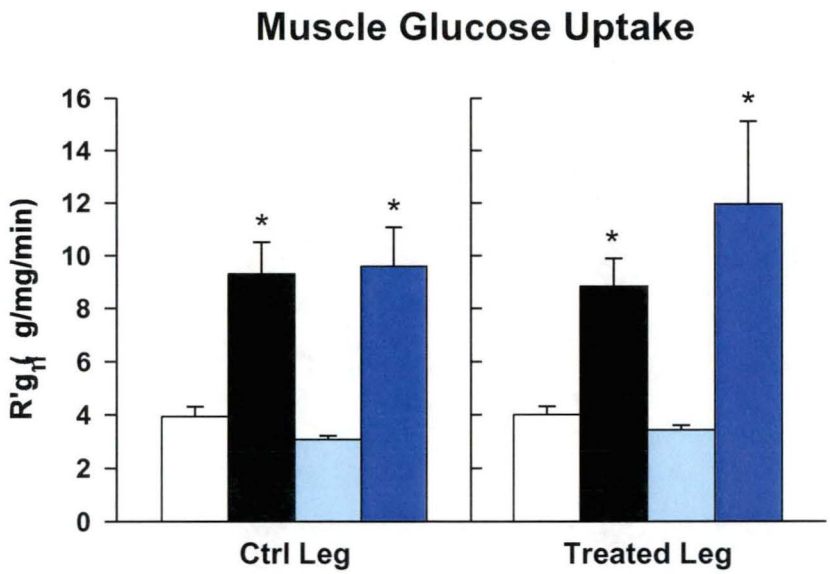

Figure 41: Muscle glucose uptake in chronic MS treated rats.
Muscle radioactive 2-DG uptake (R'g) for the contralateral leg (left panel) and the treated leg (right panel) of each group as a result of a chronic MS occlusion. 2-DG was administered as a bolus at 75 min (Figure 6) and calf muscles were excised at the completion of the experiment. Data are means ± SEM for n = 6-8. * $p<0.05$ from saline of same treatment, two-way ANOVA with *post-hoc* analysis using SNK method.
□ Sham-Saline, ■ Sham-Insulin, ◦ MS-Saline, • MS-Insulin.

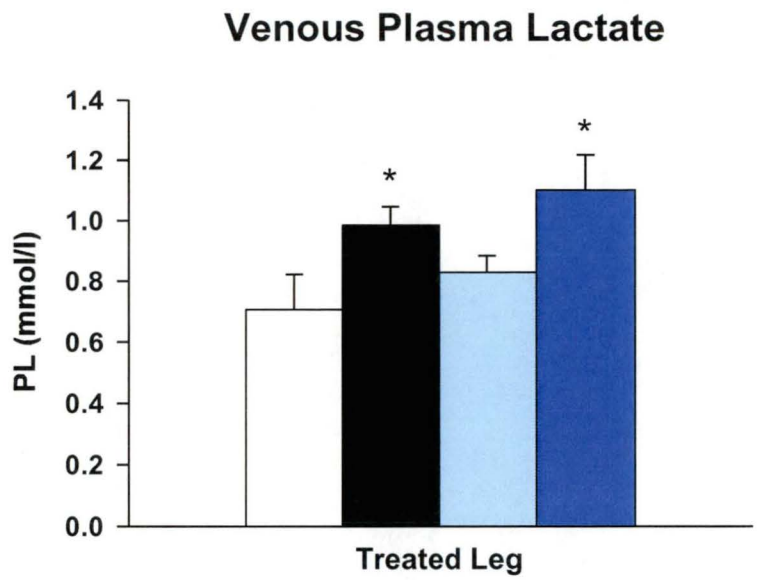

Figure 42: Venous plasma lactate in the treated leg during chronic MS occlusion.
Venous plasma lactate for the treated leg in response to a chronic MS occlusion. Data are means ± SEM for n = 6-8. * $p<0.05$ from saline of same treatment, two-way ANOVA with *post-hoc* analysis using SNK method.
□ Sham-Saline, ■ Sham-Insulin, ◦ MS-Saline, • MS-Insulin.

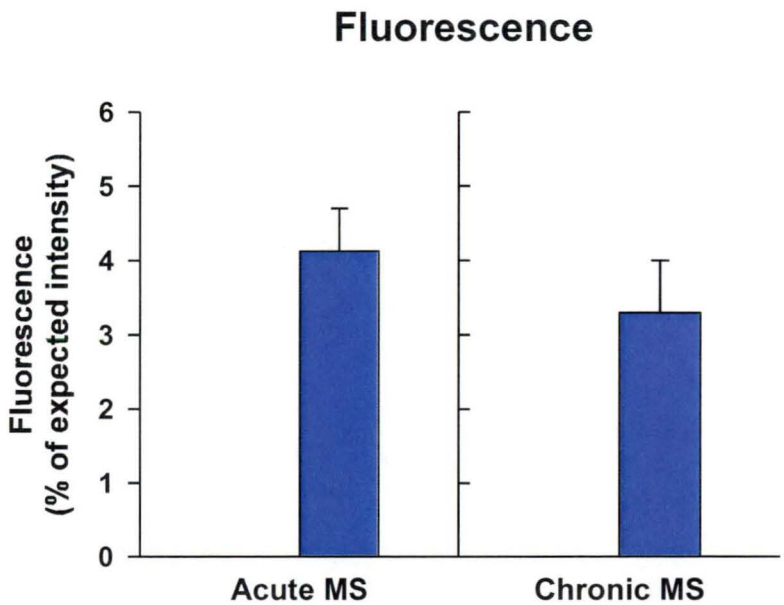

Figure 43: Tibialis anterior fluorescence in acute and chronic MS occlusion.
Fluorescence intensity of the tibialis anterior for the contralateral leg (□) and the MS treated leg (■) in response to an acute (left panel) and a chronic (right panel) MS occlusion. Fluorescence of MS-Saline and MS-Insulin were combined to compare the acute and the chronic models. Data are means ± SEM for n = 11. Comparisons were made with a one-way ANOVA.

Table 7: High-energy intermediate content of calf muscles from treated legs following chronic MS occlusion.

	Sham-Saline	Sham-Insulin	MS-Saline	MS-Insulin
Dry wt/Wet wt	0.206 ± 0.007	0.212 ± 0.003	0.206 ± 0.004	0.202 ± 0.007
Creatine (μmol/g dry weight)	74 ± 6	66 ± 2	68 ± 3	69 ± 6
Phospho-Creatine (μmol/g dry weight)	121 ± 4	111 ± 3	119 ± 0.04	105 ± 8
PCr/Cr	1.67 ± 0.12	1.67 ± 0.08	1.77 ± 0.06	1.54 ± 0.14
ATP (μmol/g dry weight)	29.46 ± 1.13	26.23 ± 0.40	29.76 ± 1.11	26.40 ± 2.14
ADP (μmol/g dry weight)	3.12 ± 0.24	3.30 ± 0.12	3.66 ± 0.18	3.22 ± 0.27
AMP (μmol/g dry weight)	0.51 ± 0.10	0.36 ± 0.07	0.30 ± 0.04	0.31 ± 0.08
NAD (μmol/g dry weight)	3.00 ± 0.09	2.66 ± 0.08	3.04 ± 0.12	2.67 ± 0.24
Energy Charge	0.937 ± 0.004	0.933 ± 0.002	0.937 ± 0.002	0.936 ± 0.002

Data are means ± SEM for n = 6-8 rats in each group. Comparisons were made with a two-way ANOVA. Calf muscles were freeze clamped then removed from rats at the completion of each experiment.

6.4 DISCUSSION

The main observation from the current study was that chronic MS occlusion of the skeletal muscle microvasculature did not result in skeletal muscle insulin resistance. The lack of myocyte insulin resistance resulting from the occlusion does not mean that the microvasculature is not important. After the 2 week treatment, occluded muscle had adapted to the condition and impaired microvascular recruitment was no longer apparent.

The indication of a reversal of the MS occlusion comes from the normal insulin-mediated microvascular recruitment in the chronic model, contrasting with the impairment in the acute model of MS occlusion. Consequently, the decrease in insulin-mediated glucose uptake observed in the acute model was not conserved after 2 weeks of recovery, leading to normal insulin responses. The insulin-mediated effects on metabolism, as seen with GIR, HGU and muscle R'g, and the vascular responses FBF and 1-MX disappearance, were unaffected by a chronic MS occlusion. Further differences to the acute model were also noted. All signs of ischemia indentified in the acute model (decreased PCr/Cr ratio, decreased dry weight/wet weight ratio, increased muscle lactate production and increased basal FBF) were absent in the chronic MS occlusion model.

A possible explanation for the loss of occlusion in the chronic MS model could be that the MS are no longer localised within the skeletal muscle. Entrapment of the MS was verified by the inclusion of fluorescent MS in the 3 x 10^6 MS mix. Fluorescence analysis revealed that the MS were still present within the tibialis anterior muscle 2 weeks post-injection (Figure 43). Furthermore, the extent of the fluorescence was similar to the level recovered in the acute model. This means that the fluorescent MS are still present to a similar extent as in the acute model.

It is likely that the muscles have adapted to the chronic MS occlusion by inducing the growth of new vessels, a phenomenon called angiogenesis (Brown

2003, Bloor 2005, Ferrara 2009). Growth of new vessels may have bypassed the occluded vessels and reversed the decreased microvascular blood delivery. Such an adaptation to the chronic presence of MS would have overcome the effects of the acute MS occlusion.

Angiogenesis occurs with large vessel ligation (Milkiewicz 2003), but since occlusion with 15 μm MS was expected to only affect the microcirculation, angiogenesis was not anticipated. However, the results indicated that an ischemic state occurred acutely with the MS injection. It is known that similar ischemic states lead to angiogenesis (Walder 1996, Milkiewicz 2003, Ferrara 2004, Economopoulou 2009, Hudlicka 2009). Therefore, additional experiments were conducted in our laboratory to confirm whether angiogenesis had occurred following the MS occlusion. Vascular Endothelial Growth Factor (VEGF) is the main molecule involved in the initiation and the control of angiogenesis (Leung 1989, Brown 2003, Ferrara 2009). Therefore, messenger RNA of VEGF and its receptor FLK-1 were measured by RT-PCR in the tibialis anterior muscle after 3 hrs, 2, 4 and 14 days post MS occlusion. It was observed that a 2.3-fold increase in VEGF expression and a significant 11-fold increase in FLK-1 expression occurred 4 days after the MS occlusion. As an increase in the expression of VEGF receptor has been shown to be upregulated during angiogenesis (Milkiewicz 2003), this supports the proposal of angiogenesis as the adaptation that has occurred in the muscle to overcome the microvascular occlusion following the MS injection. Further assessment of the angiogenic response needs to be done, either through quantitative histology (capillary:fibre ratio) or through blood flow imaging.

These findings are similar to the ischemia-induced angiogenesis that has been previously reported due to large vessel ligation. Iliac artery ligation has been shown to increase muscle VEGF mRNA levels 1 and 3 days post ligation (Milkiewicz 2006). After 7 days of ligation, the levels of VEGF mRNA had returned to basal, and a decrease in VEGF mRNA was observed between 14-35 days post-ligation as a counter regulatory mechanism (Milkiewicz 2006).

However, VEGF alone might not be as useful an index of angiogenic potential in response to ischemia as previously thought (Hudlicka 2009). Indeed, expression of VEGF receptors (Flk-1 increases angiogenesis, while Flt-1 prevents) has been shown to be crucial in the onset and control of angiogenesis (Milkiewicz 2003), with activation of the VEGF receptor Flk-1 also observed to be an important factor in the induction of capillary growth (Abumiya 2002).

The formation of new functional vessels after only 2 weeks of MS occlusion may seem rather rapid when compared with the capillary growth that occurs after large vessel ligation. Indeed, iliac ligation induces a late onset angiogenesis, with capillary:fibre ratio increased only after 35 days (Milkiewicz 2003, Milkiewicz 2006). Interestingly, ligation of the smaller feeding arteriole of the caudal-half of the spinotrapezius muscle led to a 24 % increase in the formation of new arterioles after only 5 days (Bailey 2008). Therefore, a more proximal ligation of the arteries to the microcirculation seems more efficient in promoting the angiogenic process. As the occlusion with MS most likely occurred in the terminal arterioles, the induction of angiogenesis would be expected to be quicker than that following ligation of the iliac artery.

In conclusion, the influence of the microvasculature on the development of myocyte insulin resistance could not be assessed with the present model. It appears that adaptations to the 2 week MS occlusion via the angiogenic process have reversed the impairment of the insulin-mediated microvascular recruitment seen in the acute model. Therefore, the implication of a reduced delivery on myocyte insulin resistance remains to be resolved.

CHAPTER 7:
DISCUSSION

7.1 DISCUSSION

The main aim of the present thesis was to better understand the initial step in the development of type 2 diabetes. More precisely, evaluate whether the microvasculature of the skeletal muscle is a key player in the development of insulin resistance. As outlined in chapter 1, a plethora of different hypotheses is present in the literature that suggests mechanisms for the development of insulin resistance. However, the inability to discover only one unifying mechanism for the development of insulin resistance illustrates the complexity of this disease. This may also indicate that the search for the initial defect in insulin resistance may have been too restrictive and not considered a broad enough perspective. Cellular and molecular defects *per se* may not be as important as their physiopathologic effect on the vasculature. Indeed, vascular defects could be the link between these different mechanisms resulting in the same outcome: insulin resistance.

Study of the microvascular recruitment was done for the first time in a pre-diabetic model of insulin resistance, the 4 week HFD fed rats. The data present in Chapter 3 has shown that the insulin-mediated microvascular response is impaired in this model, and this is associated with a reduction in sensitivity to the insulin-mediated metabolic actions. This suggests that a defect in the vascular action of insulin is an early event in the aetiology of type 2 diabetes, supporting the hypothesis that implicates the microvasculature as an initial defect. This microvascular defect can cause impairment of nutrient and insulin delivery to myocytes and thus, may contribute to the myocyte insulin resistance.

Muscle contraction is another process that will induce an increase in microvascular recruitment. Therefore, contraction-mediated microvascular recruitment was assessed in the 4 week HFD fed rats. This assessment was done using two different techniques: 1-MX metabolism and CEU. The main finding from Chapter 4 is that contraction-mediated metabolic and FBF response are preserved in a pre-diabetic state of insulin resistance. As contraction-mediated

glucose disposal is preserved in this model, even though the insulin-mediated response is impaired, it supports the hypothesis of different mechanisms for insulin and contraction effects. Another finding of this study was that 1-MX and CEU assessment of the microvascular recruitment yielded discrepant data. 1-MX assessment of the capillary surface area was not affected by the dietary intervention, while CEU assessment of the microvascular volume showed impairment in the HFD fed animals. This result was unexpected since 1-MX and CEU have previously yielded similar results in insulin-sensitive animals (Dawson 2002, Clark 2008). However, since HFD feeding did not affect contraction-mediated glucose uptake, this would indicate that capillary surface area is more important for the disposal of glucose than the microvascular volume. Therefore, caution should be taken in interpreting the results of CEU measures of the microvasculature. In some instances, as shown in Chapter 4, a decrease in MBV may not indicate a decrease in nutrients delivery. Future studies are needed to compare 1-MX and CEU in other models of insulin resistance.

Whether the loss of insulin-mediated microvascular recruitment can impact on myocytes insulin responsiveness was addressed in the studies described in Chapter 5. Contribution of the muscle microvasculature to the insulin-mediated glucose uptake has been assessed previously using different acute pharmaceutical treatments (Rattigan 1999, Youd 2000, Clerk 2002, Wallis 2005). However, interventions were not directly targeted to the muscle microvasculature and contributions from other tissues could not be excluded. Therefore, a novel model for the direct assessment of the microvasculature was developed. Reduced microvascular recruitment was created by blocking the terminal arterioles with 15 μm MS. This successfully prevented the insulin-mediated increases in microvascular recruitment, leading to a 46 % decrease in muscle insulin-mediated glucose uptake, creating a vascular-derived state of insulin resistance. This finding confirmed that increased microvascular recruitment is required for insulin to produce the normal metabolic effects in skeletal muscle.

The effects of a chronic (2 weeks) decrease in microvascular recruitment on muscle insulin sensitivity were investigated in Chapter 6. However, after 2 weeks of occlusion the angiogenic process had reversed the impairment of the insulin-mediated microvascular recruitment seen in the acute model. This finding prevented the assessment of impaired microvascular recruitment on myocyte insulin sensitivity. This problem of the chronic MS model may be overcome in two ways. The first approach could be to prevent the angiogenesis process by using anti-angiogenic drugs (Crawford 2009). These anti-angiogenic agents limit the growth of tumours by preventing the formation of new vessels needed by the tumour cells to maintain their high metabolic needs (Ellis 2008). The second approach could be to target more directly the nutritive route of the muscle microvasculature. This could be achieved by stimulating an increase in microvascular recruitment with insulin or contraction prior to MS injection. This would have the benefit of blocking the insulin-recruited vessels. Secondly, muscle contraction using electrical stimulation could be used to recruit vessels of the nutritive route (Clark 2000). Thus, a more targeted occlusion of the nutritive route may require less MS, and as such, decrease the ischemic response seen in Chapter 5. This may dampen the angiogenic process and allow assessment of the function of the microvasculature in the development of myocyte insulin resistance. While the chronic occlusion did not help reveal the importance of long-term impairment of insulin-mediated microvascular recruitment on the skeletal muscle insulin sensitivity, it is a good example of the high adaptability of this tissue. This should come as no surprise, given the physiological importance of the normal function of muscles for survival.

One limitation of the present thesis is that all the experiments were done in anesthetised animals, which has been shown to influence total blood flow in a dose-dependent and tissue-specific manner (Seyde 1985, James 1986). However, modification of total blood flow seen in anesthetised animals may not correlate with modification of the microvascular recruitment. As previously shown, change in total blood flow does not always correlate with change in

microvascular recruitment (Rattigan 1997). Moreover, little is known about the effect of anaesthesia on the microvascular recruitment. This is partly due to the requirement of a motionless animal for the assessment of microvascular recruitment, as an increases in movement (i.e. walking in the cage) would lead to a modification of the flow pattern. However, it is encouraging that measurements done in anesthetised animals are mirrored by those done in awake humans. Indeed, assessment of the microvascular recruitment in the awake human in response to exercise (Womack 2009) and insulin (Vincent 2006) are similar to the anesthetised rat (Dawson 2002). Furthermore, impairment in insulin-mediated microvascular recruitment seen in models of insulin-resistance are true for both the awake state (Clerk 2006) and anaesthetised animals (Clerk 2007). Nevertheless, until a technique measuring the microvascular recruitment in awake animals is developed, the effects of anaesthesia *per se* will remain unknown.

7.2 CONCLUSION

Collectively, studies in the present thesis confirm the pivotal role of the microvasculature plays in the development of skeletal muscle insulin resistance. Indeed, insulin-mediated microvascular recruitment is impaired at an early stage in the development of insulin resistance, while the contraction-mediated effects on capillary surface area are preserved. Furthermore, muscle insulin resistance can be artificially produced by blockage the microvasculature. Blockage of microvascular recruitment lead to a 46 % decrease in insulin-mediated glucose uptake, further confirming defects in microvascular recruitment as a likely candidate for the development of insulin resistance. These findings furthers our understanding of the aetiology of type 2 diabetes, beginning with loss of insulin-mediated microvascular recruitment, and emphasises the microvasculature as an interesting therapeutic target for the management of type 2 diabetes.

These findings convincingly position an impairment of microvascular recruitment in the early stage of insulin resistance. Thus, a proposed mechanism can be constructed from these and other published findings.

The western society lifestyle is characterised by increased calorie intake (with the majority in the form of fats) and decreased energy expenditure (less exercise). This imbalance translates as an increase in exposure to fatty acids, which can lead to many adverse effects: increase in adipose tissue mass, adipocytes of increased size as well as increased muscle and liver storage of fatty acid (Reaven 1988, Hamdy 2005, Goossens 2008). A further consequence is an accumulation of the fatty acid in adipocytes localised around arterioles of the microvasculature (Bakker 2009). These perivascular adipocytes of increased sized have been shown to secrete TNF-α (Chatterjee 2009). According to the vasocrine hypothesis (Yudkin 2005), paracrine secretion of inflammatory adipokines (e.g. TNF-α) by perivascular adipocytes of increase sized, as well as higher circulating level of FFA, could impair the endothelium dependent vasodilation in response to insulin. At the level of terminal arterioles, this will translate as an impairment of the insulin-mediated microvascular recruitment. Circulating levels of glucose and insulin will therefore have limited access to the myocyte of the nutritive route, resulting in decreased insulin-mediated glucose uptake. In the long-term, prolonged impairment of insulin-mediated microvascular recruitment may lead to changes in the intracellular function of the insulin signalling pathway, corresponding to the defects associated with late-stage type 2 diabetes (Defronzo 1985, Zierath 1998, Ryder 2001, Karlsson 2007).

REFERENCES

Abel, E.D., O. Peroni, J.K. Kim, Y.B. Kim, O. Boss, E. Hadro, T. Minnemann, G.I. Shulman and B.B. Kahn (2001). Adipose-selective targeting of the GLUT4 gene impairs insulin action in muscle and liver. Nature **409**(6821): 729-733.

Abramson, D.I., N. Schkloven, M.N. Margolis and I.A. Mirsky (1939). Influence of massive doses of insulin on peripheral blood flow in man. American Journal of Physiology **128**: 124-132.

Australian Bureau of Statistics (2008). Year Book Australia 2008. Viewed November 2009. http://www.abs.gov.au/.

Abumiya, T., T. Sasaguri, Y. Taba, Y. Miwa and M. Miyagi (2002). Shear stress induces expression of vascular endothelial growth factor receptor Flk-1/KDR through the CT-rich Sp1 binding site. Arteriosclerosis, Thrombosis, and Vascular Biology **22**(6): 907-913.

American Diabetes Association (2009). The American Diabetes Association. Viewed November 2009. www.diabetes.org.

Aguirre, V., T. Uchida, L. Yenush, R. Davis and M.F. White (2000). The c-Jun NH(2)-terminal kinase promotes insulin resistance during association with insulin receptor substrate-1 and phosphorylation of Ser(307). Journal of Biological Chemistry **275**(12): 9047-9054.

Alessi, D.R., M. Andjelkovic, B. Caudwell, P. Cron, N. Morrice, P. Cohen and B.A. Hemmings (1996). Mechanism of activation of protein kinase B by insulin and IGF-1. EMBO Journal **15**(23): 6541-6551.

Anastasiou, E., J.P. Lekakis, M. Alevizaki, C.M. Papamichael, J. Megas, A. Souvatzoglou and S.F. Stamatelopoulos (1998). Impaired endothelium-dependent vasodilatation in women with previous gestational diabetes. Diabetes Care **21**(12): 2111-2115.

Anderson, E.A., R.P. Hoffman, T.W. Balon, C.A. Sinkey and A.L. Mark (1991). Hyperinsulinemia produces both sympathetic neural activation and vasodilation in normal humans. Journal of Clinical Investigation **87**: 2246-2252.

Anthony, M. and R. Ramona (2009). Exercise for Prevention of Obesity and Diabetes in Children and Adolescents. Clinics in sports medicine **28**(3): 393-421.

Araki, E., M.A. Lipes, M.E. Patti, J.C. Bruning, B. Haag and R.S. Johnson (1994). Alternative pathway of insulin signalling in mice with targeted disruption of the IRS-1 gene. Nature **372**: 186-190.

Armstrong, R.B. and M.H. Laughlin (1983). Blood flows within and among rat muscles as a function of time during high speed treadmill exercise. Journal of Physiology **344**: 189-208.

Azevedo, J.L., Jr., J.O. Carey, W.J. Pories, P.G. Morris and G.L. Dohm (1995). Hypoxia stimulates glucose transport in insulin-resistant human skeletal muscle. Diabetes **44**(6): 695-698.

Bailey, A.M., T.J. O'Neill, C.E. Morris and S.M. Peirce (2008). Arteriolar remodeling following ischemic injury extends from capillary to large arteriole in the microcirculation. Microcirculation **15**(5): 389-404.

Bakker, W., E.C. Eringa, P. Sipkema and V.W. van Hinsbergh (2009). Endothelial dysfunction and diabetes: roles of hyperglycemia, impaired insulin signaling and obesity. Cell and Tissue Research **335**(1): 165-189.

Baron, A.D. (1994). Hemodynamic actions of insulin. American Journal of Physiology **267**: E187-E202.

Baron, A.D., G. Brechtel-Hook, A. Johnson and D. Hardin (1993). Skeletal muscle blood flow. A possible link between insulin resistance and blood pressure. Hypertension **21**: 129-135.

Baron, A.D. and G. Brechtel (1993). Insulin differentially regulates systemic and skeletal muscle vascular resistance. American Journal of Physiology **265**: E61-E67.

Baron, A.D. and M.G. Clark (1997). Role of blood flow in the regulation of muscle glucose uptake. Annual Review of Nutrition **17:487-99**: 487-499.

Baron, A.D., M. Laakso, G. Brechtel and S.V. Edelman (1991). Mechanism of insulin resistance in insulin-dependent diabetes mellitus: a major role for reduced skeletal muscle blood flow. Journal of Clinical Endocrinology and Metabolism **73**: 637-643.

Barrett, E.J., E.M. Eggleston, A.C. Inyard, H. Wang, G. Li, W. Chai and Z. Liu (2009). The vascular actions of insulin control its delivery to muscle and regulate the rate-limiting step in skeletal muscle insulin action. Diabetologia **52**(5): 752-764.

Bauer, T.A., J.E.B. Reusch, M. Levi and J.G. Regensteiner (2007). Skeletal Muscle Deoxygenation After the Onset of Modcrate Exercise Suggests Slowed Microvascular Blood Flow Kinetics in Type 2 Diabetes. Diabetes Care **30**(11): 2880-2885.

Bergman, R.N., G.W. Van Citters, S.D. Mittelman, M.K. Dea, M. Hamilton-Wessler, S.P. Kim and M. Ellmerer (2001). Central role of the adipocyte in the metabolic syndrome. Journal of Investigative Medicine **49**(1): 119-126.

Bertuglia, S. and A. Giusti (2005). Role of nitric oxide in capillary perfusion and oxygen delivery regulation during systemic hypoxia. American Journal of Physiology Heart and Circulatory Physiology **288**(2): H525-H531.

Bloor, C.M. (2005). Angiogenesis during exercise and training. Angiogenesis **8**(3): 263-271.

Boden, G. (2009). Endoplasmic Reticulum Stress: Another Link Between Obesity and Insulin Resistance/Inflammation? Diabetes **58**(3): 518-519.

Boden, G., X. Chen, J. Ruiz, J.V. White and L. Rossetti (1994). Mechanisms of fatty acid-induced inhibition of glucose uptake. Journal of Clinical Investigation **93**(6): 2438-2446.

Boden, G. and G.I. Shulman (2002). Free fatty acids in obesity and type 2 diabetes: defining their role in the development of insulin resistance and beta-cell dysfunction. European Journal of Clinical Investigation **32**(Suppl 3): 14-23.

Bonadonna, R.C., M.P. Saccomani, S. Del Prato, E. Bonora, R.A. Defronzo and C. Cobelli (1998). Role of tissue-specific blood flow and tissue recruitment in insulin-mediated glucose uptake of human skeletal muscle. Circulation **98**(3): 234-241.

Bonadonna, R.C., K. Zych, C. Boni, E. Ferrannini and R.A. DeFronzo (1989). Time dependence of the interaction between lipid and glucose in humans. American Journal of Physiology Endocrinology and Metabolism **257**(1 Pt 1): E49-56.

Borgstrom, P., L. Lindbom, K.E. Arfors and M. Intaglietta (1988). Beta-adrenergic control of resistance in individual vessels in rabbit tenuissimus muscle. American Journal of Physiology Heart and Circulatory Physiology **254**(4 Pt 2): H631-H635.

Boron, W.F. and E.L. Boulpaep (2003). Medical physiology : a cellular and molecular approach. Philadelphia, PA ; Toronto, W.B. Saunders.

Bradley, E.A., M.G. Clark and S. Rattigan (2006). Acute effects of wortmannin on insulin's hemodynamic and metabolic actions in vivo. American Journal of Physiology Endocrinology and Metabolism **292**(3): E779-E787.

Brown, M.D. and O. Hudlicka (2003). Modulation of physiological angiogenesis in skeletal muscle by mechanical forces: involvement of VEGF and metalloproteinases. Angiogenesis **6**(1): 1-14.

Brownlee, M. and A. Cerami (1981). The biochemistry of the complications of diabetes mellitus. Annual Review of Biochemistry **50**: 385-432.

Bruning, J.C., J. Winnay, S. Bonner-Weir, S.I. Taylor, D. Accili and C.R. Kahn (1997). Development of a novel polygenic model of NIDDM in mice heterozygous for IR and IRS-1 null alleles. Cell **88**(4): 561-572.

Bruss, M.D., E.B. Arias, G.E. Lienhard and G.D. Cartee (2005). Increased Phosphorylation of Akt Substrate of 160 kDa (AS160) in Rat Skeletal Muscle in Response to Insulin or Contractile Activity. Diabetes **54**(1): 41-50.

Bruun, J.M., A.S. Lihn, C. Verdich, S.B. Pedersen, S. Toubro, A. Astrup and B. Richelsen (2003). Regulation of adiponectin by adipose tissue-derived cytokines: in vivo and in vitro investigations in humans. American Journal of Physiology Endocrinology and Metabolism **285**(3): E527-E533.

Buettner, R., J. Scholmerich and L.C. Bollheimer (2007). High-fat Diets: Modeling the Metabolic Disorders of Human Obesity in Rodents. Obesity **15**(4): 798-808.

Burnol, A.F., A. Leturque and P.J. Girard (1983). A method for quantifying insulin sensitivity in vivo in the anesthetized rat: the euglycemic insulin

clamp technique coupled with isotopic measurement of glucose turnover. Reproduction, Nutrition, Development **23**: 429-435.

Chakir, M., G.E. Plante and P. Maheux (1998). Reduction of capillary permeability in the fructose-induced hypertensive rat. American Journal of Hypertension **11**(5): 563-569.

Chatterjee, T.K., L.L. Stoll, G.M. Denning, A. Harrelson, A.L. Blomkalns, G. Idelman, F.G. Rothenberg, B. Neltner, S.A. Romig-Martin, E.W. Dickson, S. Rudich and N.L. Weintraub (2009). Proinflammatory phenotype of perivascular adipocytes: Influence of high-fat feeding. Circulation Research **104**(4): 541-549.

Chen, H., M. Montagnani, T. Funahashi, I. Shimomura and M.J. Quon (2003). Adiponectin stimulates production of nitric oxide in vascular endothelial cells. Journal of Biological Chemistry **278**(45): 45021-45026.

Clark, M.G. (2008). Impaired microvascular perfusion: a consequence of vascular dysfunction and a potential cause of insulin resistance in muscle. American Journal of Physiology Endocrinology and Metabolism **295**(4): E732-E750.

Clark, M.G., E.Q. Colquhoun, S. Rattigan, K.A. Dora, T.P. Eldershaw, J.L. Hall and J. Ye (1995). Vascular and endocrine control of muscle metabolism. American Journal of Physiology Endocrinology and Metabolism **268**(5 Pt 1): E797-E812.

Clark, M.G., S. Rattigan and E.J. Barrett (2006). Nutritive blood flow as an essential element supporting muscle anabolism. Current Opinion in Clinical Nutrition & Metabolic Care **9**(3): 185-189.

Clark, M.G., S. Rattigan, L.H. Clerk, M.A. Vincent, A.D. Clark, J.M. Youd and J.M. Newman (2000). Nutritive and non-nutritive blood flow: rest and exercise. Acta Physiologica Scandinavica **168**(4): 519-530.

Clerk, L.H., S. Rattigan and M.G. Clark (2002). Lipid infusion impairs physiologic insulin-mediated capillary recruitment and muscle glucose uptake in vivo. Diabetes **51**(4): 1138-1145.

Clerk, L.H., M.E. Smith, S. Rattigan and M.G. Clark (2000). Increased chylomicron triglyceride hydrolysis by connective tissue flow in perfused rat hindlimb. Implications for lipid storage. Journal of Lipid Research **41**(3): 329-335.

Clerk, L.H., M.A. Vincent, E. Barrett, M.F. Lankford and J.R. Lindner (2007). Skeletal muscle capillary responses to insulin are abnormal in late-stage diabetes and are restored by angiotensin converting enzyme inhibition. American Journal of Physiology Endocrinology and Metabolism.

Clerk, L.H., M.A. Vincent, L.A. Jahn, Z. Liu, J.R. Lindner and E.J. Barrett (2006). Obesity blunts insulin-mediated microvascular recruitment in human forearm muscle. Diabetes **55**(5): 1436-1442.

Clerk, L.H., M.A. Vincent, J.R. Lindner, M.G. Clark, S. Rattigan and E.J. Barrett (2004). The vasodilatory actions of insulin on resistance and terminal

arterioles and their impact on muscle glucose uptake. Diabetes/Metabolism Research and Reviews. **20**(1): 3-12.

Clifford, P.S. and Y. Hellsten (2004). Vasodilatory mechanisms in contracting skeletal muscle. Journal of Applied Physiology **97**(1): 393-403.

Coggins, M., J. Lindner, S. Rattigan, L. Jahn, E. Fasy, S. Kaul and E. Barrett (2001). Physiologic hyperinsulinemia enhances human skeletal muscle perfusion by capillary recruitment. Diabetes **50**(12): 2682-2690.

Crawford, Y. and N. Ferrara (2009). VEGF inhibition: insights from preclinical and clinical studies. Cell and Tissue Research **335**(1): 261-269.

Crettaz, M., D. Zaninetti and B. Jeanrenaud (1981). Insulin-resistance in heart and skeletal muscles of genetically obese Zucker rats. Biochemical Society Transactions **9**(6): 524-525.

Cusi, K., K. Maezono, A. Osman, M. Pendergrass, M.E. Patti, T. Pratipanawatr, R.A. Defronzo, C.R. Kahn and L.J. Mandarino (2000). Insulin resistance differentially affects the PI 3-kinase- and MAP kinase-mediated signaling in human muscle. Journal of Clinical Investigation **105**(3): 311-320.

Dawson, D., M.A. Vincent, E.J. Barrett, S. Kaul, A. Clark, H. Leong-Poi and J.R. Lindner (2002). Vascular recruitment in skeletal muscle during exercise and hyperinsulinemia assessed by contrast ultrasound. American Journal of Physiology Endocrinology and Metabolism **282**(3): E714-E720.

De Fea, K. and R.A. Roth (1997). Modulation of insulin receptor substrate-1 tyrosine phosphorylation and function by mitogen-activated protein kinase. Journal of Biological Chemistry **272**(50): 31400-31406.

De Filippis, E., K. Cusi, G. Ocampo, R. Berria, S. Buck, A. Consoli and L.J. Mandarino (2006). Exercise-induced improvement in vasodilatory function accompanies increased insulin sensitivity in obesity and type 2 diabetes mellitus. Journal of Clinical Endocrinology and Metabolism **91**(12): 4903-4910.

de Jongh, R.T., A.D. Clark, R.G. Ijzerman, E.H. Serne, G. De Vries and C.D. Stehouwer (2004). Physiological hyperinsulinaemia increases intramuscular microvascular reactive hyperaemia and vasomotion in healthy volunteers. Diabetologia **47**(6): 978-986.

de Jongh, R.T., E.H. Serne, R.G. Ijzerman, G. De Vries and C.D. Stehouwer (2004). Impaired microvascular function in obesity: implications for obesity-associated microangiopathy, hypertension, and insulin resistance. Circulation **109**(21): 2529-2535.

Defronzo, R.A. (1988). Lilly lecture 1987. The triumvirate: beta-cell, muscle, liver. A collusion responsible for NIDDM. Diabetes **37**(6): 667-687.

Defronzo, R.A. and E. Ferrannini (1991). Insulin resistance. A multifaceted syndrome responsible for NIDDM, obesity, hypertension, dyslipidemia, and atherosclerotic cardiovascular disease. Diabetes Care **14**: 173-194.

Defronzo, R.A., R. Gunnarsson, O. Bjorkman, M. Olsson and J. Wahren (1985). Effects of insulin on peripheral and splanchnic glucose metabolism in

noninsulin-dependent (type II) diabetes mellitus. Journal of Clinical Investigation **76**: 149-155.

Dela, F., J.J. Larsen, K.J. Mikines, T. Ploug, L.N. Petersen and H. Galbo (1995). Insulin-stimulated muscle glucose clearance in patients with NIDDM - Effects of one-legged physical training. Diabetes **44**: 1010-1020.

Douen, A.G., T. Ramlal, S. Rastogi, P.J. Bilan, G.D. Cartee, M. Vranic, J.O. Holloszy and A. Klip (1990). Exercise induces recruitment of the "insulin-responsive glucose transporter". Journal of Biological Chemistry **265**: 13427-13430.

Dresner, A., D. Laurent, M. Marcucci, M.E. Griffin, S. Dufour, G.W. Cline, L.A. Slezak, D.K. Andersen, R.S. Hundal, D.L. Rothman, K.F. Petersen and G.I. Shulman (1999). Effects of free fatty acids on glucose transport and IRS-1-associated phosphatidylinositol 3-kinase activity. Journal of Clinical Investigation **103**(2): 253-259.

Dunaif, A., J. Xia, C.B. Book, E. Schenker and Z. Tang (1995). Excessive insulin receptor serine phosphorylation in cultured fibroblasts and in skeletal muscle. A potential mechanism for insulin resistance in the polycystic ovary syndrome. Journal of Clinical Investigation **96**(2): 801-810.

Dyck, D.J., G.J. Heigenhauser and C.R. Bruce (2006). The role of adipokines as regulators of skeletal muscle fatty acid metabolism and insulin sensitivity. Acta Physiologica (Oxford) **186**(1): 5-16.

Ebeling, P., R. Bourey, L. Koranyi, J.A. Tuominen, L.C. Groop, J. Henriksson, M. Mueckler, A. Sovijarvi and V.A. Koivisto (1993). Mechanism of enhanced insulin sensitivity in athletes. Increased blood flow, muscle glucose transport protein (GLUT-4) concentration, and glycogen synthase activity. Journal of Clinical Investigation **92**: 1623-1631.

Economopoulou, M., H.F. Langer, A. Celeste, V.V. Orlova, E.Y. Choi, M. Ma, A. Vassilopoulos, E. Callen, C. Deng, C.H. Bassing, M. Boehm, A. Nussenzweig and T. Chavakis (2009). Histone H2AX is integral to hypoxia-driven neovascularization. Nature Medicine **15**(5): 553-558.

Eggleston, E.M., L.A. Jahn and E.J. Barrett (2007). Hyperinsulinemia rapidly increases human muscle microvascular perfusion but fails to increase muscle insulin clearance: evidence that a saturable process mediates muscle insulin uptake. Diabetes **56**: 2958-2963.

Eizirik, D.L., A.K. Cardozo and M. Cnop (2008). The Role for Endoplasmic Reticulum Stress in Diabetes Mellitus. Endocrine Reviews **29**(1): 42-61.

Ellis, L.M. and D.J. Hicklin (2008). VEGF-targeted therapy: mechanisms of anti-tumour activity. Nature Reviews Cancer **8**(8): 579-591.

Erdei, N., A. Toth, E.T. Pasztor, Z. Papp, I. Edes, A. Koller and Z. Bagi (2006). High-fat diet-induced reduction in nitric oxide-dependent arteriolar dilation in rats: role of xanthine oxidase-derived superoxide anion. American Journal of Physiology Heart and Circulatory Physiology **291**(5): H2107-H2115.

Ferrannini, E., E.J. Barrett and S. Bevilacqua (1983). Effect of fatty acids on glucose production and utilization in man. Journal of Clinical Investigation **72**: 1737-1747.

Ferrara, N. (2004). Vascular endothelial growth factor: basic science and clinical progress. Endocrine Reviews **25**(4): 581-611.

Ferrara, N. (2009). Vascular endothelial growth factor. Arteriosclerosis, Thrombosis, and Vascular Biology **29**(6): 789-791.

Folli, F., M.J. Saad, J.M. Backer and C.R. Kahn (1992). Insulin stimulation of phosphatidylinositol 3-kinase activity and association with insulin receptor substrate 1 in liver and muscle of the intact rat. Journal of Biological Chemistry **267**: 22171-22177.

Frisbee, J.C. (2005). Hypertension-independent microvascular rarefaction in the obese Zucker rat model of the metabolic syndrome. Microcirculation **12**(5): 383-392.

Fueger, P.T., R.S. Lee-Young, J. Shearer, D.P. Bracy, S. Heikkinen, M. Laakso, J.N. Rottman and D.H. Wasserman (2007). Phosphorylation Barriers to Skeletal and Cardiac Muscle Glucose Uptakes in High-Fat Fed Mice: Studies in Mice With a 50% Reduction of Hexokinase II. Diabetes **56**(10): 2476-2484.

Furnsinn, C., S. Neschen, O. Wagner, M. Roden, M. Bisschop and W. Waldhausl (1997). Acute and chronic exposure to tumor necrosis factor-alpha fails to affect insulin-stimulated glucose metabolism of isolated rat soleus muscle. Endocrinology **138**(7): 2674-2679.

Gao, Z., D. Hwang, F. Bataille, M. Lefevre, D. York, M.J. Quon and J. Ye (2002). Serine phosphorylation of insulin receptor substrate 1 by inhibitor kappa B kinase complex. Journal of Biological Chemistry **277**(50): 48115-48121.

Garland, P.B., P.J. Randle and E.A. Newsholme (1963). Citrate as an Intermediary in the Inhibition of Phosphofructokinase in Rat Heart Muscle by Fatty Acids, Ketone Bodies, Pyruvate, Diabetes, and Starvation. Nature **200**: 169-170.

Goodyear, L.J. and B.B. Kahn (1998). Exercise, glucose transport, and insulin sensitivity. Annual Review of Medicine **49**: 235-261.

Goossens, G.H. (2008). The role of adipose tissue dysfunction in the pathogenesis of obesity-related insulin resistance. Physiology and Behavior **94**(2): 206-218.

Griffin, M.E., M.J. Marcucci, G.W. Cline, K. Bell, N. Barucci, D. Lee, L.J. Goodyear, E.W. Kraegen, M.F. White and G.I. Shulman (1999). Free fatty acid-induced insulin resistance is associated with activation of protein kinase C theta and alterations in the insulin signaling cascade. Diabetes **48**(6): 1270-1274.

Gual, P., Y. Le Marchand-Brustel and J.F. Tanti (2005). Positive and negative regulation of insulin signaling through IRS-1 phosphorylation. Biochimie **87**(1): 99-109.

Guo, Z. (2007). Intramyocellular lipid kinetics and insulin resistance. Lipids in Health and Disease **6**(1): 18.

Hallsten, K., K.A. Virtanen, F. Lonnqvist, H. Sipila, A. Oksanen, T. Viljanen, T. Ronnemaa, J. Viikari, J. Knuuti and P. Nuutila (2002). Rosiglitazone but not metformin enhances insulin- and exercise-stimulated skeletal muscle glucose uptake in patients with newly diagnosed type 2 diabetes. Diabetes **51**(12): 3479-3485.

Hamdy, O. (2005). Lifestyle modification and endothelial function in obese subjects. Expert Review of Cardiovascular Therapy **3**(2): 231-241.

Hamilton-Wessler, M., M. Ader, M.K. Dea, D. Moore, M. Loftager, J. Markussen and R.N. Bergman (2002). Mode of transcapillary transport of insulin and insulin analog NN304 in dog hindlimb: evidence for passive diffusion. Diabetes **51**(3): 574-582.

Han, D.H., P.A. Hansen, H.H. Host and J.O. Holloszy (1997). Insulin resistance of muscle glucose transport in rats fed a high-fat diet: a reevaluation. Diabetes **46**(11): 1761-1767.

Hansen, P.A., D.H. Han, B.A. Marshall, L.A. Nolte, M.M. Chen, M. Mueckler and J.O. Holloszy (1998). A high fat diet impairs stimulation of glucose transport in muscle. Functional evaluation of potential mechanisms. Journal of Biological Chemistry **273**(40): 26157-26163.

Hardie, D.G. (2003). Minireview: the AMP-activated protein kinase cascade: the key sensor of cellular energy status. Endocrinology **144**(12): 5179-5183.

Hattori, Y., Y. Nakano, S. Hattori, A. Tomizawa, K. Inukai and K. Kasai (2008). High molecular weight adiponectin activates AMPK and suppresses cytokine-induced NF-kappaB activation in vascular endothelial cells. FEBS Letters **582**(12): 1719-1724.

Hayashi, T., J.F. Wojtaszewski and L.J. Goodyear (1997). Exercise regulation of glucose transport in skeletal muscle. American Journal of Physiology **273**(6 Pt 1): E1039-E1051.

Henriksen, E.J. (2002). Invited Review: Effects of acute exercise and exercise training on insulin resistance. Journal of Applied Physiology **93**(2): 788-796.

Hofmann, C., K. Lorenz, S.S. Braithwaite, J.R. Colca, B.J. Palazuk, G.S. Hotamisligil and B.M. Spiegelman (1994). Altered gene expression for tumor necrosis factor-alpha and its receptors during drug and dietary modulation of insulin resistance. Endocrinology **134**(1): 264-270.

Honig, C.R., C.L. Odoroff and J.L. Frierson (1982). Active and passive capillary control in red muscle at rest and in exercise. American Journal of Physiology **243**: H196-H206.

Hotamisligil, G.S. (1999). The role of TNFalpha and TNF receptors in obesity and insulin resistance. Journal of Internal Medicine **245**(6): 621-625.

Hotamisligil, G.S. (2006). Inflammation and metabolic disorders. Nature **444**(7121): 860-867.

Hotamisligil, G.S., P. Arner, J.F. Caro, R.L. Atkinson and B.M. Spiegelman (1995). Increased adipose tissue expression of tumor necrosis factor-alpha in human obesity and insulin resistance. Journal of Clinical Investigation **95**(5): 2409-2415.

Hotamisligil, G.S., A. Budavari, D. Murray and B.M. Spiegelman (1994). Reduced tyrosine kinase activity of the insulin receptor in obesity-diabetes. Central role of tumor necrosis factor-alpha. Journal of Clinical Investigation **94**: 1543-1549.

Hotamisligil, G.S., P. Peraldi, A. Budavari, R. Ellis, M.F. White and B.M. Spiegelman (1996). IRS-1-mediated inhibition of insulin receptor tyrosine kinase activity in TNF-à- and obesity-induced insulin resistance. Science **271**: 665-668.

Hotamisligil, G.S., N.S. Shargill and B.M. Spiegelman (1993). Adipose expression of tumor necrosis factor-alpha: Direct role in obesity-linked insulin resistance. Science **259**: 87-91.

Hubinger, A., A. Franzen and F.A. Gries (1987). Hormonal and metabolic response to physical exercise in hyperinsulinemic and non-hyperinsulinemic type 2 diabetics. Diabetes Research **4**(2): 57-61.

Hudlicka, O. and M.D. Brown (2009). Adaptation of Skeletal Muscle Microvasculature to Increased or Decreased Blood Flow: Role of Shear Stress, Nitric Oxide and Vascular Endothelial Growth Factor. Journal of Vascular Research **46**(5): 504-512.

Hughes, V.A., M.A. Fiatarone, R.A. Fielding, B.B. Kahn, C.M. Ferrara, P. Shepherd, E.C. Fisher, R.R. Wolfe, D. Elahi and W.J. Evans (1993). Exercise increases muscle GLUT-4 levels and insulin action in subjects with impaired glucose tolerance. American Journal of Physiology Endocrinology and Metabolism **264**(6 Pt 1): E855-862.

Itani, S.I., N.B. Ruderman, F. Schmieder and G. Boden (2002). Lipid-Induced Insulin Resistance in Human Muscle Is Associated With Changes in Diacylglycerol, Protein Kinase C, and IÎºB-Î±. Diabetes **51**(7): 2005-2011.

Ivy, J.L. (1997). Role of exercise training in the prevention and treatment of insulin resistance and non-insulin-dependent diabetes mellitus. Sports Medicine **24**(5): 321-336.

Jackson, R.A., J.B. Hamling, P.M. Blix, B.M. Sim, M.I. Hawa, J.B. Jaspan, J. Belin and J.D. abarro (1986). The influence of graded hyperglycemia with and without physiological hyperinsulinemia on forearm glucose uptake and other metabolic responses in man. Journal of Clinical Endocrinology and Metabolism **63**(3): 594-604.

James, D.E., K.M. Burleigh, L.H. Storlien, S.P. Bennett and E.W. Kraegen (1986). Heterogeneity of insulin action in muscle: influence of blood flow. American Journal of Physiology **251**: E422-E430.

Jansson, P.A. (2007). Endothelial dysfunction in insulin resistance and type 2 diabetes. Journal of Internal Medicine **262**(2): 173-183.

Jarasch, E.D., G. Bruder and H.W. Heid (1986). Significance of xanthine oxidase in capillary endothelial cells. Acta Physiologica Scandinavica Supplementum **548**: 39-46.

Jayaweera, A.R., K. Wei, M. Coggins, J.P. Bin, C. Goodman and S. Kaul (1999). Role of capillaries in determining CBF reserve: new insights using myocardial contrast echocardiography. American Journal of Physiology Heart and Circulatory Physiology **277**(6 Pt 2): H2363-2372.

Jessen, N. and L.J. Goodyear (2005). Contraction signaling to glucose transport in skeletal muscle. Journal of Applied Physiology **99**(1): 330-337.

Jiang, Z.Y., Y.W. Lin, A. Clemont, E.P. Feener, K.D. Hein, M. Igarashi, T. Yamauchi, M.F. White and G.L. King (1999). Characterization of selective resistance to insulin signaling in the vasculature of obese zucker (fa/fa) rats. Journal of Clinical Investigation **104**(4): 447-457.

Jonk, A.M., A.J. Houben, R.T. de Jongh, E.H. Serne, N.C. Schaper and C.D. Stehouwer (2007). Microvascular dysfunction in obesity: a potential mechanism in the pathogenesis of obesity-associated insulin resistance and hypertension. Physiology (Bethesda) **22**: 252-260.

Joyner, M.J. and B.W. Wilkins (2007). Exercise hyperaemia: is anything obligatory but the hyperaemia? Journal of Physiology **583**(Pt 3): 855-860.

Karlsson, H.K. and J.R. Zierath (2007). Insulin signaling and glucose transport in insulin resistant human skeletal muscle. Cell Biochemistry and Biophysics **48**(2-3): 103-113.

Kasner, S.E. and J.C. Grotta (1997). Emergency identification and treatment of acute ischemic stroke. Annals of Emergency Medicine **30**(5): 642-653.

Kearney, M.T., E.R. Duncan, M. Kahn and S.B. Wheatcroft (2008). Insulin resistance and endothelial cell dysfunction: studies in mammalian models. Experimental Physiology **93**(1): 158-163.

Kennedy, J.W., M.F. Hirshman, E.V. Gervino, J.V. Ocel, R.A. Forse, S.J. Hoenig, D. Aronson, L.J. Goodyear and E.S. Horton (1999). Acute exercise induces GLUT4 translocation in skeletal muscle of normal human subjects and subjects with type 2 diabetes. Diabetes **48**(5): 1192-1197.

Kern, P.A., S. Ranganathan, C. Li, L. Wood and G. Ranganathan (2001). Adipose tissue tumor necrosis factor and interleukin-6 expression in human obesity and insulin resistance. American Journal of Physiology Endocrinology and Metabolism **280**(5): E745-E751.

Kim, F., M. Pham, E. Maloney, N.O. Rizzo, G.J. Morton, B.E. Wisse, E.A. Kirk, A. Chait and M.W. Schwartz (2008). Vascular inflammation, insulin resistance, and reduced nitric oxide production precede the onset of peripheral insulin resistance. Arteriosclerosis, Thrombosis, and Vascular Biology **28**(11): 1982-1988.

Kim, F., K.A. Tysseling, J. Rice, B. Gallis, L. Haji, C.M. Giachelli, E.W. Raines, M.A. Corson and M.W. Schwartz (2005). Activation of IKK beta by

glucose is necessary and sufficient to impair insulin signaling and nitric oxide production in endothelial cells. Journal of Molecular and Cellular Cardiology **39**(2): 327-334.

Kim, F., K.A. Tysseling, J. Rice, M. Pham, L. Haji, B.M. Gallis, A.S. Baas, P. Paramsothy, C.M. Giachelli, M.A. Corson and E.W. Raines (2005). Free fatty acid impairment of nitric oxide production in endothelial cells is mediated by IKKbeta. Arteriosclerosis, Thrombosis, and Vascular Biology **25**(5): 989-994.

Kim, J.A., M. Montagnani, K.K. Koh and M.J. Quon (2006). Reciprocal relationships between insulin resistance and endothelial dysfunction: molecular and pathophysiological mechanisms. Circulation **113**(15): 1888-1904.

Kim, J.Y., L.A. Nolte, P.A. Hansen, D.H. Han, K. Ferguson, P.A. Thompson and J.O. Holloszy (2000). High-fat diet-induced muscle insulin resistance: relationship to visceral fat mass. American Journal of Physiology Regulatory, Integrative and Comparative Physiology. **279**(6): R2057-R2065.

King, G.L. and S.M. Johnson (1985). Receptor-mediated transport of insulin across endothelial cells. Science **227**: 1583-1586.

Klitzman, B., D.N. Damon, R.J. Gorczynski and B.R. Duling (1982). Augmented tissue oxygen supply during striated muscle contraction in the hamster. Relative contributions of capillary recruitment, functional dilation, and reduced tissue PO2. Circulation Research **51**: 711-721.

Koshinaka, K., Y. Oshida, Y.Q. Han, M. Kubota, A.Y. Viana, M. Nagasaki and Y. Sato (2004). Insulin-nonspecific reduction in skeletal muscle glucose transport in high-fat-fed rats. Metabolism: Clinical and Experimental **53**(7): 912-917.

Kraegen, E.W., P.W. Clark, A.B. Jenkins, E.A. Daley, D.J. Chisholm and L.H. Storlien (1991). Development of muscle insulin resistance after liver insulin resistance in high- fat-fed rats. Diabetes **40**: 1397-1403.

Kraegen, E.W. and G.J. Cooney (2008). Free fatty acids and skeletal muscle insulin resistance. Current Opinion in Lipidology **19**(3): 235-241.

Kraegen, E.W., D.E. James, A.B. Jenkins and D.J. Chisholm (1985). Dose-response curves for in vivo insulin sensitivity in individual tissues in rats. American Journal of Physiology **248**: E353-E362.

Kraegen, E.W., D.E. James, L.H. Storlien, K.M. Burleigh and D.J. Chisholm (1986). In vivo insulin resistance in individual peripheral tissues of the high fat fed rat: assessment by euglycaemic clamp plus deoxyglucose administration. Diabetologia **29**: 192-198.

Krook, A., M. Bjornholm, D. Galuska, X.J. Jiang, R. Fahlman, M.G. Myers, Jr., H. Wallberg-Henriksson and J.R. Zierath (2000). Characterization of signal transduction and glucose transport in skeletal muscle from type 2 diabetic patients. Diabetes **49**(2): 284-292.

Krssak, M., K.F. Petersen, R. Bergeron, T. Price, D. Laurent, D.L. Rothman, M. Roden and G.I. Shulman (2000). Intramuscular glycogen and intramyocellular lipid utilization during prolonged exercise and recovery in man: a 13C and 1H nuclear magnetic resonance spectroscopy study. Journal of Clinical Endocrinology & Metabolism **85**(2): 748-754.

Kulkarni, R.N., J.C. Bruning, J.N. Winnay, C. Postic, M.A. Magnuson and C.R. Kahn (1999). Tissue-specific knockout of the insulin receptor in pancreatic beta cells creates an insulin secretory defect similar to that in type 2 diabetes. Cell **96**(3): 329-339.

Kusunoki, M., L.H. Storlien, J. MacDessi, N.D. Oakes, C. Kennedy, D.J. Chisholm and E.W. Kraegen (1993). Muscle glucose uptake during and after exercise is normal in insulin-resistant rats. American Journal of Physiology Endocrinology and Metabolism **264**(2): E167-172.

Laakso, M., S.V. Edelman, G. Brechtel and A.D. Baron (1990). Decreased effect of insulin to stimulate skeletal muscle blood flow in obese man. Journal of Clinical Investigation **85**: 1844-1852.

Lang, C.H., C. Dobrescu and G.J. Bagby (1992). Tumor necrosis factor impairs insulin action on peripheral glucose disposal and hepatic glucose output. Endocrinology **130**(1): 43-52.

Lee, D.-E., S. Kehlenbrink, H. Lee, M. Hawkins and J.S. Yudkin (2009). Getting the message across: mechanisms of physiological cross talk by adipose tissue. American Journal of Physiology Endocrinology and Metabolism **296**(6): E1210-1229.

Lesniewski, L.A., A.J. Donato, B.J. Behnke, C.R. Woodman, M.H. Laughlin, C.A. Ray and M.D. Delp (2008). Decreased NO signaling leads to enhanced vasoconstrictor responsiveness in skeletal muscle arterioles of the ZDF rat prior to overt diabetes and hypertension. American Journal of Physiology Heart and Circulatory Physiology **294**(4): H1840-1850.

Leung, D.W., G. Cachianes, W.J. Kuang, D.V. Goeddel and N. Ferrara (1989). Vascular endothelial growth factor is a secreted angiogenic mitogen. Science **246**(4935): 1306-1309.

Levy, B.I., G. Ambrosio, A.R. Pries and H.A. Struijker-Boudier (2001). Microcirculation in hypertension: a new target for treatment? Circulation **104**(6): 735-740.

Li, G., E.J. Barrett, M.O. Barrett, W. Cao and Z. Liu (2007). Tumor necrosis factor-alpha induces insulin resistance in endothelial cells via a p38 mitogen-activated protein kinase-dependent pathway. Endocrinology **148**(7): 3356-3363.

Li, H. and U. Forstermann (2000). Nitric oxide in the pathogenesis of vascular disease. Journal of Pathology **190**(3): 244-254.

Li, R., W.Q. Wang, H. Zhang, X. Yang, Q. Fan, T.A. Christopher, B.L. Lopez, L. Tao, B.J. Goldstein, F. Gao and X.L. Ma (2007). Adiponectin improves endothelial function in hyperlipidemic rats by reducing oxidative/nitrative stress and differential regulation of eNOS/iNOS

activity. American Journal of Physiology Endocrinology and Metabolism **293**(6): E1703-E1708.

Liang, C., J.U. Doherty, R. Faillace, K. Maekawa, S. Arnold, H. Gavras and W.B. Hood, Jr. (1982). Insulin infusion in conscious dogs. Effects on systemic and coronary hemodynamics, regional blood flows, and plasma catecholamines. Journal of Clinical Investigation **69**(6): 1321-1336.

Lihn, A.S., S.B. Pedersen and B. Richelsen (2005). Adiponectin: action, regulation and association to insulin sensitivity. Obesity Reviews **6**(1): 13-21.

Lindner, J.R. and K. Wei (2002). Contrast echocardiography. Current Problems in Cardiology **27**(11): 454-519.

Liu, R.H., M. Mizuta, T. Kurose and S. Matsukura (2002). Early events involved in the development of insulin resistance in Zucker fatty rat. International Journal of Obesity and Related Metabolic Disorders **26**(3): 318-326.

Liu, S., V.E. Baracos, H.A. Quinney and M.T. Clandinin (1996). Dietary fat modifies exercise-dependent glucose transport in skeletal muscle. Journal of Applied Physiology **80**(4): 1219-1224.

Machann, J., H. Haring, F. Schick and M. Stumvoll (2004). Intramyocellular lipids and insulin resistance. Diabetes, Obesity and Metabolism **6**(4): 239-248.

Mahajan, H., S.M. Richards, S. Rattigan and M.G. Clark (2004). Local methacholine but not bradykinin potentiates insulin-mediated glucose uptake in muscle in vivo by augmenting capillary recruitment. Diabetologia **47**(12): 2226-2234.

Masek, J. and P. Fabry (1959). High-fat diet and the development of obesity in albino rats. Experientia **15**: 444-445.

Mauvais-Jarvis, F. and C.R. Kahn (2000). Understanding the pathogenesis and treatment of insulin resistance and type 2 diabetes mellitus: what can we learn from transgenic and knockout mice? Diabetes and Metabolism **26**(6): 433-448.

Meyer, M.M., K. Levin, T. Grimmsmann, N. Perwitz, A. Eirich, H. Beck-Nielsen and H.H. Klein (2002). Troglitazone treatment increases protein kinase B phosphorylation in skeletal muscle of normoglycemic subjects at risk for the development of type 2 diabetes. Diabetes **51**(9): 2691-2697.

Milkiewicz, M., O. Hudlicka, R. Shiner, S. Egginton and M.D. Brown (2006). Vascular endothelial growth factor mRNA and protein do not change in parallel during non-inflammatory skeletal muscle ischaemia in rat. Journal of Physiology **577**(2): 671-678.

Milkiewicz, M., O. Hudlicka, J. Verhaeg, S. Egginton and M.D. Brown (2003). Differential expression of Flk-1 and Flt-1 in rat skeletal muscle in response to chronic ischaemia: favourable effect of muscle activity. Clinical Science **105**(4): 473-482.

Minokoshi, Y., Y.B. Kim, O.D. Peroni, L.G. Fryer, C. Muller, D. Carling and B.B. Kahn (2002). Leptin stimulates fatty-acid oxidation by activating AMP-activated protein kinase. Nature **415**(6869): 339-343.

Minuk, H.L., M. Vranic, E.B. Marliss, A.K. Hanna, A.M. Albisser and B. Zinman (1981). Glucoregulatory and metabolic response to exercise in obese noninsulin- dependent diabetes. American Journal of Physiology **240**: E458-E464.

Moncada, S., A.G. Herman and P. Vanhoutte (1987). Endothelium- derived relaxing factor is identified as nitric oxide. Trends in Pharmacological Sciences **8**: 365-368.

Mora, A., D. Komander, D.M. van Aalten and D.R. Alessi (2004). PDK1, the master regulator of AGC kinase signal transduction. Seminars in Cell and Developmental Biology **15**(2): 161-170.

Mullen, K.L., J. Pritchard, I. Ritchie, L.A. Snook, A. Chabowski, A. Bonen, D. Wright and D.J. Dyck (2009). Adiponectin resistance precedes the accumulation of skeletal muscle lipids and insulin resistance in high-fat-fed rats. American Journal of Physiology Regulatory, Integrative and Comparative Physiology **296**(2): R243-251.

Muniyappa, R., M. Montagnani, K.K. Koh and M.J. Quon (2007). Cardiovascular Actions of Insulin. Endocrine Reviews **28**(5): 463-491.

Murrant, C.L. and I.H. Sarelius (2000). Coupling of muscle metabolism and muscle blood flow in capillary units during contraction. Acta Physiologica Scandinavica **168**(4): 531-541.

Newman, J.M., J.T. Steen and M.G. Clark (1997). Vessels supplying septa and tendons as functional shunts in perfused rat hindlimb. Microvascular Research **54**(1): 49-57.

Newman, J.M.B., R.M. Dwyer, P. St-Pierre, S.M. Richards, M.G. Clark and S. Rattigan (2009). Decreased microvascular vasomotion and myogenic response in rat skeletal muscle in association with acute insulin resistance. The Journal of Physiology **587**(11): 2579-2588.

Nieuwdorp, M., H.L. Mooij, J. Kroon, B. Atasever, J.A. Spaan, C. Ince, F. Holleman, M. Diamant, R.J. Heine, J.B. Hoekstra, J.J. Kastelein, E.S. Stroes and H. Vink (2006). Endothelial glycocalyx damage coincides with microalbuminuria in type 1 diabetes. Diabetes **55**(4): 1127-1132.

Nieuwdorp, M., T.W. van Haeften, M.C. Gouverneur, H.L. Mooij, M.H. van Lieshout, M. Levi, J.C. Meijers, F. Holleman, J.B. Hoekstra, H. Vink, J.J. Kastelein and E.S. Stroes (2006). Loss of endothelial glycocalyx during acute hyperglycemia coincides with endothelial dysfunction and coagulation activation in vivo. Diabetes **55**(2): 480-486.

Nilsson, H. and C. Aalkjaer (2003). Vasomotion: mechanisms and physiological importance. Molecular Interventions **3**(2): 79-89, 51.

Nolte, L.A., P.A. Hansen, M.M. Chen, J.M. Schluter, E.A. Gulve and J.O. Holloszy (1998). Short-term exposure to tumor necrosis factor-alpha does

not affect insulin-stimulated glucose uptake in skeletal muscle. Diabetes **47**(5): 721-726.

Noon, J.P., B.R. Walker, D.J. Webb, A.C. Shore, D.W. Holton, H.V. Edwards and G.C.M. Watt (1997). Impaired microvascular dilatation and capillary rarefaction in young adults with a predisposition to high blood pressure. Journal of Clinical Investigation **99**(8): 1873-1879.

Nuutila, P., M. Raitakari, H. Laine, O. Kirvela, T. Takala, T. Utriainen, S. Makimattila, O.P. Pitkanen, U. Ruotsalainen, H. Iida, J. Knuuti and H. Yki-Jarvinen (1996). Role of blood flow in regulating insulin-stimulated glucose uptake in humans. Studies using bradykinin, [15O]water, and [18F]fluoro-deoxy- glucose and positron emission tomography. Journal of Clinical Investigation **97**(7): 1741-1747.

Olsen, A.K., E.M. Bladbjerg, A.K. Hansen and P. Marckmann (2002). A High Fat Meal Activates Blood Coagulation Factor VII in Rats. Journal of Nutrition **132**(3): 347-350.

Ozcan, U., Q. Cao, E. Yilmaz, A.H. Lee, N.N. Iwakoshi, E. Ozdelen, G. Tuncman, C. Gorgun, L.H. Glimcher and G.S. Hotamisligil (2004). Endoplasmic reticulum stress links obesity, insulin action, and type 2 diabetes. Science **306**(5695): 457-461.

Pappenheimer, J.R. (1941). Vasoconstrictor nerves and oxygen consumption in the isolated perfused hindlimb muscles of the dog. Journal of Physiology **99**(2): 182-200.

Parks, D.A. and D.N. Granger (1986). Xanthine oxidase: biochemistry, distribution and physiology. Acta Physiologica Scandinavica **548**: 87-99.

Parthasarathi, K. and H.H. Lipowsky (1999). Capillary recruitment in response to tissue hypoxia and its dependence on red blood cell deformability. American Journal of Physiology Heart and Circulatory Physiology **277**(6 Pt 2): H2145-H2157.

Pauli, J.R., E.R. Ropelle, D.E. Cintra, M.A. Carvalho-Filho, J.C. Moraes, C.T. De Souza, L.A. Velloso, J.B.C. Carvalheira and M.J.A. Saad (2008). Acute physical exercise reverses S-nitrosation of the insulin receptor, insulin receptor substrate 1 and protein kinase B/Akt in diet-induced obese Wistar rats. Journal of Physiology **586**(2): 659-671.

Perseghin, G., T.B. Price, K.F. Petersen, M. Roden, G.W. Cline, K. Gerow, D.L. Rothman and G.I. Shulman (1996). Increased glucose transport-phosphorylation and muscle glycogen synthesis after exercise training in insulin-resistant subjects. New England Journal of Medicine **335**(18): 1357-1362.

Peterson, T.E., V. Poppa, H. Ueba, A. Wu, C. Yan and B.C. Berk (1999). Opposing Effects of Reactive Oxygen Species and Cholesterol on Endothelial Nitric Oxide Synthase and Endothelial Cell Caveolae. Circulation Research **85**(1): 29-37.

Plomgaard, P., K. Bouzakri, R. Krogh-Madsen, B. Mittendorfer, J.R. Zierath and B.K. Pedersen (2005). Tumor necrosis factor-alpha induces skeletal

muscle insulin resistance in healthy human subjects via inhibition of Akt substrate 160 phosphorylation. Diabetes **54**(10): 2939-2945.

Potenza, M.A., F. Addabbo and M. Montagnani (2009). Vascular actions of insulin with implications for endothelial dysfunction. American Journal of Physiology Endocrinology and Metabolism **297**(3): E568-577.

Raitakari, M., P. Nuutila, U. Ruotsalainen, H. Laine, M. Teras, H. Iida, S. Makimattila, T. Utriainen, V. Oikonen and H. Sipila (1996). Evidence for dissociation of insulin stimulation of blood flow and glucose uptake in human skeletal muscle - Studies using [15 O]H 2 O, [18 F]fluoro-2-deoxy-D-glucose, and positron emission tomography. Diabetes **45**: 1471-1477.

Randle, P.J., P.B. Garland, E.A. Newsholmet and C.N. Hales (1965). The Glucose Fatty Acid Cycle in Obesity and Maturity Onset Diabetes Mellitus. Annals of the New York Academy of Sciences **131**(Adipose Tissue Metabolism and Obesity): 324-333.

Rask-Madsen, C., H. Dominguez, N. Ihlemann, T. Hermann, L. Kober and C. Torp-Pedersen (2003). Tumor necrosis factor-alpha inhibits insulin's stimulating effect on glucose uptake and endothelium-dependent vasodilation in humans. Circulation **108**(15): 1815-1821.

Rattigan, S., G.J. Appleby, K.A. Miller, J.T. Steen, K.A. Dora, E.Q. Colquhoun and M.G. Clark (1997). Serotonin inhibition of 1-methylxanthine metabolism parallels its vasoconstrictor activity and inhibition of oxygen uptake in perfused rat hindlimb. Acta Physiologica Scandinavica **161**(2): 161-169.

Rattigan, S., M.G. Clark and E.J. Barrett (1997). Hemodynamic actions of insulin in rat skeletal muscle: evidence for capillary recruitment. Diabetes **46**(9): 1381-1388.

Rattigan, S., M.G. Clark and E.J. Barrett (1999). Acute vasoconstriction-induced insulin resistance in rat muscle in vivo. Diabetes **48**(3): 564-569.

Rattigan, S., M.G. Wallis, J.M. Youd and M.G. Clark (2001). Exercise training improves insulin-mediated capillary recruitment in association with glucose uptake in rat hindlimb. Diabetes **50**(12): 2659-2665.

Rattigan, S., C. Wheatley, S.M. Richards, E.J. Barrett and M.G. Clark (2005). Exercise and insulin-mediated capillary recruitment in muscle. Exercise and Sport Sciences Reviews **33**(1): 43-48.

Reaven, G.M. (1988). Role of insulin resistance in human disease. Diabetes **37**: 1595-1607.

Reaven, G.M., C. Hollenbeck, C.Y. Jeng, M.S. Wu and Y.D. Chen (1988). Measurement of plasma glucose, free fatty acid, lactate, and insulin for 24 h in patients with NIDDM. Diabetes **37**(8): 1020-1024.

Reitsma, S., D.W. Slaaf, H. Vink, M.A. van Zandvoort and M.G. Oude Egbrink (2007). The endothelial glycocalyx: composition, functions, and visualization. Pflugers Archiv **454**(3): 345-359.

Roden, M., T.B. Price, G. Perseghin, K.F. Petersen, D.L. Rothman, G.W. Cline and G.I. Shulman (1996). Mechanism of free fatty acid-induced insulin resistance in humans. Journal of Clinical Investigation **97**(12): 2859-2865.

Rose, A.J. and E.A. Richter (2005). Skeletal Muscle Glucose Uptake During Exercise: How is it Regulated? Physiology (Bethesda) **20**(4): 260-270.

Rosholt, M.N., P.A. King and E.S. Horton (1994). High-fat diet reduces glucose transporter responses to both insulin and exercise. American Journal of Physiology Regulatory, Integrative and Comparative Physiology **266**: R95-R101.

Ross, R.M., K. Downey, J.M. Newman, S.M. Richards, M.G. Clark and S. Rattigan (2008). Contrast-enhanced ultrasound measurement of microvascular perfusion relevant to nutrient and hormone delivery in skeletal muscle: A model study in vitro. Microvascular Research **75**(3): 323-329.

Ross, R.M., G.D. Wadley, M.G. Clark, S. Rattigan and G.K. McConell (2007). Local NOS inhibition reduces skeletal muscle glucose uptake but not capillary blood flow during in situ muscle contraction in rats. Diabetes **56**: 2885-2892.

Rothman, D.L., I. Magnusson, G. Cline, D. Gerard, C.R. Kahn, R.G. Shulman and G.I. Shulman (1995). Decreased muscle glucose transport/phosphorylation is an early defect in the pathogenesis of non-insulin-dependent diabetes mellitus. Proceedings of the National Academy of Sciences of the United States of America **92**: 983-987.

Roy, D. and A. Marette (1996). Exercise induces the translocation of GLUT4 to transverse tubules from an intracellular pool in rat skeletal muscle. Biochemical and Biophysical Research Communications **223**: 147-152.

Roy, D., M. Perreault and A. Marette (1998). Insulin stimulation of glucose uptake in skeletal muscles and adipose tissues in vivo is NO dependent. American Journal of Physiology Endocrinology and Metabolism **274**(4 Pt 1): E692-E699.

Rucker, M., O. Strobel, B. Vollmar, F. Roesken and M.D. Menger (2000). Vasomotion in critically perfused muscle protects adjacent tissues from capillary perfusion failure. American Journal of Physiology Heart and Circulatory Physiology **279**(2): H550-558.

Ryder, J.W., A.V. Chibalin and J.R. Zierath (2001). Intracellular mechanisms underlying increases in glucose uptake in response to insulin or exercise in skeletal muscle. Acta Physiologica Scandinavica **171**(3): 249-257.

Saghizadeh, M., J.M. Ong, W.T. Garvey, R.R. Henry and P.A. Kern (1996). The expression of TNF alpha by human muscle. Relationship to insulin resistance. Journal of Clinical Investigation **97**(4): 1111-1116.

Sakai, K., T. Imaizumi, H. Masaki and A. Takeshita (1993). Intra-arterial infusion of insulin attenuates vasoreactivity in human forearm. Hypertension **22**: 67-73.

Sato, T., Y. Nara, Y. Kato and Y. Yamori (1996). Long-term effects of high calorie sucrose-enriched diet and streptozotocin-induced diabetes on insulin resistance in spontaneously hypertensive rats. Clinical and Experimental Pharmacology and Physiology **23**(8): 669-674.

Schenk, S. (2008). Insulin sensitivity: modulation by nutrients and inflammation. The Journal of Clinical Investigation **118**(9): 2992-3002.

Scherrer, U., D. Randin, P. Vollenweider, L. Vollenweider and P. Nicod (1994). Nitric oxide release accounts for insulin's vascular effects in humans. Journal of Clinical Investigation **94**(6): 2511-2515.

Schneider, S.H., L.F. Amorosa, A.K. Khachadurian and N.B. Ruderman (1984). Studies on the mechanism of improved glucose control during regular exercise in Type 2 (non-insulin-dependent) diabetes. Diabetologia **26**: 355-360.

Schrauwen-Hinderling, V.B., M.K. Hesselink, P. Schrauwen and M.E. Kooi (2006). Intramyocellular lipid content in human skeletal muscle. Obesity (Silver Spring) **14**(3): 357-367.

Schrauwen-Hinderling, V.B., M.E. Kooi, M.K. Hesselink, E. Moonen-Kornips, G. Schaart, K.J. Mustard, D.G. Hardie, W.H. Saris, K. Nicolay and P. Schrauwen (2005). Intramyocellular lipid content and molecular adaptations in response to a 1-week high-fat diet. Obesity Reviews **13**(12): 2088-2094.

Schroder, M. and R.J. Kaufman (2005). The mammalian unfolded protein response. Annual Review of Biochemistry **74**: 739-789.

Segal, S.S. (2000). Integration of blood flow control to skeletal muscle: key role of feed arteries. Acta Physiologica Scandinavica **168**(4): 511-518.

Segal, S.S. and B.R. Duling (1986). Communication between feed arteries and microvessels in hamster striated muscle: segmental vascular responses are functionally coordinated. Circulation Research **59**: 283-290.

Serne, E.H., R.T. de Jongh, E.C. Eringa, R.G. Ijzerman and C.D. Stehouwer (2007). Microvascular dysfunction: a potential pathophysiological role in the metabolic syndrome. Hypertension **50**(1): 204-211.

Serne, E.H., R.O. Gans, J.C. ter Maaten, G.J. Tangelder, A.J. Donker and C.D. Stehouwer (2001). Impaired skin capillary recruitment in essential hypertension is caused by both functional and structural capillary rarefaction. Hypertension **38**(2): 238-242.

Serne, E.H., R.O. Gans, J.C. ter Maaten, P.M. ter Wee, A.J. Donker and C.D. Stehouwer (2001). Capillary recruitment is impaired in essential hypertension and relates to insulin's metabolic and vascular actions. Cardiovascular Research **49**(1): 161-168.

Serne, E.H., C.D. Stehouwer, J.C. ter Maaten, P.M. ter Wee, J.A. Rauwerda, A.J. Donker and R.O. Gans (1999). Microvascular Function Relates to Insulin Sensitivity and Blood Pressure in Normal Subjects. Circulation **99**(7): 896-902.

Seyde, W.C., L. McGowan, N. Lund, B. Duling and D.E. Longnecker (1985). Effects of anesthetics on regional hemodynamics in normovolemic and hemorrhaged rats. American Journal of Physiology Heart and Circulatory Physiology **249**(1 Pt 2): H164-173.

Sheriff, D.D., L.B. Rowell and A.M. Scher (1993). Is rapid rise in vascular conductance at onset of dynamic exercise due to muscle pump? American Journal of Physiology **265**: H1227-H1234.

Shulman, G.I. (2000). Cellular mechanisms of insulin resistance. Journal of Clinical Investigation **106**(2): 171-176.

Sierra-Honigmann, M.R., A.K. Nath, C. Murakami, G. Garcia-Cardena, A. Papapetropoulos, W.C. Sessa, L.A. Madge, J.S. Schechner, M.B. Schwabb, P.J. Polverini and J.R. Flores-Riveros (1998). Biological action of leptin as an angiogenic factor. Science **281**(5383): 1683-1686.

Sonne, B. and H. Galbo (1985). Carbohydrate metabolism during and after exercise in rats: studies with radioglucose. Journal of Applied Physiology **59**: 1627-1639.

St-Pierre, P., L. Bouffard and P. Maheux (2004). Rosiglitazone increases extravasation of macromolecules and endothelial nitric oxide synthase in skeletal muscles of the fructose-fed rat model. Biochemical Pharmacology **67**(10): 1997-2004.

St-Pierre, P., L. Bouffard, M.E. Papirakis and P. Maheux (2006). Increased extravasation of macromolecules in skeletal muscles of the Zucker rat model. Obesity **14**(5): 787-793.

Stefanovska, A., M. Bracic and H.D. Kvernmo (1999). Wavelet analysis of oscillations in the peripheral blood circulation measured by laser Doppler technique. IEEE Transactions on Biomedical Engineering **46**(10): 1230-1239.

Steil, G.M., M. Ader, D.M. Moore, K. Rebrin and R.N. Bergman (1996). Transendothelial insulin transport is not saturable in vivo - No evidence for a receptor-mediated process. Journal of Clinical Investigation **97**: 1497-1503.

Steinberg, H.O. and A.D. Baron (1999). Insulin-mediated vasodilation: why one's physiology could be the other's pharmacology. Diabetologia **42**(4): 493-495.

Steinberg, H.O., G. Brechtel, A. Johnson, N. Fineberg and A.D. Baron (1994). Insulin-mediated skeletal muscle vasodilation is nitric oxide dependent. A novel action of insulin to increase nitric oxide release. Journal of Clinical Investigation **94**: 1172-1179.

Steinberg, H.O., G. Paradisi, G. Hook, K. Crowder, J. Cronin and A.D. Baron (2000). Free fatty acid elevation impairs insulin-mediated vasodilation and nitric oxide production. Diabetes **49**(7): 1231-1238.

Stenbit, A.E., T.S. Tsao, J. Li, R. Burcelin, D.L. Geenen, S.M. Factor, K. Houseknecht, E.B. Katz and M.J. Charron (1997). GLUT4 heterozygous

knockout mice develop muscle insulin resistance and diabetes. Nature Medicine **3**(10): 1096-1101.

Storlien, L.H., A.B. Jenkins, D.J. Chisholm, W.S. Pascoe, S. Khouri and E.W. Kraegen (1991). Influence of dietary fat composition on development of insulin resistance in rats. Diabetes **40**: 280-289.

Suh, S.H., I.Y. Paik and K. Jacobs (2007). Regulation of blood glucose homeostasis during prolonged exercise. Molecules and Cells **23**(3): 272-279.

Summers, S.A. (2006). Ceramides in insulin resistance and lipotoxicity. Progress in Lipid Research **45**(1): 42-72.

Sweeney, T.E. and I.H. Sarelius (1989). Arteriolar control of capillary cell flow in striated muscle. Circulation Research **64**: 112-120.

Tack, C.J., J.A. Lutterman, G. Vervoort, T. Thien and P. Smits (1996). Activation of the sodium-potassium pump contributes to insulin-induced vasodilation in humans. Hypertension **28**(3): 426-432.

Tan, K.C., A. Xu, W.S. Chow, M.C. Lam, V.H. Ai, S.C. Tam and K.S. Lam (2004). Hypoadiponectinemia is associated with impaired endothelium-dependent vasodilation. Journal of Clinical Endocrinology & Metabolism **89**(2): 765-769.

Tanaka, S., T. Hayashi, T. Toyoda, T. Hamada, Y. Shimizu, M. Hirata, K. Ebihara, H. Masuzaki, K. Hosoda, T. Fushiki and K. Nakao (2007). High-fat diet impairs the effects of a single bout of endurance exercise on glucose transport and insulin sensitivity in rat skeletal muscle. Metabolism **56**(12): 1719-1728.

Torres, S.H., J.B. De Sanctis, L.B. de, N. Hernandez and H.J. Finol (2004). Inflammation and nitric oxide production in skeletal muscle of type 2 diabetic patients. Journal of Endocrinology **181**(3): 419-427.

Ueda, S., J.R. Petrie, S.J. Cleland, H.L. Elliott and J.M. Connell (1998). The vasodilating effect of insulin is dependent on local glucose uptake: a double blind, placebo-controlled study. Journal of Clinical Endocrinology and Metabolism **83**(6): 2126-2131.

Utriainen, T., R. Malmstrom, S. Makimattila and H. Yki-Jarvinen (1995). Methodological aspects, dose-response characteristics and causes of interindividual variation in insulin stimulation of limb blood flow in normal subjects. Diabetologia **38**(5): 555-564.

Uysal, K.T., S.M. Wiesbrock, M.W. Marino and G.S. Hotamisligil (1997). Protection from obesity-induced insulin resistance in mice lacking TNF-alpha function. Nature **389**(6651): 610-614.

Valerio, A., A. Cardile, V. Cozzi, R. Bracale, L. Tedesco, A. Pisconti, L. Palomba, O. Cantoni, E. Clementi, S. Moncada, M.O. Carruba and E. Nisoli (2006). TNF-alpha downregulates eNOS expression and mitochondrial biogenesis in fat and muscle of obese rodents. Journal of Clinical Investigation **116**(10): 2791-2798.

Vanhoutte, P.M., H. Shimokawa, E.H. Tang and M. Feletou (2009). Endothelial dysfunction and vascular disease. Acta Physiologica (Oxford) **196**: 193-222.

Vincent, M.A., E.J. Barrett, J.R. Lindner, M.G. Clark and S. Rattigan (2003). Inhibiting NOS blocks microvascular recruitment and blunts muscle glucose uptake in response to insulin. American Journal of Physiology Endocrinology and Metabolism **285**(1): E123-E129.

Vincent, M.A., L.H. Clerk, J.R. Lindner, A.L. Klibanov, M.G. Clark, S. Rattigan and E.J. Barrett (2004). Microvascular recruitment is an early insulin effect that regulates skeletal muscle glucose uptake in vivo. Diabetes **53**(6): 1418-1423.

Vincent, M.A., L.H. Clerk, J.R. Lindner, W.J. Price, L.A. Jahn, H. Leong-Poi and E.J. Barrett (2006). Mixed meal and light exercise each recruit muscle capillaries in healthy humans. American Journal of Physiology Endocrinology and Metabolism **290**(6): E1191-E1197.

Vincent, M.A., D. Dawson, A.D. Clark, J.R. Lindner, S. Rattigan, M.G. Clark and E.J. Barrett (2002). Skeletal muscle microvascular recruitment by physiological hyperinsulinemia precedes increases in total blood flow. Diabetes **51**(1): 42-48.

Vincent, M.A., M. Montagnani and M.J. Quon (2003). Molecular and physiologic actions of insulin related to production of nitric oxide in vascular endothelium. Current Diabetes Reports **3**(4): 279-288.

Vincent, M.A., S. Rattigan and M.G. Clark (2001). Size-dependent effects of microspheres on vasoconstrictor-mediated change in oxygen uptake by perfused rat hindlimb. Microvascular Research **62**(3): 306-314.

Vincent, M.A., S. Rattigan, M.G. Clark, S.L. Bernard and R.W. Glenny (2001). Spatial distribution of nutritive and nonnutritive vascular routes in perfused rat hindlimb muscle using microspheres. Microvascular Research **61**(1): 111-121.

Vollenweider, P., L. Tappy, D. Randin, P. Schneiter, E. Jequier, P. Nicod and U. Scherrer (1993). Differential effects of hyperinsulinemia and carbohydrate metabolism on sympathetic nerve activity and muscle blood flow in humans. Journal of Clinical Investigation **92**: 147-154.

Vollus, G.C., E.A. Bradley, M.K. Roberts, J.M. Newman, S.M. Richards, S. Rattigan, E.J. Barrett and M.G. Clark (2007). Graded occlusion of perfused rat muscle vasculature decreases insulin action. Clinical Science **112**: 457-466.

Walder, C.E., C.J. Errett, S. Bunting, P. Lindquist, J.R. Ogez, H.G. Heinsohn, N. Ferrara and G.R. Thomas (1996). Vascular endothelial growth factor augments muscle blood flow and function in a rabbit model of chronic hindlimb ischemia. Journal of Cardiovascular Pharmacology **27**(1): 91-98.

Wallberg-Henriksson, H. and J.O. Holloszy (1984). Contractile activity increases glucose uptake by muscle in severely diabetic rats. Journal of Applied Physiology **57**: 1045-1049.

Wallis, M.G., M.E. Smith, C.M. Kolka, L. Zhang, S.M. Richards, S. Rattigan and M.G. Clark (2005). Acute glucosamine-induced insulin resistance in muscle in vivo is associated with impaired capillary recruitment. Diabetologia **48**: 2131-2139.

Wallis, M.G., C.M. Wheatley, S. Rattigan, E.J. Barrett, A.D. Clark and M.G. Clark (2002). Insulin-mediated hemodynamic changes are impaired in muscle of zucker obese rats. Diabetes **51**(12): 3492-3498.

Wang, H., Z. Liu, G. Li and E.J. Barrett (2006). The vascular endothelial cell mediates insulin transport into skeletal muscle. American Journal of Physiology Endocrinology and Metabolism **291**(2): E323-E332.

Wei, K., A.R. Jayaweera, S. Firoozan, A. Linka, D.M. Skyba and S. Kaul (1998). Quantification of myocardial blood flow with ultrasound-induced destruction of microbubbles administered as a constant venous infusion. Circulation **97**(5): 473-483.

Wellen, K.E. and G.S. Hotamisligil (2005). Inflammation, stress, and diabetes. Journal of Clinical Investigation **115**(5): 1111-1119.

Weltman, N.Y., S.A. Saliba, E.J. Barrett and A. Weltman (2009). The use of exercise in the management of type 1 and type 2 diabetes. Clinical Sports Medicine **28**(3): 423-439.

Wheatley, C.M., S. Rattigan, S.M. Richards, E.J. Barrett and M.G. Clark (2004). Skeletal muscle contraction stimulates capillary recruitment and glucose uptake in insulin-resistant obese Zucker rats. American Journal of Physiology Endocrinology and Metabolism **287**(4): E804-E809.

White, M.F. and C.R. Kahn (1994). The insulin signaling system. Journal of Biological Chemistry **269**: 1-4.

World Health Organisation (2009). The World Health Organisation. Viewed November 2009. http://www.who.int/diabetes/facts/world_figures/en/.

Williams, S.B., J.A. Cusco, M.A. Roddy, M.T. Johnstone and M.A. Creager (1996). Impaired nitric oxide-mediated vasodilation in patients with non-insulin-dependent diabetes mellitus. Journal of the American College of Cardiology **27**(3): 567-574.

Womack, L., D. Peters, E.J. Barrett, S. Kaul, W. Price and J.R. Lindner (2009). Abnormal Skeletal Muscle Capillary Recruitment During Exercise in Patients With Type 2 Diabetes Mellitus and Microvascular Complications. Journal of the American College of Cardiology **53**(23): 2175-2183.

Xu, H., K.T. Uysal, J.D. Becherer, P. Arner and G.S. Hotamisligil (2002). Altered tumor necrosis factor-alpha (TNF-alpha) processing in adipocytes and increased expression of transmembrane TNF-alpha in obesity. Diabetes **51**(6): 1876-1883.

Ye, J., M.G. Clark and E.Q. Colquhoun (1996). Creatine phosphate as the preferred early indicator of ischemia in muscular tissues. Journal of Surgical Research **61**(1): 227-236.

Yki-Jarvinen, H. and T. Utriainen (1998). Insulin-induced vasodilatation: physiology or pharmacology? Diabetologia **41**(4): 369-379.

Yki-Jarvinen, H., A.A. Young, C. Lamkin and J.E. Foley (1987). Kinetics of glucose disposal in whole body and across the forearm in man. Journal of Clinical Investigation **79**(6): 1713-1719.

Youd, J.M., S. Rattigan and M.G. Clark (2000). Acute impairment of insulin-mediated capillary recruitment and glucose uptake in rat skeletal muscle in vivo by TNFa. Diabetes **49**(11): 1904-1909.

Young, M.E. and B. Leighton (1998). Evidence for altered sensitivity of the nitric oxide/cGMP signalling cascade in insulin-resistant skeletal muscle. Biochemical Journal **329**(Pt 1): 73-79.

Youngren, J.F., J. Paik and R.J. Barnard (2001). Impaired insulin-receptor autophosphorylation is an early defect in fat-fed, insulin-resistant rats. Journal of Applied Physiology **91**(5): 2240-2247.

Yu, C., Y. Chen, G.W. Cline, D. Zhang, H. Zong, Y. Wang, R. Bergeron, J.K. Kim, S.W. Cushman, G.J. Cooney, B. Atcheson, M.F. White, E.W. Kraegen and G.I. Shulman (2002). Mechanism by which fatty acids inhibit insulin activation of insulin receptor substrate-1 (IRS-1)-associated phosphatidylinositol 3-kinase activity in muscle. Journal of Biological Chemistry **277**(52): 50230-50236.

Yudkin, J.S., E. Eringa and C.D. Stehouwer (2005). "Vasocrine" signalling from perivascular fat: a mechanism linking insulin resistance to vascular disease. Lancet **365**(9473): 1817-1820.

Zeng, G., F.H. Nystrom, L.V. Ravichandran, L.N. Cong, M. Kirby, H. Mostowski and M.J. Quon (2000). Roles for insulin receptor, PI3-kinase, and Akt in insulin-signaling pathways related to production of nitric oxide in human vascular endothelial cells. Circulation **101**(13): 1539-1545.

Zhang, K. and R.J. Kaufman (2008). From endoplasmic-reticulum stress to the inflammatory response. Nature **454**(7203): 455-462.

Zhang, L., M.A. Vincent, S.M. Richards, L.H. Clerk, S. Rattigan, M.G. Clark and E.J. Barrett (2004). Insulin sensitivity of muscle capillary recruitment in vivo. Diabetes **53**(2): 447-453.

Zhang, L., C.M. Wheatley, S.M. Richards, E.J. Barrett, M.G. Clark and S. Rattigan (2003). TNF-alpha acutely inhibits vascular effects of physiological but not high insulin or contraction. American Journal of Physiology Endocrinology and Metabolism **285**(3): E654-E660.

Ziel, F.H., N. Venkatesan and M.B. Davidson (1988). Glucose transport is rate limiting for skeletal muscle glucose metabolism in normal and STZ-induced diabetic rats. Diabetes **37**: 885-890.

Zierath, J.R., A. Krook and H. Wallberg-Henriksson (1998). Insulin action in skeletal muscle from patients with NIDDM. Molecular and Cellular Biochemistry **182**(1-2): 153-160.

Zierler, K.L. (1961). Theory of the use of Arteriovenous Concentration Differences for Measuring Metabolism in Steady and Non-Steady States. Journal of Clinical Investigation **40**(12): 2111-2125.

Zisman, A., O.D. Peroni, E.D. Abel, M.D. Michael, F. Mauvais-Jarvis, B.B. Lowell, J.F. Wojtaszewski, M.F. Hirshman, A. Virkamaki, L.J. Goodyear, C.R. Kahn and B.B. Kahn (2000). Targeted disruption of the glucose transporter 4 selectively in muscle causes insulin resistance and glucose intolerance. Nature Medicine **6**(8): 924-928.

Zou, B., M. Suwa, H. Nakano, Y. Higaki, T. Ito, S. Katsuta and S. Kumagai (2003). Adaptation of skeletal muscle characteristics to a high-fat diet in rats with different intra-abdominal-obesity susceptibilities. Journal of Nutritional Science and Vitaminology **49**(4): 241-246.